Universität Potsdam
Mathematisch-Naturwissenschaftliche Fakultät
Institut für Physik und Astronomie

Helmholtz-Zentrum Berlin für Materialien und Energie
Institut für Methoden und Instrumentierung
der Forschung mit Synchrotronstrahlung

Accessing Active Sites of Molecular Proton Dynamics

Publikationsbasierte Dissertation

zur Erlangung des akademischen Grades
doctor rerum naturalium
(Dr. rer. nat.)
in der Wissenschaftsdisziplin
Experimentalphysik

eingereicht an der
Mathematisch-Naturwissenschaftlichen Fakultät
der Universität Potsdam

von
Sebastian Oliver Eckert

Disputation am
04.03.2019

Hauptbetreuer	Prof. Dr. Alexander Föhlisch
Zweitbetreuer	Prof. Dr. Peter Saalfrank
Gutachter	Prof. Dr. Alexander Föhlisch
	Prof. Dr. Markus Gühr
	Prof. Dr. Mathias Richter

Abstract

The unceasing impact of intense sunlight on earth constitutes a continuous source of energy fueling countless natural processes. On a molecular level, the energy contained in the electromagnetic radiation is transferred through photochemical processes into chemical or thermal energy. In the course of such processes, photo-excitations promote molecules into thermally inaccessible excited states. This induces adaptations of their molecular geometry according to the properties of the excited state. Decay processes towards energetically lower lying states in transient molecular geometries result in the formation of excited state relaxation pathways. The photo-chemical relaxation mechanisms depend on the studied system itself, the interactions with its chemical environment and the character of the involved states. This thesis focuses on systems in which photo-induced deprotonation processes occur at specific atomic sites.

To detect these excited-state proton dynamics at the affected atoms, a local probe of molecular electronic structure is required. Therefore, site-selective and orbital-specific K-edge soft X-ray spectroscopy techniques are used here to detect photo-induced proton dynamics in gaseous and liquid sample environments. The protonation of nitrogen (N) sites in organic molecules and the oxygen (O) atom in the water molecule are probed locally through transitions between 1s orbitals and the p-derived molecular valence electronic structure. The used techniques are X-ray absorption spectroscopy (XAS) and resonant inelastic X-ray scattering (RIXS). Both yield access to the unoccupied local valence electronic structure, whereas the latter additionally probes occupied states.

We apply these probes in optical pump X-ray probe experiments to investigate valence excited-state proton transfer capabilities of aqueous 2-thiopyridone. A characteristic shift of N K-edge X-ray absorption resonances as well as a distinct X-ray emission line are established by us as spectral fingerprints of N deprotonation in the system. We utilize them to identify photo-induced N deprotonation of 2-thiopyridone on femtosecond timescales, in optical pump N K-edge RIXS probe measurements. We further establish excited state proton transfer mechanisms on picosecond and nanosecond timescales along the dominant relaxation pathways of 2-thiopyridone using transient N K-edge XAS.

Despite being an excellent probe mechanism for valence excited-state proton dynamics, the K-edge core-excitation itself also disturbs the electronic structure at specific sites of a molecule. The rapid reaction of protons to 1s photo-excitations can yield directional structural distortions within the femtosecond core-excited state lifetime. These directional proton dynamics can change the energetic separation of eigenstates of the system and alter probabilities for radiative decay between them. Both effects yield spectral signatures of the dynamics in RIXS spectra.

Using these signatures of RIXS transitions into electronically excited states, we investigate proton dynamics induced by N K-edge excitation in the amino-acid histidine. The minor core-excited state dynamics of histidine in basic and neutral chemical environments allow us to establish XAS and RIXS spectral signatures of different N protonation states at its imidazole N sites. Based on these signatures, we identify an excitation-site-independent N-H dissociation for N K-edge excitation under acidic conditions.

Such directional structural deformations, induced by core-excitations, also make proton dynamics in electronic ground states accessible through RIXS transitions into vibrationally excited states. In that context, we interpret high resolution RIXS spectra of the water molecule for three O K-edge resonances based on quantum-chemical wave packet propagation simulations. We show that highly oriented ground state vibrational modes of coupled nuclear motion can be populated through RIXS processes by preparation of core-excited state nuclear wave packets with the same directionality. Based on that, we analytically derive the possibility to extract one-dimensional directional cuts through potential energy surfaces of molecular systems from the corresponding RIXS spectra. We further verify this concept through the extraction of the gas-phase water ground state potential along three coordinates from experimental data in comparison to quantum-chemical simulations of the potential energy surface.

This thesis also contains contributions to instrumentation development for investigations of photo-induced molecular dynamics at high brilliance X-ray light sources. We characterize the setup used for the transient valence-excited state XAS measurements of 2-thiopyridone. Therein, a sub-micrometer thin liquid sample environment is established employing in-vacuum flat-jet technology, which enables a transmission experimental geometry. In combination with a MHz-laser system, we achieve a high detection sensitivity for photo-induced X-ray absorption changes. Additionally, we present conceptual improvements for temporal X-ray optical cross-correlation techniques based on transient changes of multilayer optical properties, which are crucial for the realization of femtosecond time-resolved studies at synchrotrons and free-electron lasers.

Zusammenfassung

Die stetige Bestrahlung der Erde mit intensivem Sonnenlicht stellt einen permanente Energiequelle dar, die zahllose natürliche Prozesse antreibt. Auf molekularer Ebene wird die Energie der elektromagnetischen Strahlung durch photochemische Prozesse in chemische und thermische Energie umgewandelt. Während dieser Prozesse werden thermisch nicht erreichbare angeregte Zustände von Molekülen durch Photoanregungen bevölkert. Dies führt zu Änderungen der Molekülgeometrie, die abhängig von den Eigenschaften der angeregten Zustände sind. Zerfallsprozesse in energetisch tieferliegende Zustände in transienten Molekülgeometrien führen zur Ausbildung von Relaxationspfaden angeregter Zustände. Die Relaxationsmechanismen sind dabei abhängig vom untersuchten System selbst, den Wechselwirkungen mit seiner chemischen Umgebung und den Eigenschaften der beteiligten angeregten Zustände. In dieser Arbeit werden Systeme untersucht, in denen die Protonierung bestimmter Atome im Molekül durch eine Photoanregung geändert werden kann.

Um Protonendynamik an den betreffenden Atomen zu untersuchen, wird ein lokaler Zugang zur elektronischen Struktur des Moleküls benötigt. Daher wird in dieser Arbeit K-Kanten Weichröntgenspektroskopie genutzt, um photo-induzierte Protonendynamik in gasförmigen und flüssigen Proben zu untersuchen. Zusätzlich zur Selektivität bzgl. des Elements und des chemischen Zustands des betreffenden Atoms bietet diese Zugang zum Charakter und zur Lokalisierung der bindungsformenden Valenzorbitale. Die Protonierung von Stickstoffatomen (N) in organischen Systemen und die des Sauerstoffatoms (O) im Wassermolekül wird dabei durch Übergänge zwischen stark lokalisierten 1s- und Valenzorbitalen mit 2p-Charakter detektiert. Die verwendeten Spektroskopiemethoden Röntgenabsorption (engl. X-ray absorption spectroscopy, XAS) und resonate inelastische Röntgenstreuung (engl. resonant inelastic X-ray scattering, RIXS) bieten dabei einen lokalen Zugang zur unbesetzten bzw. im Fall von RIXS auch zur besetzten elektronischen Struktur der untersuchten Moleküle.

Mit Hilfe der genannten Methoden haben wir in zeitaufgelösten Anrege-Abfrage (engl. pump-probe) Experimenten durch Valenzanregungen induzierte Protonentransfer-Prozesse (engl. excited state proton transfer, ESPT) des Moleküls 2-Thiopyridon in wässriger Lösung untersucht. Eine Verschiebung der N K-Kanten Röntgenabsorpti-

onsresonanzen, sowie eine charakteristische Röntgenemissionslinie werden von uns als spektrale Signaturen einer N Deprotonierung des Systems etabliert. Eine potenzielle photo-induzierte N Deprotonierung des Moleküls wird anhand dieser Signaturen auf femtosekunden Zeitskalen über zeitaufgelöste N K-Kanten RIXS Messungen identifiziert. Protonentransfer-Mechanismen auf Pico- und Nanosekunden Zeitskalen entlang der dominanten Relaxationspfade des Systems werden mit zeitaufgelöstem N K-Kanten XAS untersucht.

K-Kanten Rumpfanregungen eignen sich nicht nur ideal zur Detektion von Protonendynamik in valenzangeregten Zuständen, da die Rumpfanregungen selbst auch eine lokalisierte Störung der elektronischen Struktur darstellen. Vor allem die Reaktion von Protonen auf diese Störung innerhalb der 1s Rumpfloch-Lebensdauer von wenigen Femtosekunden kann zu einer gerichteten Verzerrung der Molekülstruktur führen. Die damit verbundenen Änderungen von Übergangsenergien und -wahrscheinlichkeiten sind als Signaturen dieser gerichteten Protonendynamik in RIXS Spektren zugänglich.

Anhand von RIXS Übergängen in elektronisch angeregte Zustände untersuchen wir Protonendynamik, die durch N K-Kanten Anregungen an den N Atomen im Imidazolring der Aminosäure Histidin induziert wird. Die schwache Dynamik in basischen und neutralen wässrigen Lösungen erlauben es uns, die Protonierung dieser N Atome mit charakteristischen spektralen Signaturen zu korrelieren. Mit Hilfe dieser Signaturen identifizieren wir eine durch K-Kanten Anregung verursachte N-H Dissoziation in saurer Lösung. Dieser Prozess ist unabhängig davon, an welchem der N Atome des Imidazolrings die Rumpfanregung lokalisiert ist.

Solche, durch Rumpfanregungen verursachten, gerichteten Verzerrungen der Molekülstruktur ermöglichen einen Zugang zu Protonendynamik im elektronischen Grundzustand über RIXS Prozesse in dessen vibrationsangeregte Zustände. In diesem Zusammenhang vergleichen wir hochaufgelöste O K-Kanten RIXS Spektren des Wassermoleküls in der Gasphase mit quantenchemischen Simulationen zur Wellenpaketpropagation in den rumpfangeregten Zuständen. Dabei wird deutlich, dass die gerichtete Verzerrung der Molekülstruktur im rumpfangeregten Zustand eine Bevölkerung von Vibrationsmoden des Grundzustandes mit der gleichen Ausrichtung durch den RIXS Prozess verursacht. Anhand dieser Ergebnisse leiten wir ab, unter welchen Bedingungen eine Extraktion eindimensionaler Querschnitte der Potentialfläche des Grundzustandes aus den entsprechenden RIXS Spektren möglich ist. Wir verifizieren diese Methode anhand der Extraktion der Grundzustandspotentialfläche des Wassermoleküls entlang drei unterschiedlicher Richtungen im Vergleich zu den quantenchemischen Rechnungen.

Diese Arbeit enthält zudem Beiträge zur Entwicklung von Instrumentierung für Untersuchungen valenzangeregter Moleküldynamik an Röntgenquellen mit hoher Brillianz. Der experimentelle Aufbau, der für die zeitaufgelösten XAS Messungen an 2-Thiopyridon verwendet wurde, wird vorgestellt. Ein sub-Mikrometer dünner Flüssigkeitsflachstrahl erlaubt dabei Messungen in einer Transmissionsgeometrie. In Kombination mit einem MHz-Lasersystem können transiente Absorptionsänderungen effizient detektiert werden. Zudem präsentieren wir Konzepte zur zeitlichen Korrelati-

on von Röntgen- und optischen Lichtpulsen, basierend auf Änderungen der optischen Eigenschaften von Dünnschichtsystemen, die essenziell für Studien transienter Prozesse an Synchrotrons und Freie-Elektronen Lasern mit Femtosekunden Zeitauflösung sind.

Preface

This thesis summarizes the research I performed under supervision of Prof. Dr. Alexander Föhlisch at the University of Potsdam and at the Institute for Methods and Instrumentation for Synchrotron Radiation of the Helmholtz-Zentrum Berlin.

It is prepared in a cumulative fashion and composed of eight selected publications which I (co-)authored in the past years. Seven of them are published in peer-reviewed journals and one is in manuscript. My affiliation changed from Helmholtz-Zentrum Berlin to University of Potsdam while the research for this thesis was performed. Hence, either one or both affiliations are attributed to me in the publications, depending on the time at which the individual projects were carried out.

The presented work is grouped into three contentual parts. First, we present a study of optically induced dynamics in a dilute molecular system investigated with N 1s X-ray absorption spectroscopy (XAS) and resonant inelastic X-ray scattering (RIXS). The X-ray spectroscopic signatures correlated with structural changes of the system as well as the population of transient excited states through optical excitation are addressed in the publications I–III. The second group of publications IV, V and VI utilize the duration of resonant inelastic X-ray scattering events to extract properties of ground and core-excited state potentials of molecular systems from RIXS spectra. Publications VII and VIII represent parts of the development of methods and instrumentation for X-ray/optical pump-probe measurements I contributed to. Background information and motivation for each of these groups is provided in the chapters 1–4 of this thesis. The Appendix contains information on occasions at which the results were presented and Supporting Information to individual publications included in this thesis.

The majority of this research was carried out at the synchrotron light source BESSY II in Berlin, Germany. Optically induced molecular dynamics in publication II were investigated with RIXS using the soft X-ray beamline at the Linac Coherent Light Source (LCLS) in Stanford, USA. The results on femtosecond core-excited state dynamics from electronically elastic high resolution RIXS in publications V and VI were achieved using the SAXES spectrometer at the ADRESS beamline of the Swiss Light Source (SLS) in Villigen, Switzerland.

List of Publications

Eight publications forming the **core of my thesis** are listed here. Different authors were involved in the various stages of the presented studies, as all of them are results of collaborative efforts. Here, I only mention activities in which I added a major contribution.

I **Molecular structures and protonation state of 2-Mercaptopyridine in aqueous solution**
S. Eckert, P. S. Miedema, W. Quevedo, B. O'Cinneide, M. Fondell, M. Beye, A. Pietzsch, M. Ross, M. Khalil, and A. Föhlisch
Chemical Physics Letters ***647****, 103-106 (2016)*

I planned the experiment, acquired, analyzed and interpreted the data and wrote the manuscript.

II **Ultrafast Independent N-H and N-C Bond Deformation Investigated with Resonant Inelastic X-Ray Scattering**
S. Eckert, J. Norell, P. S. Miedema, M. Beye, M. Fondell, W. Quevedo, B. Kennedy, M. Hantschmann, A. Pietzsch, B. van Kuiken, M. Ross, M. P. Minitti, S. P. Moeller, W. F. Schlotter, M. Khalil, M. Odelius, and A. Föhlisch
Angewandte Chemie International Edition ***56****, 6088-6092 (2017)*
Angewandte Chemie ***129****, 6184–6188 (2017)*

I planned the experiments, acquired, analyzed and interpreted the data and wrote the manuscript.

III **T_1 Population as the Driver of Excited-State Proton Transfer in 2-Thiopyridone**
S. Eckert, J. Norell, R. M. Jay, M. Fondell, R. Mitzner, M. Odelius, and A. Föhlisch
Submitted to Chemistry – A European Journal (under review) *

*This manuscript was published in a revised form in *Chemistry – A European Journal* ***25****, 1733–1739 (2019)* between the submission and the defense of this thesis.

I planned the experiment, acquired, analyzed and interpreted the data and wrote the manuscript.

IV **Valence orbitals and local bond dynamics around N atoms of histidine under X-ray irradiation**
S. Eckert, J. Niskanen, R. M. Jay, P. S. Miedema, M. Fondell, B. Kennedy, W. Quevedo, M. Iannuzzi, and A. Föhlisch
Physical Chemistry Chemical Physics ***19****, 32091–32098 (2017)*

I planned the experiment, acquired, analyzed and interpreted the data and wrote the manuscript.

V **Selective gating to vibrational modes through resonant X-ray scattering**
R. C. Couto, V. Vaz da Cruz, E. Ertan, S. Eckert, M. Fondell, M. Dantz, B. Kennedy, T. Schmitt, A. Pietzsch, F. F. Guimarães, H. Ågren, F. Gel'mukhanov, M. Odelius, V. Kimberg, and A. Föhlisch
Nature Communications ***8****, 14165 (2017)*

I commissioned the used heatable cell, acquired and analyzed the presented experimental data and commented on the manuscript.

VI **One-dimensional cuts through multidimensional potential energy surfaces by tunable x rays**
S. Eckert, V. Vaz da Cruz, F. Gel'mukhanov, E. Ertan, N. Ignatova, S. Polyutov, R. C. Couto, M. Fondell, M. Dantz, B. Kennedy, T. Schmitt, A. Pietzsch, M. Odelius, and A. Föhlisch
Physical Review A ***97****, 053410 (2018)*

I commissioned the used heatable cell, acquired and analyzed the presented experimental data and performed the potential extraction together with V. Vaz da Cruz (KTH, Stockholm). I took part in writing the manuscript.

VII **Time-Resolved Soft X-ray Absorption Spectroscopy in Transmission Mode on Liquids at MHz Repetition Rates**
M. Fondell, S. Eckert, R. M. Jay, C. Weniger, W. Quevedo, J. Niskanen, B. Kennedy, F. Sorgenfrei, D. Schick, E. Giangrisostomi, R. Ovsyannikov, K. Adamczyk, N. Huse, Ph. Wernet, R. Mitzner, and A. Föhlisch
Structural Dynamics ***4*** *054902 (2017)*

I commissioned the end-station, performed the measurements, participated in data analysis and wrote the manuscript in close collaboration with M. Fondell, R. Jay and R. Mitzner.

VIII **Versatile soft X-ray-optical cross-correlator for ultrafast applications**
D. Schick, S. Eckert, N. Pontius, R. Mitzner, A. Föhlisch, K. Holldack, and F. Sorgenfrei
*Structural Dynamics **3**, 054304 (2016)*

I implemented the pump-probe setup for the all optical measurements in the laser laboratory of the FG-ISRR at the Helmholtz-Zentrum Berlin. I performed the all optical measurements and commented on the manuscript.

I list additional publications of which some are closely **related** to the research topics discussed above and are co-authored by me but left out from this thesis. The related core manuscripts of this thesis are assigned.

A **A study of the water molecule using frequency control over nuclear dynamics in resonant X-ray scattering**
V. Vaz da Cruz, E. Ertan, R. C. Couto, S. Eckert, M. Fondell, Marcus Dantz, B. Kennedy, T. Schmitt, A. Pietzsch, F. F. Guimarães, H. Ågren, F. Gel'mukhanov, M. Odelius, and A. Föhlisch, and V. Kimberg
*Physical Chemistry Chemical Physics **19**, 19573–19589 (2017)*

I commissioned the used heatable cell, acquired and analyzed the presented experimental data and proofread the manuscript, which is closely related to publications V and VI.

B **Ultrafast dissociation features in RIXS spectra of the water molecule**
E. Ertan, V. Savchenko, N. Ignatova, V. Vaz da Cruz, R. C. Couto, S. Eckert, M. Fondell, M. Dantz, B. Kennedy, T. Schmitt, A. Pietzsch, A. Föhlisch, F. Gelmukhanov, M. Odelius, and V. Kimberg
*Physical Chemistry Chemical Physics **20**, 14384-14397 (2018)*

I commissioned the used heatable cell, acquired and analyzed the presented experimental data, contributed to figure production and commented on the manuscript, which is closely related to publications V and VI.

C **A Setup for Resonant Inelastic Soft X-Ray Scattering on Liquids at Free Electron Laser Light Sources**
K. Kunnus, I. Rajkovic, S. Schreck, W. Quevedo, S. Eckert, M. Beye, E. Suljoti, C. Weniger, C. Kalus, S. Grübel, M. Scholz, D. Nordlund, W. Zhang, R. W. Hartsock, K. J. Gaffney, W. F. Schlotter, J. J. Turner, B. Kennedy, F. Hennies, S. Techert, Ph. Wernet, and A. Föhlisch
*Review of Scientific Instruments **83**, 123109 (2012)*

The setup in which the experimental data for publications I, II, IV and VII was acquired is presented. I characterized the performance of the RIXS spectrometer

in combination with an in-vacuum liquid jet as the source of X-ray fluorescence. I acquired and analyzed parts of the presented data and commented on the manuscript.

D **Principles of femtosecond X-ray/optical cross-correlation with X-ray induced transient optical reflectivity in solids**
S. Eckert, M. Beye, A. Pietzsch, W. Quevedo, M. Hantschmann, M. Ochmann, M. Ross, M. P. Minitti, J. J. Turner , S. P. Moeller, W. F. Schlotter, G. L. Dakovski, M. Khalil, N. Huse, and A. Föhlisch
Applied Physics Letters ***106****, 061104 (2015)*

The presented concepts and results can be applied to optimize temporal cross-correlation measurements at free-electron lasers, as it was done for the measurements presented in publication II. I acquired and analyzed the data and wrote the manuscript.

Furthermore, I list the following publications I coauthored, but which **deviate thematically** from the central scope of this thesis.

E **Reabsorption of Soft X-Ray Emission at High X-Ray Free-Electron Laser Fluences**
S. Schreck, M. Beye, J. A. Sellberg, T. McQueen, H. Laksmono, B. Kennedy, S. Eckert, D. Schlesinger, D. Nordlund, H. Ogasawara, R. G. Sierra, V. H. Segtnan, K. Kubicek, W. F. Schlotter, G. L. Dakovski, S. P. Moeller, U. Bergmann, S. Techert, L. G. M. Pettersson, Ph. Wernet, M. J. Bogan, Y. Harada, A. Nilsson, and A. Föhlisch
Physical Review Letters ***113****, 153002 (2014)*

F **X-ray emission spectroscopy of bulk liquid water in "no-man's land"**
J. A. Sellberg, T. A. McQueen, H. Laksmono, S. Schreck, M. Beye, D. P. DePonte, B. Kennedy, D. Nordlund, R. G. Sierra, D. Schlesinger, T. Tokushima, I. Zhovtobriukh, S. Eckert, V. H. Segtnan, H. Ogasawara, K. Kubicek, S. Techert, U. Bergmann, G. L. Dakovski, W. F. Schlotter, Y. Harada, M. J. Bogan, Ph. Wernet, A. Föhlisch, L. G. M. Pettersson, and A. Nilsson
The Journal of Chemical Physics ***142****, 044505 (2015)*

G **Fingerprints of electronic, spin and structural dynamics from resonant inelastic soft X-ray scattering in transient photo-chemical species**
J. Norell, R. M. Jay, M. Hantschmann, S. Eckert, M. Guo, K. J. Gaffney, Ph. Wernet, M. Lundberg, A. Föhlisch, and M. Odelius
Physical Chemistry Chemical Physics ***20****, 7243–7253 (2018)*

H **Disentangling Transient Charge Density and Metal- Ligand Covalency in Photo-Excited Ferricyanide with Femtosecond Resonant Inelastic Soft X-ray Scattering**
R. M. Jay, J. Norell, S. Eckert, M. Hantschmann, M. Beye, B. Kennedy, W. Quevedo, W. F. Schlotter, G. L. Dakovski, M. P. Minitti, M. C. Hoffmann, A. Mitra, S. P. Moeller, D. Nordlund, W. Zhang, H. W. Liang, K. Kunnus, K. Kubicek, S. A. Techert, M. Lundberg, Ph. Wernet, K. J. Gaffney, M. Odelius, and A. Föhlisch
The Journal of Physical Chemistry Letters ***9****, 3538–3543 (2018)*

I **The nature of frontier orbitals under systematic ligand exchange in (pseudo-)octahedral Fe(II) complexes**
R. M. Jay, S. Eckert, M. Fondell, P. S. Miedema, J. Norell, A. Pietzsch, W. Quevedo, J. Niskanen, K. Kunnus, and A. Föhlisch
Physical Chemistry Chemical Physics (2018)

List of Abbreviations

2-TP	2-thiopyridone
BESSY	Berliner Elektronenspeicherring(-Gesellschaft) für Synchrotronstrahlung
CAS	complete active space
CCD	charge coupled device
DFT	density functional theory
ESPT	excited state proton transfer
FEL	free-electron laser
FG–ISRR	Forschungsbereich Großgeräte–Institut für Methoden und Instrumentierung der Forschung mit Synchrotronstrahlung
HF	Hartree Fock
HZB	Helmholtz-Zentrum Berlin
IC	internal conversion
ISC	intersystem crossing
LCLS	Linac Coherent Light Source
MCP	multi-channel plate
NEXAFS	near-edge X-ray absorption fine structure
PES	potential energy surface
RAS	restricted active space
RIXS	resonant inelastic X-ray scattering

SLS	Swiss Light Source
XAS	X-ray absorption spectroscopy
XES	X-ray emission spectroscopy

Contents

Chapter 1

Introduction

Photochemical processes have an ubiquitous impact on life, ranging from the essential constructive role of transition metal complexes in e.g. photosynthesis and artificial light-harvesting applications[1–4] to harmful effects induced by e.g. exposure of human tissue to ionizing radiation[5,6] or intense sunlight[7–10]. They result from a photo-induced population of thermally inaccessible electronic states. The photochemical processes are triggered by the thereby altered chemical properties of the system and subsequent, excited state dependent, deformations of the molecular geometry. This work focuses on the role of protons in molecular photo-chemical processes. Their low mass results in high mobility and yields the ability to form fluctuating bonding networks in condensed-phase systems. Thus, protons adapt rapidly to transient changes of the coupled molecular electronic and nuclear structure.[11–13] This allows for protonation changes at specific atomic sites along photochemical relaxation pathways, sometimes mediated by interactions with the surrounding solvent molecules.[13–15] It is therefore essential to establish reliable experimental signatures of protonation changes as fingerprints of proton dynamics in photochemical processes.

Spectroscopy techniques utilize cross-sections of photo-induced transitions between eigenstates of molecules, to provide experimental evidence for the presence of specific chemical states and to determine electronic properties of the investigated systems. As Zewail discussed in his Nobel-lecture on *Femtochemistry*,[16] pump-probe spectroscopy techniques in different spectral ranges of electromagnetic radiation are established tools to investigate different aspects of transient molecular dynamics. They yield information on the transient processes, subsequent to photo-excitations, based on reliable spectroscopic fingerprints. To monitor the protonation at specific atomic sites, an element-specific and chemical state selective spectroscopic technique accessing the local molecular electronic structure is required. Upon restriction to protonation and proton dynamics at nitrogen (N) and oxygen (O) sites, the used spectroscopy technique needs to probe bond-mediating p-derived molecular orbitals sensitively.

These demands are fulfilled by K-edge soft X-ray spectroscopy,[17] giving access to the p-character and the localization of valence orbitals through electronic transitions changing the occupation of localized 1s orbitals. Combining optical and X-ray light

sources therefore enables to locally monitor photo-induced protonation changes along relaxation pathways via valence-excited states. Different X-ray light sources qualify for such time-resolved studies of molecular dynamics, depending on the used X-ray spectroscopy technique and the investigated timescale. Third generation synchrotrons can be used routinely for time-resolved soft X-ray absorption studies, probing transient local unoccupied valence density of states, with picosecond temporal resolution.[18–24] At femtoslicing facilities a hundred femtosecond temporal resolution can be achieved at a largely reduced photon flux.[24,25] Recent developments of dedicated, optical-laser driven, high harmonic generation sources show potential for X-ray absorption studies on femtosecond timescales.[26–31] Resonant inelastic X-ray scattering (RIXS) gives additional access to the occupied local valence density of states of a system. This is achieved by the detection of photon energies for radiative decay processes into valence-excited states subsequent to core-excitations. The yield of such processes is in the percentage range for soft-X-ray photon energies and they can only be detected with a limited efficiency. Pump-probe femtosecond molecular dynamics studies employing RIXS can therefore currently only be performed at free-electron laser light sources.[32–35]

The discussed techniques are used in the first three publications of this thesis to study the valence-excited state proton transfer process in 2-thiopyridone. A photo-induced proton transfer capability between the N and the S site of the system was assigned previously by Du et al..[36] They identified the thiol tautomer 2-mercaptopyridine to be present on nanosecond timescales after an optical excitation based on resonance Raman spectroscopic signatures, without determining a distinct proton transfer pathway. Picosecond S K-edge spectroscopy indicates that the proton transfer dynamics possibly depend on the used solvent and excitation wavelength.[37] Here, we resolve relaxation mechanisms yielding excited state proton transfer in 2-thiopyridone using transient N K-edge X-ray absorption spectroscopy as well as resonant inelastic X-ray scattering. In **publication I**, we establish X-ray absorption spectroscopic signatures for N deprotonation of 2-thiopyridone. In a second step, we identify transient spectroscopic signatures in optical pump N 1s RIXS probe measurements of 2-thiopyridone (aq) on femtosecond timescales, which coincide with signatures of chemically induced N deprotonation, as shown in **publication II**. Conclusively, we investigate the proton transfer dynamics of 2-thiopyridone in a range of tens of picoseconds to tens of nanoseconds after the optical excitation using transient X-ray absorption spectroscopy in dependence on the excitation wavelength in **publication III**.

Highly directional molecular proton dynamics occur as an initial response to photo-excitations using X-ray radiation. A K-edge excitation dominantly affects the local electronic structure at the core-excited atom. Insight on the structural deformations within the lifetime of a core-excitation can be gained from RIXS spectral signatures. The propagation of core-excited state nuclear wave packets, representing the nuclear displacement induced by the change in orbital occupancy, alters the probability to populate specific vibrational modes on the electronic ground or valence-excited

potentials as RIXS final states.[38–47] Hence, information on both, the core-excited and the final state potentials, can be drawn from RIXS intensities. The impact of different parts of the core-excited state nuclear wave packet on the RIXS intensity can be altered by choice of the excitation energy. This yields the possibility to change the effective scattering duration and thus access the femtosecond core-excited state proton dynamics with synchrotron radiation without a dedicated pulse pattern.[38,47,48]

Based on spectral signatures of RIXS final states characterized by electronic excitations, we investigate the N 1s core-excited state dynamics of the amino-acid histidine dependent on the chemical environment in **publication IV**. It is known that the system exhibits pH-value-dependent protonation states at its three N sites in aqueous environments.[49] One of the N sites forms an amino group, whereas the other two are located within a conjugated imidazole ring. For the latter, we establish characteristic N K-edge X-ray absorption, as well as RIXS signatures of different protonation states. These allow us to unravel the propensity for deprotonation of one specific N site in the imidazole ring in the N 1s core-excited states of histidine in an acidic environment, through a comparison between experimental RIXS spectra and simulations based on the Z+1 equivalent core approximation.

In contrast, RIXS final states characterized exclusively by vibrational excitations are used to access directional proton dynamics in the molecular electronic ground state in publications V and VI. We show in **publication V** that the preparation of well-oriented wave packets in the O 1s core-excited states of the gas-phase water molecule yields a selective excitation of vibrational modes, with the same directionality, upon radiative decay to the electronic ground state. We combine vibrationally resolved O K-edge RIXS spectra with quantum chemical wave packet propagation and spectrum simulations. Thereby we demonstrate that properties of the ground state potential, defining interactions with the chemical environment and thus chemical reaction pathways, could be probed selectively for molecules in solution. In particular, we derive the possibility to extract directional cuts through molecular potential energy surfaces from vibrationally resolved RIXS spectra analytically in **publication VI**. The proposed method is used to extract cuts through the ground state potential of the gas phase water molecule, defining the dynamics of the protons with respect to the oxygen atom, in three distinct directions from O 1s RIXS spectra with vibrational resolution.

The development of concepts and instrumentation for the investigation of optically induced dynamics with X-ray spectroscopic methods are discussed in publications VII and VIII of the thesis. Specifically, the demands of time-resolved soft X-ray studies for in-vacuum sample environments providing sufficient sample replenishment and efficient measurement schemes to compensate for the limited available X-ray photon flux are addressed.

A rapidly replenishing sample environment suitable for soft X-ray absorption measurements in a transmission experimental geometry has recently proven to be provided by sub-μm thin liquid flat-jets.[50] The combination of a flat-jet with a MHz optical-laser system at the beamline UE52-SGM (BESSY II) for low-noise optical

pump X-ray absorption probe spectroscopy of dilute molecular systems is presented in **publication VII**.

Considering beamtime limitations in addition to long necessary data acquisition times, temporal cross-correlation of X-ray and optical pulses prior to the actual measurement is essential for pump-probe studies with femtosecond temporal resolution. We have established concepts to optimize the contrast for temporal cross-correlation at free electron lasers based on X-ray-induced transient optical reflectivity changes exploiting thin film interference effects.[51] However, this method is inapplicable at light sources providing a low X-ray flux per pulse, as it requires a high X-ray-induced excitation density in an insulating thin film material. We have therefore developed an alternative cross-correlator based on optically induced X-ray reflectivity changes of a metal-insulator multilayer sample, which is presented in **publication VIII**. This efficient cross-correlation method, utilizing again transiently altered interference, can be used at low-flux X-ray sources. It is therefore essential for future transient X-ray absorption studies with femtosecond temporal resolution at synchrotron femtoslicing facilities and optical laser driven X-ray sources.

Chapter 2

Molecular Proton Dynamics: Concepts and Experimental Access

The methods to access molecular proton dynamics applied throughout the publications will be introduced in this section. A theoretical framework for the description of coupled electronic and nuclear dynamics on ground and excited state potential energy surfaces will be given. Based on these concepts, the fundamentals of X-ray absorption spectroscopy and RIXS as tools to access them will further be derived. Considering these concepts is essential to establish possible molecular relaxation pathways and identify configurations along them which can yield transiently altered protonation. Additionally, they illustrate the suitability of K-edge spectroscopy, with its sensitivity for p-derived valence density of states, to probe bonds in molecules consisting of light elements. The combination of these concepts is crucial to predict and interpret X-ray spectroscopic signatures of protonation changes through selection rules and quantum chemical spectrum simulations.

The following descriptions of concepts used to access excited state dynamics are based on the derivations by Lee and Heller[52], if not declared differently. The nomenclature was adapted for compatibility with the reasoning in this thesis. The quantum mechanical state of a system is defined by its Hamiltonian $\hat{H}$ and a wavefunction Ψ as a solution of the time-dependent many body Schrödinger equation. We consider the Hamiltonian of a molecular system consisting of s electrons and N nuclei with $\underline{r} = (\underline{r}_1, ..., \underline{r}_s)$ electronic and $\underline{R} = (R_1, .., R_{3N})^*$ nuclear degrees of freedom experiencing a time-dependent perturbation $\hat{\mathcal{H}}^{int}(\underline{r}, \underline{R}, t)$.

*Here we do not reduce the nuclear degrees of freedom to $3N - 6$ internal coordinates through a coordinate transformation, e.g. use of the center of mass and relative coordinates. This can generally yield mass polarization terms for the case of coupled nuclear motion, which are omitted in the formulation of Lee and Heller.[52]

$$i\hbar\partial_t\Psi(\underline{r},\underline{R},t) = \hat{H}\Psi(\underline{r},\underline{R},t) = [\hat{H}_m + \hat{\mathcal{H}}^{int}(\underline{r},\underline{R},t)]\Psi(\underline{r},\underline{R},t), \tag{2.1}$$

$$\hat{H}_m = -\sum_{n=1}^{3N}\frac{\hbar^2\partial^2_{R_n}}{2M_n} - \sum_{i=1}^{s}\frac{\hbar^2\Delta_i}{2m} + U(\underline{r},\underline{R})$$

M_n and m are the masses of the nuclei and electrons, $U(\underline{r},\underline{R})$ is the electrostatic potential between the electrons and nuclei and $\hbar$ is the reduced Planck constant. It is unfeasible to find an analytical solution for Ψ in this physical many body problem as soon as the complexity of the studied system exceeds that of the hydrogen atom. Among others, the Born Oppenheimer approximation[53] is well established to find an approximate solution also for more complex systems and understand or predict their quantum-mechanical properties. Mathematically the Born-Oppenheimer approximation results from a Produktansatz for Ψ which separates a nuclear $\chi_j(\underline{R},t)$ and an electronic part $\psi_j(\underline{r},\underline{R})$ of the wavefunction.

$$\Psi(\underline{r},\underline{R},t) = \sum_{j=1}^{\infty}\chi_j(\underline{R},t)\psi_j(\underline{r},\underline{R}) \tag{2.2}$$

This Ansatz decouples the explicit time dependence from the electronic coordinates. Hence, a time-dependent perturbation $\hat{\mathcal{H}}^{int}(\underline{r},\underline{R},t)$ can only alter the population of the electronic states $\psi_j(\underline{r},\underline{R})$ through the time-dependent coefficients $\chi_j(\underline{R},t)$. Inserting Ansatz 2.2 in the Schrödinger equation 2.1 generates coupling terms between χ_j and ψ_j of the form $\frac{\hbar^2}{M_n}\partial_{R_n}\chi_j(\underline{R},t)\partial_{R_n}\psi_j(\underline{r},\underline{R})$ and $\frac{\hbar^2}{2M_n}\chi_j(\underline{R},t)\partial^2_{R_n}\psi_j(\underline{r},\underline{R})$. The coupling terms are proportional to the inverse mass of the nuclei M_n^{-1} are thus expected to be small compared to the electron kinetic energy contribution to the Schrödinger equation.[54†] Omitting these coupling terms allows for a separate treatment of the electronic part of the wavefunction $\psi_j(\underline{r},\underline{R})$ which is parametric in $\underline{R}$.

[†] We follow the argumentation by Steinfeld.[54, p. 78] We assume that the derivatives of the electronic wavefunctions with respect to the nuclear coordinates $\partial_{R_n}\psi_j$ and the l-th component of the k-th electron $\partial_{r_{kl}}\psi_j$ are of similar scale, as we consider the same molecular dimensions for both operators. The contribution of a typical coupling term (see main text) can then be estimated as

$$\frac{\hbar^2}{2M_n}\chi_j(\underline{R},t)\partial^2_{R_n}\psi_j(\underline{r},\underline{R}) \approx \frac{\hbar^2}{2M_n}\chi_j(\underline{R},t)\partial^2_{r_{kl}}\psi_j = \frac{m}{M_n}\chi_j(\underline{R},t)\frac{\hbar^2\partial^2_{r_{kl}}\psi_j}{2m}.$$

The last factor resembles a contribution in the electron kinetic energy (see second last term of $\hat{H}_m$ in equation 2.1). The scaling factor $m/M_m \sim 1/10000$ justifies an omission of this coupling term. The Born-Oppenheimer approximation fails to describe molecular systems in geometries exhibiting close lying electronic states. There, the electronic wavefunction is formed as a linear combination of the wavefunctions for the different states. The contribution of each state to the total electronic wavefunction is altered by changes of the nuclear coordinates. The character of the electronic wavefunction therefore depends sensitively on R_n. Consequently, the derivatives along nuclear and electronic coordinates can no longer be expected to be of similar magnitude in these configurations.

$$\left[-\sum_{i=1}^{s}\frac{\hbar^2\Delta_i}{2m}+U(\underline{r},\underline{R})\right]\psi_j(\underline{r},\underline{R})=E_j(\underline{R})\psi_j(\underline{r},\underline{R}) \tag{2.3}$$

It also yields coupled differential equations for the time-dependent coefficients $\chi_j(\underline{R},t)$

$$i\hbar\partial_t\chi_j(\underline{R},t)=H_j(\underline{R})\chi_j(\underline{R},t)-\sum_{k=1}^{\infty}\left[\hat{\mathcal{H}}^{int}_{jk}(\underline{R},t)\right]\chi_k(\underline{R},t) \tag{2.4}$$

$$H_j(\underline{R})=-\sum_{n=1}^{3N}\frac{\hbar^2\partial^2_{R_n}}{2M_n}+E_j(\underline{R}),$$

with $\hat{\mathcal{H}}^{int}_{jk}(\underline{R},t)=\langle\psi_j(\underline{r},\underline{R})|\hat{\mathcal{H}}^{int}(\underline{r},\underline{R},t)|\psi_k(\underline{r},\underline{R})\rangle_{\underline{r}}$. For unperturbed systems with $\hat{\mathcal{H}}^{int}(\underline{r},\underline{R},t)=0$ equation 2.4 yields the vibrational states for the potential $E_j(\underline{R})$ defined by equation 2.3. The dynamics of a system are thus defined by the (molecular geometry dependent) energy eigenvalue of the electronic part of the wavefunction forming a Potential Energy Surface (PES).

2.1 Electronic Structure from Quantum Chemistry

PESs of molecular systems at specific atomic configurations, with their possible connections across potential energy barriers are the basis of the theoretical description of chemical reactivity. They can be utilized to determine the origins for preferences of specific molecular geometries in chemical environments and yield the option to understand and quantify thermally driven and photochemical processes. It is therefore essential to approximate the solution of Schrödinger's equation for the molecular geometry dependent electronic part of the wavefunction. This can be achieved numerically using different approaches. Which quantum chemical method is most suitable to simulate the electronic structure for molecular systems strongly depends on the size and elemental composition of the investigated system and its interaction with its chemical environment. Here, the general concepts of Hartree-Fock (HF) in combination with selected post-HF methods and density functional theory are outlined based on the description by Atkins.[55, p. 288–320]

The HF method approximates a solution for the electronic part of the wavefunction from equation 2.3. One Slater determinant of s single electron wavefunctions is used as an Ansatz for ψ_j for a given set of nuclear coordinates. The wavefunctions in this determinant are adapted to minimize the associated energy expectation value. Electron correlation effects are treated in a mean field approach by this approximation of the electronic wavefunction. The HF equations (or Roothaan equations, if the orbitals are expanded in a specific basis set) yield the orthogonal occupied and the virtual (unoccupied) HF orbitals, which are used to generate a single determinant of occupied single electron wavefunctions to describe the entire electronic system.

The resulting neglect of electron correlation effects can be compensated for in a post-HF method called configuration interaction (CI), which will be introduced briefly. Including determinants in which occupied orbitals are replaced by virtual ones resulting from the HF calculation in a linear combination with the HF-ground state wavefunction and optimizing their expansion coefficients can yield a wavefunction with a lower energy expectation value. Determinants including virtual instead of occupied states are termed to contain an excitation between the exchanged orbitals. Including determinants containing excitations can yield a better approximation of the total electronic wavefunction. In principle, all orthogonal occupied and virtual orbitals resulting from an HF calculation can be used to form a complete basis of determinants for the description of any antisymmetric s-electron wavefunction. Hence, excited states of the studied system can also be simulated with the CI method. The number of determinants defines the accuracy of the approximated wavefunction, but it also increases the computational weight of the simulation. Different approaches that restrict the number of orbitals between which the excitations can occur and/or the excitations between them. The complete- and restricted-active-space methods (CAS,RAS) are used to reduce the computational weight compared to a full-CI calculation of a given system. These restrictions can also be used to simulate selected excited states characterized by excitations from specific orbitals, which is of high interest for the simulation of X-ray spectra.[56]

Computationally much lighter quantum chemical density functional theory (DFT) simulations make use of Hohenberg-Kohns' theorems, which show that in an s-electron system, in the non-degenerate electronic ground state, the potential and thus the wavefunction are defined as a unique functional of the electron density. Generating the electron density from a Slater determinant of s single electron wavefunctions yields the Kohn-Sham (KS) equations, which are analogous to Schrödinger's equation for single electrons in the KS potential. The KS potential is defined as the sum of the external potential defined by the nuclei, the Hartree Potential as the Coulomb repulsion induced by the presence of electron density and the exchange correlation interaction potential, which depends on the unknown exchange-correlation functional. Different exchange correlation functional approximation dependent on the electron density and its derivatives are available for the use in quantum chemistry codes. Self consistent solutions of the KS equations yield again occupied and virtual KS orbitals. Additionally, time-dependent (TD) DFT can be used to estimate the interaction between electromagnetic fields and the investigated molecule. The interaction with the field is implemented through TD potentials, which yields TD Kohn-Sham equations. They can be treated perturbatively. This approach can be used to estimate transition dipole moments between the ground and excited states of the system. Alternatively, spectrum simulations in the slater transition state model are possible.[57–59]

The post-HF methods, which increase the accuracy of simulations but also their computational weight, impose size and/or symmetry restrictions for HF based electronic structure simulations of ground and excited states. Hence, only small systems with very limited inclusion of interaction with a chemical environment can

be modeled. We chose such methods to reliably simulate both ground and excited state electronic structure and X-ray spectra in publications II, III and V for the compound 2-thiopyridone and the gas phase water molecule.

The computationally lighter DFT can explicitly model solute-solvent interaction even for larger systems combined with the ability to estimate spectroscopic observables for systems in their electronic ground state.[60–62] In the publications I and IV we utilize DFT to access the electronic structure of 2-thiopyridone (and connected molecular species) and the amino acid histidine, partially with an explicit treatment of the chemical environment, in multiple molecular geometries and solute-solvent configurations.

2.2 Dynamics on Potential Energy Surfaces

Mapping out possible trajectories of a sample on electronic ground and excited state PES under specific experimental conditions is a key step to estimate the localization of protons in transient states of the system. A possible trajectory across a system of PES, which is discussed conceptually in this section, is depicted in Fig. 2.1, before the theoretical description of transitions between PESs and the propagation on them are introduced in section 2.2.

The coordinate the PESs are projected on can resemble e.g. an inter-atomic distance in a diatomic gas-phase molecule or a complex reaction pathway through a multidimensional potential energy landscape in larger systems. In the second case, the simple one-dimensional sketch drawn here has to be extended to allow for deformations of the molecule and its chemical environment along all possible nuclear coordinates. Still, the simplified picture illustrates the concept of dynamics on valence-excited state potential energy landscapes and its most important steps.

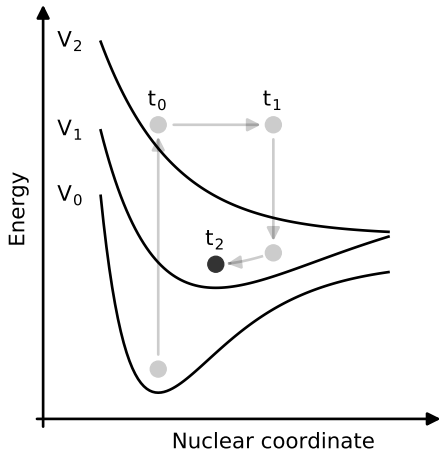

Figure 2.1: *Dynamics on valence-excited state potential energy surfaces.* An excitation from the ground (V_0) into a valence-excited state (V_2) at the time t_0 is followed by a structural relaxation according to the excited state potential. Different decay channels yield a statistical depopulation with a time constant $\tau = t_1 - t_0$ into lower lying valence-excited states (V_1) or back into the V_0 resulting in further subsequent adaptations of the molecular geometry including possible energy dissipation to the chemical environment.

The rigidity of a sample in its stable ground state is overcome by the introduction of energy into the system, which transfers it onto an energetically higher lying PES. We start out from an excitation of the investigated system in its ground state V_0 onto a valence-excited state PES, the state V_2, e.g. induced by the absorption of an optical photon at the time t_0 as illustrated in Fig. 2.1. We assume that the timescale on which the system evolves according to the properties of the populated electronic state is long compared to the timescale on which the actual transition between the states occurs. Under these conditions, an exponential decay of the population of the state V_2 onto the ground state or energetically lower lying electronically excited state PESs occurs with a rate Γ_2 that statistically defines the excited state lifetime $\tau = t_1 - t_0$. In this time-frame the molecule adapts its geometry according to the properties of the V_2 potential. From the gradient of the potential in combination with Γ_2 the yield for a certain molecular deformation during the excited state lifetime can be estimated. In this context the quantum mechanical nature of the motion of the nuclei has to be taken into account. The molecular geometries marked in the reduced picture drawn in Fig. 2.1 shall be understood as transient populations of the coupled electronic and nuclear wavefunctions. As will be shown in section 2.2, the excitation resembles a projection of the ground state nuclear wavefunction onto the set of nuclear wavefunctions of the valence-excited state creating a wave packet which propagates in the time after the excitation. Hence, interference between the excited nuclear modes, in addition to the shape of the involved PESs, can have an impact on the preference for specific molecular geometries at a certain time after the excitation and the subsequent decay pathways. Solute solvent interactions can cause dissipation of kinetic energy from the system to the solvent through vibrational cooling. Therefore molecules are expected to reside in local minima of potentials, as illustrated for the time t_2, given sufficient relaxation-time after the transition between the PES and an even longer lifetime of the state V_1.

The characteristics of involved potentials and their coupling define dominant relaxation pathways in excited state dynamics, i.e. the transient population of specific intermediate molecular configurations. To quantitatively describe dynamics on PESs and estimate rates of transitions between them, the theoretical concept of wave packet propagation within the framework of the Born-Oppenheimer approximation can be applied, which is described in the following.

Computational Access to Dynamics on Potential Energy Surfaces

The dynamics occurring subsequently to an excitation of a quantum-mechanical system is reflected in the time-dependent nuclear wavefunction.[‡] Using time-dependent perturbation theory, the coefficients $\chi_j(\underline{R}, t)$ from equation 2.4 can be expanded with

[‡]The presented concepts are still based on the derivations by Lee and Heller.[52]

respect to powers of the perturbation amplitude. The Ansatz reads

$$\chi_j(\underline{R},t) = \sum_{k=0}^{\infty} \chi_j^{(k)}(\underline{R},t). \tag{2.5}$$

Using the stationary state solutions for a given PES with the index j

$$\chi_{jm}^{(0)}(\underline{R},t) = \chi_{jm}^{(0)}(\underline{R})e^{-iE_{jm}t/\hbar},$$
$$H_j(\underline{R})\chi_{jm}^{(0)}(\underline{R}) = E_{jm}\chi_{jm}^{(0)}(\underline{R}),$$

and a population of modes on the inital electronic state PES $\chi_1^{(0)}(\underline{R},0)$ at $t=0$ with the energy E_1 (given by $H_1\chi_1^{(0)}(\underline{R},0) = E_1\chi_1^{(0)}(\underline{R},0)$), the first and second order wave packet amplitudes on the PES j at a time $t=T$ are given by

$$i\hbar\chi_j^{(1)}(\underline{R},T) = \int_0^T du\, e^{-i(H_j-i\Gamma_j)(T-u)/\hbar}\hat{\mathcal{H}}_{j1}^{int}(\underline{R},u)e^{-iH_1u/\hbar}\chi_1^{(0)}(\underline{R},0) \tag{2.6}$$

and

$$\begin{aligned} i\hbar\chi_j^{(2)}(\underline{R},T) = &\sum_k \int_0^T ds \int_0^s du\, e^{-i(H_j-i\Gamma_j)(T-s)/\hbar}\hat{\mathcal{H}}_{jk}^{int}(\underline{R},s) \\ &\times e^{-i(H_k-i\Gamma_k)(s-u)/\hbar}\hat{\mathcal{H}}_{k1}^{int}(\underline{R},u)e^{-iH_1u/\hbar}\chi_1^{(0)}(\underline{R},0). \end{aligned} \tag{2.7}$$

Hence, all scattering events with the temporal evolution following the scheme

$$\chi_1^{(0)}(\underline{R},0) \xrightarrow[e^{-iH_1u/\hbar}]{t=0 \quad t=u} \hat{\mathcal{H}}_{j1}^{int}(\underline{R},u) \xrightarrow[e^{-i(H_j-i\Gamma_j)(T-u)/\hbar}]{t=u \quad t=T} \chi_j^{(1)}(\underline{R},T)$$

corresponding to a single interaction with the electromagnetic field in the temporal interval $[0,T]$ are considered in the first order wave packet amplitude given by equation 2.6. Two interaction events according to the temporal structure

$$\chi_1^{(0)}(\underline{R},0) \xrightarrow[e^{-iH_1u/\hbar}]{t=0 \quad t=u} \hat{\mathcal{H}}_{k1}^{int}(\underline{R},u) \xrightarrow[e^{-i(H_k-i\Gamma_k)(s-u)/\hbar}]{t=u \quad t=s} \hat{\mathcal{H}}_{jk}^{int}(\underline{R},s) \xrightarrow[e^{-i(H_j-i\Gamma_j)(T-s)/\hbar}]{t=s \quad t=T} \chi_j^{(2)}(\underline{R},T)$$

result from the second order wave packet amplitude in equation 2.7. Limited lifetimes for the intermediate and final states populated between the transitions have been introduced in the model through the decay rates Γ_i. We thus suspect a comparably long lifetime of the initial state 1. We should emphasize that the interactions mediating radiative and non-radiative transitions between the different PESs are implemented through the perturbation $\hat{\mathcal{H}}_{jk}^{int}(\underline{R},t)$, allowing to consider all possible sequences of transitions between the electronic states.

The state and scattering duration dependent propagation of the electronically excited state wave packets, considering two transitions between the surfaces, can be simulated using equation 2.7. The involved states define the driven nuclear coordinates and thus affect the scattering amplitude to subsequently populated states in different molecular geometries. Consideration of higher order wave packet

amplitudes allows to take further transitions between the states into account, based only on the the initial wave packet $\chi_1^{(0)}(\underline{R}, 0)$ and the system of PESs involved in the scattering events.

Wave packet propagation formalisms based on these transient populations of nuclear wavefunctions have been used successfully to describe valence[63–66] as well as core-excited[40,42,47,67] state dynamics in compact molecular systems. The concept was developed to describe photo absorption and Raman scattering processes[52] and is thus also applicable to X-ray absorption induced transitions[68] which will be discussed in section 2.3. In the context of this thesis, it has been employed to model the O 1s core-excited state dynamics of the water molecule in publications V and VI, as well as in the related publications[69,70]. These will be discussed in section 3.3.

The propagation can only be simulated for systems where the multidimensional potential energy surface can be simulated in a sufficiently large range of molecular geometries. Alternatively, a semi-classical treatment of the nuclear motion in combination with a distribution of statistical starting conditions for the molecular geometry has allowed to determine preferential pathways across valence-excited state potential energy surfaces for larger systems.[71] In this surface hopping formalism, the system is propagated on a single PES and the transition probability towards the other PESs in the temporally evolving molecular geometry is evaluated at each simulated time step. The system is subsequently propagated on a different surface if the transition probability to this surface lies above a threshold value. A recent implementation allows treatment of transitions between states with different multiplicity in this framework.[72,73] The surface hopping method has proven to generate results comparable to full quantum dynamical simulations for small systems[72] and was applied e.g. to disentangle photo-induced dynamics in cyclo-organic systems.[74,75] In the context of this thesis, the surface hopping method is currently applied to gain computational access to the relaxation dynamics of the photo-excited cyclo-organic compound 2-thiopyridone. Experimental signatures of N-H proton dynamics on femtosecond timescales are discussed in publication II, which require a mechanistic explanation based on relaxation pathways from quantum-chemistry.

Interaction Operators for Electronic Transitions

Radiative transitions between different PESs are mediated by the dipole moment operator $\underline{d} = e\sum_{i=1}^{s} \underline{r}_i$ in the interaction Hamiltonian $\hat{\mathcal{H}}_{jk}^{int}(\underline{R}, t) = -D_{jk}(\underline{R}) \cdot \underline{\mathcal{E}}(t)$ with the transition dipole moments $D_{jk}(\underline{R}) = \kappa\,\hbar\omega_{jk}\langle\psi_j(\underline{r}, \underline{R})|\underline{d}|\psi_k(\underline{r}, \underline{R})\rangle_{\underline{r}}$ between the electronic states j and k and the time-dependent electric field $\underline{\mathcal{E}}(t)$.[52] The factor $\kappa\,\hbar\omega_{jk}$, with the constant κ and $\hbar\omega_{jk} = E_j - E_k$, results from the dipole approximation.[76] The core dipole moments $\underline{d}_N = e\sum_{i=1}^{N} Z_i\underline{R}_i$ for the cores with charges Z_i can be omitted, when transitions between different electronic surfaces are considered.[55, p. 388]

The **non-radiative** transitions considered here for cases of core and valence-excited state dynamics are resonant photo-emission and Auger processes, internal conversion IC processes between valence-excited and ground states with the same multiplicity

and inter-system crossing ISC processes characterized by coupling between states with different multiplicity. In the following, we discuss aspects of them which are important in the context of this thesis.

- **Resonant photo-emission and Auger** processes yield singly and doubly ionized final states of the system. Upon Auger decay a vacancy in an orbital is populated from an energetically higher lying occupied single electron state. The excess energy is transferred into kinetic energy of an electron, which is emitted from the system.[§] The operator coupling the discrete initial and the continuum of final states is the Hamiltonian of the electronic system[38,81] from equation 2.3. Using a slater determinant to describe the electronic state in a frozen orbital approximation (see section 2.3.3) reduces the interaction operator to $\hat{\mathcal{H}}^{int}_{jk}(\underline{R}) = \langle\psi_j(\underline{r},\underline{R})|e^2\eta(\underline{r_1}-\underline{r_2})^{-1}|\psi_k(\underline{r},\underline{R})\rangle_{\underline{r}}$, which corresponds to the Coulomb interaction between the electrons involved in the decay process.[82,83] η is a scaling parameter including creation and annihilation operators for spin orbitals to allow for changes of spin states upon the auger transition. Here, it is important to note that Auger processes dominate the decay pathways and lifetimes of soft X-ray core-excited states, whereas radiative decay is a minority decay channel with a yield in the percentage range.[84]

- The **IC** processes between valence-excited and ground states occur in geometries with close lying electronic states, and are mediated by the energy perturbation $\hat{\mathcal{H}}^{int}_{jk}(\underline{R}) = \langle\psi_j|-\sum_{n=1}^{3N-6}\frac{\hbar^2\partial^2_{R_n}}{2M_n}|\psi_k\rangle$ describing the vibrational coupling between the involved states. One should note that the operator contains derivatives with respect to nuclear coordinates. It therefore also operates on the nuclear part of the wavefunction in equations 2.6 and 2.7. Considering IC processes in the framework discussed here is a perturbative treatment of the coupling between nuclear and electronic wavefunctions, which is neglected in the Born-Oppenheimer approximation (see footnote† on page 6).[¶] The corresponding matrix elements between states with different multiplicities are zero.[86]

- **ISC** is, in contrast, mediated by perturbations mixing states with different multiplicity. Spin orbit coupling induces this mixing through matrix elements of the form $\hat{\mathcal{H}}^{int}_{jk}(\underline{R}) = \langle\psi_j|\sum_{i=1}^{s}\xi(\underline{r}_i)\underline{l}_i\cdot\underline{s}_i|\psi_k(\underline{r},\underline{R})\rangle_{\underline{r}}$, where $\underline{l}_i$ and $\underline{s}_i$ are orbital momentum and spin operators. $\xi(\underline{r}_i)$ defines the amplitude of spin orbit

[§] The kinetic energy of the emitted electrons carries information on the molecular electronic structure and can be used to determine molecular dynamics using electron spectroscopy techniques.[77–80] These are complementary to the methods applied in the context of this thesis. Electron spectroscopy is particularly suited for studies of gas-phase systems, which are compatible with the vacuum requirements of electron spectrometers and avoid contamination of spectra by electrons emitted from the solvent molecules.

[¶] A different way to treat the coupling between close lying adiabatic Born-Oppenheimer PESs is the diabatic representation.[85] Therein the basis used to expand the electronic part of the wavefunction is rotated to diagonalize the derivative-containing coupling terms in the Hamiltonian. The resulting diabatic potential curves can be used to simulate dynamical processes beyond the Born-Oppenheimer approximation considering only a scalar coupling between the states.

coupling and is in a semi-classical framework proportional to the magnetic field generated by the electronic motion. For hydrogenic atoms with a nuclear charge Z, it can be shown that spin orbit coupling effects are proportional to Z^4, which indicates that ISC probabilities are enhanced by the presence of heavy atoms in molecules.[55, p. 395,p. 214-215]

Additionally, interactions with the chemical surrounding have to be considered when the system is in a solution environment. Scattering processes with solvent molecules can e.g. induce dissipation of kinetic energy or/and breakage of molecular symmetries and thus cause relaxation on individual, as well as transfers between different PESs. Association between different solute molecules induced by an electronic excitation also has to be considered dependent on sample concentrations and the properties of the solute and the solvent molecules.[55, p. 396-405]

2.3 X-ray Tools to Access Molecular Proton Dynamics

Based on the formalism illustrated above, not only excited state populations opening possible (de-)protonation pathways during relaxation processes can be modeled and identified, but it also allows for quantitative estimates of transition probabilities for X-ray absorption, as well as RIXS processes. These cross-sections depend on the molecular valence electronic structure and are used throughout the studies in this thesis to probe protonation of N and O atoms molecular systems. To model processes involving the absorption and emission of photons, we consider the interaction Hamiltonian $\hat{\mathcal{H}}^{int}_{jk}(\underline{R},t) = -D_{jk}(\underline{R}) \cdot \underline{\mathcal{E}}(t)$. The generation or annihilation of photons with energies $\hbar\omega$ are described through $\underline{\mathcal{E}}(t) = \eta\omega^{-1/2}\underline{\mathcal{E}}e^{i\omega t}$ and $\underline{\mathcal{E}}(t) = \eta\omega^{-1/2}\underline{\mathcal{E}}e^{-i\omega t}$ respectively.[52,76] η is a normalization constant.

2.3.1 X-ray Absorption Spectroscopy

The scattering amplitudes for single photon absorption or emission events into the state $\chi^{(0)}_{jm}(\underline{R},t)$ result from implementation of $\underline{\mathcal{E}}(t)$ into equation 2.6, assuming $\hbar\omega_{jk} \approx \hbar\omega$ for the transitions dipole moments, projection onto the state and integration for $T \to \infty$. This results in Fermi's golden rule for the photon energy $\hbar\omega$ dependent absorption cross section σ, which was derived by Dirac in 1927.[87]. It reads

$$\sigma^{\mathrm{XAS}}_{V_i}(\hbar\omega) \propto \hbar\omega \sum_j \left| \frac{\underline{\mathcal{E}} \cdot \langle C_j|\underline{d}|V_i\rangle}{E_{C_j} - E_{V_i} - \hbar\omega + i\Gamma_{C_j}} \right|^2 . \tag{2.8}$$

Here, $|V_\mathrm{i}\rangle$ is the full wavefunction of the state populated before the photo absorption event and $|C_\mathrm{i}\rangle$ are the accessible states through the absorption process. The accessibility is defined by the energy difference $\Delta E_{C_j,V_i} = E_{C_j} - E_{V_i}$ between the involved states in relation to the photon energy and the decay rates Γ_{C_j}. In studies of valence-excited state dynamics V_i are populated ground state or valence-excited states. C_j are, when X-ray absorption induced transitions are considered, core-excited

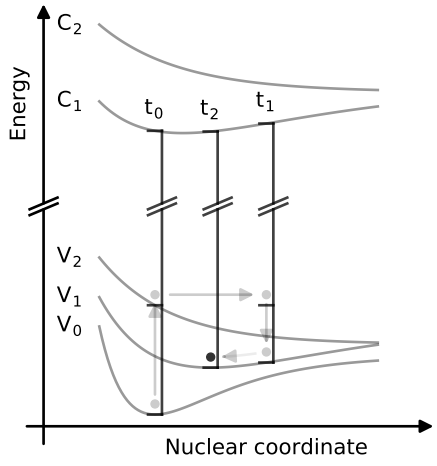

Figure 2.2: *Valence-excited state dynamics seen from core-excited states.* Transient populations of electronic states in different molecular geometries of the system are reflected in the energetic separation of valence and core-excited state potential energy surfaces $\Delta E_{C_j,V_i}$. At a time t_k XAS probes this energy difference for occupied valence-excited states V_i, while RIXS yields access to $\Delta E_{C_j,V_i}$ for many valence and core-excited states. This increases the probability to unambiguously identify the pathway across the excited state potential energy surfaces.

states characterized by an unpopulated, energetically low lying electronic orbital centered at a specific atomic site in the investigated molecule. The transition energies depend on the element and the chemical environment of the specific atom the orbital is centered at. This makes X-ray spectroscopy a sensitive probe for local electronic structure at specific elemental sites in the investigated system.

For energetically well separated core-excited states, σ is a sum of lifetime broadened Lorentzian peaks centered at photon energies $\hbar\omega = \Delta E$. The dipole matrix element in the numerator defines the amplitude of each absorption line and introduces a dependence of the cross section on characteristics of the electronic states involved in the absorption process. Depending on the model used to generate a solution for the electronic part of the wave function, a specific electronic configuration/orbital occupation can be attributed to the states $|C_j\rangle$ and $|V_i\rangle$. In K-edge X-ray spectroscopy, the photon energy used to induce the transition $V_i \xrightarrow[\text{core exc.}]{\text{X-ray abs.}} C_j$ is correlated with a reduction of the occupation of a 1s orbital in the investigated system in exchange of an increased occupation of a valence or continuum orbital. Hence, the matrix elements $\langle C_j|\underline{d}|V_i\rangle$ are restricted by the expansion of the 1s orbital (see paragraph 2.3.3 on frozen orbital and local approximation below) making soft X-ray K-edge spectroscopy a site selective probe for local molecular valence electronic structure and its occupation, which is required to get access to molecular proton dynamics specifically at N and O sites.

Fig. 2.2 depicts how the coupled transient, molecular geometry dependent, electronic structure on valence-excited state potential energy surfaces is accessible through optical pump X-ray probe spectroscopy schemes. The energy difference ΔE between the occupied ground ground state or valence-excited states and the core-excited states C_1 is different in each of the depicted electronic states in the different molecular geometries. Hence, an X-ray probe mechanism which detects a signal with state-

population dependent intensity in combination with ΔE at a well defined time after the excitation can be utilized to extract the temporal evolution of the populations of the states V_i. Even though the unambiguous assignment of the valence-excited states through ΔE is not a necessity for any valence-excited state dynamical decay, the access to spectral signatures of multiple core-excited states through precise X-ray photon energy adjustments at modern X-ray light sources increases the probability to detect distinct signatures of transient states along the decay pathway.

2.3.2 Resonant Inelastic X-ray Scattering

So far it has been illustrated how the K-edge X-ray absorption cross section given in equation 2.8 reflects electronic and structural changes based on the molecular geometry dependent energy differences between populated the ground state or valence-excited states and core-excited states. The detection of X-ray emission processes following the 1s core-excitation yields access to this energy difference also for unpopulated valence-excited states, which can gain additional information for an unambiguous assignment of the ongoing dynamical processes.

In that context, we consider two photon processes resembling subsequent absorption and emission of photons, with energies $\hbar\omega_I$ and $\hbar\omega_S$ respectively, for which cross-sections can be estimated in the framework described in section 2.2 in equation 2.7. Two-photon absorption and emission as well as a term resembling the initial emission of a photon followed by the absorption of a photon can also be described by equation 2.7 but are ommitted in favor of the subsequent absorption-emission processes which can be resonantly amplified. Substitution of the propagation time of the wave packet on the intermediate surface k $v = s - u$ yields equation 2.7 for the resonant Raman process

$$
\begin{aligned}
i\hbar\chi_j^{(2)}(\underline{R},T) =& \frac{\eta^2}{\sqrt{\omega_I\omega_S}} \int_0^T ds\, e^{-i(H_j - i\Gamma_j)T/\hbar} e^{i(H_j - E_1 - \hbar(\omega_I - \omega_S) - i\Gamma_j)s/\hbar} \sum_k [-D_{jk}(\underline{R}) \cdot \underline{\mathcal{E}}_S] \\
& \times \left\{ \int_0^s dv\, e^{-i(H_k - E_1 - \hbar\omega_I - i\Gamma_k)v/\hbar} \right\} [-D_{k1}(\underline{R}) \cdot \underline{\mathcal{E}}_I] \chi_1^{(0)}(\underline{R},0). \qquad (2.9)
\end{aligned}
$$

The core-excited state, incident and emission energy dependent intensity distribution resulting from resonant (in)elastic X-ray scattering processes $V_i \xrightarrow[\text{core exc.}]{\text{X-ray abs.}} C_j \xrightarrow[\text{deexc.}]{\text{X-ray em.}} V_k$ is named, after its discoverers, Kramers-Heisenberg formula[88]. It follows from equation 2.9 in steps similar to the ones used to derive Fermi's golden rule from equation 2.6, using in addition the completeness relation for the nuclear

modes on each of the electronic PESs. It is given in its differential form [76]

$$\frac{d\sigma_{V_i}^{\mathrm{RIXS}}}{d\Omega}(\hbar\omega_I,\hbar\omega_S) \propto (\hbar\omega_S)^3\hbar\omega_I \sum_f \left| \overbrace{\sum_j \frac{(\underline{\mathcal{E}}_S \cdot \langle V_f|\underline{d}|C_j\rangle)(\underline{\mathcal{E}}_I \cdot \langle C_j|\underline{d}|V_i\rangle)}{E_{C_j} - E_{V_i} - \hbar\omega_I + i\Gamma_{C_j}}}^{\text{scattering amplitude}} \right|^2 \times \frac{const.}{(\hbar\omega_S + E_{V_f} - E_{V_i} - \hbar\omega_I)^2 + \Gamma_{V_f}^2}, \tag{2.10}$$

as only a limited solid angle Ω of scattered photons can be detected.

For larger systems with a high number of nuclear degrees of freedom, it is not feasible to simulate the nuclear modes on all PESs involved in the studied RIXS process. Therefore, the Kramers-Heisenberg formula is evaluated only considering the dipole transitions moments between the electronic states in the ground state molecular geometry. This frozen geometry approximation is applicable for rigid systems consisting of heavy atoms. However, non-negligible structural relaxation in the core-excited state can have an impact on scattering cross-sections. This is of particular importance for systems with light bonding partners, as will be discussed below. In the following, we focus on the transition dipole moments in equation 2.10 which can be calculated from the electronic part of the product wavefunction of the investigated system in the Born-Oppenheimer approximation.

2.3.3 Orbital Selectivity and Limitations

We will now show that X-ray spectroscopy selectively probes specific molecular orbitals using the so-called **frozen orbital approximation** [89, p. 42]. This simplification allows to estimate X-ray absorption and RIXS transition rates qualitatively, without consideration of the full eigenstates of the multi-body system. Instead, matrix elements contract to integrals involving only orbitals, which change occupation during the X-ray absorption or emission process.

To justify this reduction, we suppose that the antisymmetric many electron ground state wavefunction of the investigated system is dominated by one slater determinant of single electron wavefunctions. The frozen orbital approximation implies that the orbitals used to form the determinant are the same in the core-excited state and only occupations are altered in combination with photo-absorption or emission processes. This yields a drastic reduction of the complexity of the dipole moments contributing to the X-ray absorption and RIXS cross-sections in equations 2.8 and 2.10, to

$$\langle \Psi_{C_j}|\underline{d}|\Psi_{V_i}\rangle \approx \langle N_1 N_2 \dots N_k - 1 \dots N_l + 1|\underline{d}|N_1 N_2 \dots\rangle = \langle \xi_l|\underline{d}|\xi_k\rangle. \tag{2.11}$$

Here, $|N_1 N_2 ...\rangle = \frac{1}{\sqrt{s!}} \sum_\sigma \mathrm{sgn}(\sigma)\xi_1(r_{\sigma_1}) \dots \xi_s(r_{\sigma_s})$ are slater determinants of the s single electron wavefunctions ξ_n. $N_n \in \{0, 1\}$ defines the presence/absence of ξ_n in the determinant. ξ_k and ξ_l hence represent the orbitals which either de- or increase occupation within the X-ray absorption or emission process. The scattering

amplitudes for X-ray absorption and emission are therefore given by overlap of active orbitals in this approximation. Based on these considerations it is possible to assign molecular orbitals directly to spectroscopically detected transitions.

For our aim to study proton dynamics at N and O sites, a local probe for bond mediating valence orbitals with p character is required. In this context, the **local approximation**[90] clarifies the importance of the local character of molecular orbitals with respect to the core-excited atom. We will show that a high sensitivity for the p-derived local density of states at the investigated atom can be gained through spectroscopic investigations of transitions changing the occupation of 1s orbitals. To illustrate the concept, we follow the nomenclature by Kunnus[91] and expand the molecular orbitals ξ_l within the basis of atomic orbitals ϕ_m^n centered at the sites n in the considered system,

$$\xi_l = \sum_n \sum_m \phi_m^n c_m^n.$$

$c_m^l = \langle \phi_m^l | \xi_l \rangle$ are the expansion coefficients. Assuming that the core-excitation depopulates a molecular orbital with dominant atomic character at the site p, which can be well approximated by the atomic wavefunction ϕ_o^p, the dipole moment 2.11 can be expressed as

$$\langle \Psi_{C_j} | \underline{d} | \Psi_{V_i} \rangle = \langle \xi_l | \underline{d} | \xi_k \rangle = \sum_n \sum_m c_m^n \langle \phi_m^n | \underline{d} | \phi_o^p \rangle. \tag{2.12}$$

If we further reduce the sum to atomic orbitals centered at site p, which are expected to exhibit the largest overlap with the core orbital ϕ_o^p, expression 2.12 reduces to

$$\langle \Psi_{C_j} | \underline{d} | \Psi_{V_i} \rangle \approx \sum_m c_m^p \langle \phi_m^p | \underline{d} | \phi_o^p \rangle. \tag{2.13}$$

The dipole **selection rules** for radiative transitions between atomic orbitals[55, p. 210]

$$\Delta l = \pm 1; \quad \Delta m_l = 0, \pm 1;$$

can now be applied to the considered matrix elements. Here, l is the angular momentum and m_l is the magnetic quantum number. We now consider ϕ_o^p to be a N or O 1s orbital. Applying dipole selection rules, the group of orbitals m centered at the core-excited site p reduces to the 2p orbitals. Hence, in the framework of the applied approximations, K-edge spectroscopy probes the local 2p character of valence molecular orbitals. This concept has initially been used to describe dominant transitions in 1s X-ray emission spectra[90] and reflects the elemental site selectivity and orbital sensitivity of X-ray spectroscopy methods.

Within the frozen orbital approximation, only single electron transitions, where one occupied orbital in the slater determinant is exchanged by a virtual one, are allowed. The transition dipole moments between states, which differ in occupation of more than one frozen molecular orbital, are zero. **Relaxation** of the electronic structure in the core-excited state allows such transitions to be induced by the

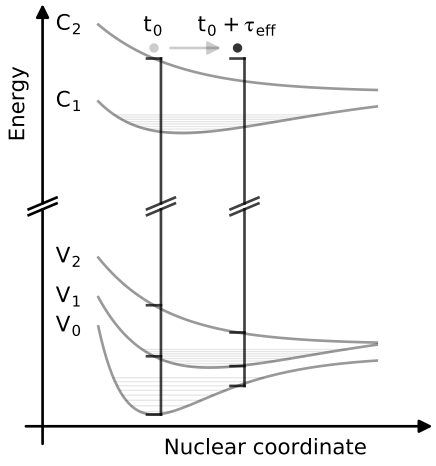

Figure 2.3: *Accessing vibrational interference/core-excited state dynamics using RIXS.* The interference of different excited modes on the core-excited state PESs is modeled through the propagation of the nuclear wave packet. It changes overlap with the nuclear wavefunctions of the ground or valence-excited electronic states, which alters the scattering amplitude for these final states of the RIXS process. Energy and amplitude shifts and, if sufficient resolution is available, altered vibrational substructure of RIXS features are the result of dynamics within the tunable effective scattering duration τ_{eff}.

absorption or emission of a photon. In the framework of configuration interaction the states differing by multiple excitations in their dominant determinants have non-zero contribution of single transition determinants to their electronic wave function through their CI-expansion coefficients. These contributions generate amplitude in the transition dipole moments scaled by the corresponding CI coefficients and thus make the corresponding states visible for spectroscopy methods. Specifically, multiplet structures are present in spectra in addition to transitions allowed in the frozen orbital approximation, which can e.g. yield estimates for transition energies between valence orbitals of the investigated system.

All intermediate states within an energy range, defined by the core-hole lifetime, around the used excitation photon energy, e.g. the previously mentioned states characterized by multiple electron transitions, have non-negligible contribution to the scattering amplitude in the emission energy dependent RIXS intensity in equation 2.10. Hence, energetically close lying electronic states introduce **interference effects** as the absolute square of the scattering amplitude is taken after the summation over the intermediate states.[92–94] The fact that $|V_i\rangle$ and $|C_j\rangle$ are combined electronic and nuclear product wavefunctions has to be considered regarding the discussed interference effects. As illustrated in Fig. 2.3, the nuclear wavefunctions of core-excited PESs exhibit either discrete, energetically close lying, eigenenergies in the bound regions of the PESs or continua for dissociative conditions. Hence, interference between vibrational states of individual or multiple core-excited PESs has an impact on the RIXS cross-section.[39,40] Such vibrational interference effects, correlated with dynamics in the core-excited state, are nicely accessible within the time-dependent concept of the RIXS process discussed section 2.3.4.

The width of spectral lines, in both cases X-ray absorption and RIXS, is defined by the lifetime of the final state of the detected transitions. Thus, XAS linewidths

are on the order of hundreds of meV for core-hole lifetimes of few femtoseconds for the O and N K-edges studied here. On the contrary, the RIXS final states are valence-excited states involving only low energy excitations, exhibiting longer lifetimes. The corresponding spectral lines can therefore be much sharper and their width is, in most cases, dominated by a fluctuating chemical environment of the probed site or instrumental **broadening** effects. The chemical environment imposes an additional dipolar broadening Γ_{env} proportional to the product of $|\Delta\mu_{if}|$, the dipole moment difference between the initial and the final state of the investigated process, and $|\mu_S|$, the dipole moment of the solvent molecules

$$\Gamma_{\text{env}} \propto |\Delta\mu_{if}||\mu_S|$$

on the detected transitions in RIXS spectra.[39] The elastic RIXS transitions are thus least affected by such dipolar broadening effects, because an altered final state dipole moment can only originate from structural distortions of the molecule and not from changes of orbital population.

2.3.4 Dynamics in Core-Excited States

The concept of excited state dynamics presented in section 2.2 is also applicable to X-ray photo-excitations, which have been introduced as detection schemes for valence-excited state dynamics so far. Nuclear displacements also occur in the core-excited states, even though the core hole lifetime is on the order of few femtoseconds for 1s excitations of light elements ($Z \leq 10$)[84]. The high mobility of protons lets them react most drastically to the core-excitation within that time-frame. In the following section we will illustrate how such core-excited state proton dynamics can be accessed with RIXS based on time-dependent description of resonant inelastic X-ray scattering events.

Theoretically this aspect is reflected in the dipole moments of the X-ray absorption and scattering cross sections in equations 2.8 and 2.10, for which the nuclear wavefunction of the initial state of the considered transition has to be expanded in the basis of the nuclear wavefunctions of the state reached either through the absorption or the emission of a photon. Fermis Golden rule in equation 2.8 and the Kramers Heisenberg formula 2.10 intrinsically consider scattering through intermediate into final states with molecular geometries other than vertical transitions in a frozen geometry, in which the molecular structure remains unaltered during the RIXS process. The dynamical aspect is represented by the projection of the initial nuclear wavefunction of the state V_i onto the vibrational states of C_j. These are projected onto the set of nuclear wave-functions of final states V_f weighted with the nuclear coordinate dependent dipole moments of the involved electronic states in the RIXS process.[52] The impact of this projection is reflected, e.g. in a vibrational substructure of X-ray absorption lines corresponding to excitations into selected vibrational states of bound core-excited states, which is in contrast absent, if an excitation into a dissociative core-excited state with continuous nuclear states is considered.

An equivalent, but conceptually and computationally more appealing access to these non-vertical contributions to the scattering amplitudes is given by the time (instead of energy) dependent formulation of the photo absorption and emission process given by equation 2.9 on page 16. This concept of wave packet propagation was presented by Lee and Heller in 1979.[52] With the increasing brilliance of X-ray light sources and technical advancements of X-ray optics, RIXS investigations became feasible at synchrotron light sources. Gel'mukhanov and Ågren discussed the consequences of wave packet propagation in X-ray spectroscopy studies in 1996.[68] The aspects which are essential for the results shown in this thesis are outlined here based on their review[38], if not declared differently. We consider a wave packet, which is generated through the X-ray absorption process on the PES of the state k. It propagates according to the properties of the PES of the considered core-excited state in the time v. Even for well separated vibrational energy levels and a monochromatic excitation, the wave packet can be formed by populating multiple modes on the PES of the state k, because the width of the individual vibrational X-ray absorption peaks corresponding to the same electronic transition is given by the core hole lifetime.

The consequences of this propagation for the RIXS process can be estimated from the reduced scheme of core-excited state dynamics drawn in Fig. 2.3. The decay from the core-excited state potential energy surface does not occur in the ground state geometry. It is a statistical process from a distribution of molecular geometries. In these different geometries, the overlap of the core-excited state wave packet with the wavefunctions of the bound ground or valence-excited state potential energy surfaces can vary. For a system which is only weakly perturbed by fluctuations of its chemical environment and with sufficient experimental resolution, vibrational excitations can be detected as RIXS final states on bound electronic PESs with sufficiently long lifetimes.[39–47] Special attention should be drawn to the electronically elastic RIXS process which, as the lifetime of the electronic ground state is infinite, does not impose any electronic state lifetime broadening onto the vibrational spectral lines.

Investigations of low energy excitations using elastic RIXS are also least affected by dipolar broadening as discussed in the previous section. Such excitations can be studied with a currently instrumentally limited energy resolution of $E/\Delta E \approx 10000$, yielding linewidths of few ten meV for soft X-ray energies, with site and q-selective RIXS in dedicated modern instruments (see section 4.4).[95]

In these RIXS studies of molecular core-excited state dynamics, the intensity of the vibrational progression is strongly dependent on the excitation photon energy in relation to the maximum of the excited X-ray absorption resonance. This can be understood from analysis of the exponent in the propagator $e^{-i(H_k - E_1 - \hbar\omega_I - i\Gamma_k)v/\hbar}$ in equation 2.9. It lets us manipulate the time span of core-excited state dynamics which have an impact on the recorded RIXS spectra. We define $\mathcal{H}_k = H_k - E_1 - \overline{E}_k$ with $\overline{E}_k$ as the average energy difference between state 1 and k and $\tilde{\Omega}_k = \overline{E}_k - \hbar\omega_I$ as the detuning of the excitation photon energy from the resonance energy. This yields an exponent for the propagator on the intermediate PES k of $-i(\mathcal{H}_k + \tilde{\Omega}_k - i\Gamma_k)v/\hbar$. Hence, non-zero $\tilde{\Omega}_k$ cause oscillatory temporal changes of the integrand. The therefore

reduced impact of longer scattering times on the total scattering amplitude can be interpreted as an excited state specific and detuning-dependent complex scattering duration

$$\tau_k = \hbar/(\Gamma - i\tilde{\Omega}_k).$$

This concept has been successfully used to accurately describe detuning-dependent vibrational progressions,[47,48] estimate core-excited state induced fragmentation,[70] as well as to distinguish between information content on electronic structure in the ground state molecular geometry and RIXS features resulting from ultrafast core-excited state dynamics for systems in hydrogen bonding networks.[44]

An alternative and in comparison to wave packet propagation computationally much lighter method to model molecular dynamics specifically upon core-excitations is the Z+1 equivalent core approximation.[96] It has been successfully applied to model scattering duration affected X-ray emission spectra.[97–100] In this semi-classical approach, the relaxation of the electronic structure and the nuclear displacement in the core-excited state is expected to be induced by the reduced screening of the core-potential at the excited atomic site. To model this effect, the charge of the nucleus at the core-excited site is increased by one elementary charge Z+1. The electronic ground state of this system, considering an equivalent increase of the number of electrons, is expected to represent the energetically lowest core-excited state of the molecule. In contrast, retaining the initial number of electrons results in a simulation of molecular properties in its core-ionized state. In this framework, core-excitation induced dynamics are simulated according to the forces introduced by the change in nuclear charge. Emission spectra can be calculated along the resulting trajectories. This method to access core-excited state dynamics has a crucial limitation. In publication V, we show for example that gas-phase water is distorted along three different directions upon excitation to three O 1s core-excited states. Such state-specific directional molecular distortions can not be modeled using the Z+1 equivalent core approximation. Hence, the agreement of Z+1 simulations with experimental RIXS data recorded upon resonant excitation below the ionization threshold either confirms or excludes that the reduced screening of the core is the mechanism driving the dynamics upon core-excitation. Besides this trade-off in physical accuracy, the method yields a tremendous reduction of computational effort. For a numerical wave packet propagation the multidimensional core-excited state PES is required in a wide range of nuclear coordinates. In contrast, only a one-dimensional trajectory has to be simulated in the Z+1 model. Such simulations were performed on a DFT level for the amino-acid histidine surrounded by water molecules. They are presented in publication IV. The dynamics and spectra could be simulated on a commercial desktop computer within days, without the need for supercomputer resources.

Chapter 3

Photo-Induced Proton Dynamics

Using the methods discussed in chapter 2, we can now focus on photo-induced molecular proton dynamics discussed in the publications I–VI. The involved active atomic sites are accessed using K-edge soft X-ray spectroscopy methods. The discussed different levels of theory allow for comparisons between the experimental spectra and quantum chemical simulations for each presented case.

3.1 Excited-State Proton-Transfer in 2-Thiopyridone

Intra- and intermolecular excited state proton transfer (ESPT) processes involve photo-induced changes of protonation at specific sites in molecular systems. Due to the high proton mobility, these processes are potentially fast and reversible. Therefore, they are discussed to be essential for photo-protection of biomolecules, e.g. DNA[7] and melanin[8–10], and require a mechanistic understanding. The characterization of an optically induced ESPT in the organo-sulforic model compound 2-thiopyridone (2-TP, see Fig. 3.1 for structure) using N 1s spectroscopy is the central scope of publications I-III. The system exhibits a chemical environment dependent tautomerism. In polar environments the N site protonated (thione) tautomer 2-TP is dominantly present.[101–103] It was categorized as an ESPT compound by Du et al. based on spectral signatures detected with transient resonant raman spectroscopy.[36] They identified the presence of the sulfur (S) site protonated tautomer 2-mercaptopyridine (2-MP) on nanosecond timescales after a photo-excitation initially populating the fourth singlet excited state S_4 of 2-TP. Van Kuiken et al. investigated the relaxation of initially S_2 excited 2-TP in acetonitrile solution based on transient S K-edge X-ray absorption data.[37] They revealed rich dynamics on pico- and nanosecond timescales. A possible ESPT pathway, contradicting the ESPT schemes of Du et al. in water, was proposed but not conclusively determined.

The potential proton transfer dynamics affect the protonation and thus also the local electronic structure at the N site of 2-TP. Therefore, N K-edge XAS and RIXS spectral fingerprints of N site protonation changes of 2-TP in were established as a

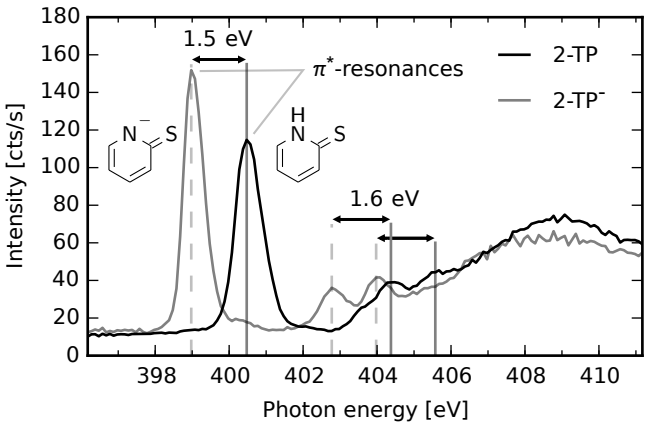

Figure 3.1: *N 1s XAS signatures of (de-)protonation in 2-thiopyridone.* In aqueous solution the dominant thione (N protonated) tautomer 2-thiopyridone (2-TP) exhibits an intense N 1s π^* absorption resonance at 400.5 eV. N deprotonation in a basic environment forming 2-TP$^-$ induces a $\sim$ 1.5 eV shift of the absorption resonances towards lower photon energies. Figure taken and adapted from **publication I**.

foundation for time-resolved investigations. The N K-edge XAS spectrum of 2-TP (aq.) is characterized in **publication I**. As shown in Fig. 3.1, the spectrum exhibits an intense π^*-absorption resonance at 400.5 eV which is well separated from energetically higher resonances on top of the continuum absorption. The absence of a potential concentration-dependent dimerization is confirmed in the study by comparison of spectra in a range of concentrations between 81 and 400 mM. By introducing the system to a basic environment the N site is chemically deprotonated. This induces a shift of all N 1s X-ray absorption resonances on the order of 1.5 eV towards lower photon energies. This shift completely separates the intense π^*-resonances of species with different protonation states. It yields a crucial advantage compared to S 1s spectroscopy. There the resonances of N site deprotonated species overlap with ones that exhibit a N-protonation as well as with the continuum absorption.[37] Comparison to DFT spectrum simulations of different molecular species confirm that the detected shift of the π^*-absorption resonance is a robust spectral signature of N deprotonation in the system. The origin of the red-shift of the resonances and its high importance for the performed investigations of excited state N-H dynamics will be explained in the following.

We demonstrate in **publication II** that the chemical N deprotonation of 2-TP induces a contraction of the formerly N-H sigma bonding orbital onto the N site. Through the orbital contraction, the screening of the N core potential is altered. This dominantly affects the N 1s energy level due to is strong localization at the N site. As the energy of the valence orbitals is not largely altered, the chemical N deprotonation induces the previously mentioned shift of the X-ray absorption resonances. These findings are based on experimental N K-edge RIXS spectra of aqueous 2-TP and the deprotonated species 2-TP$^-$ in combination with ab-initio RAS-SCF quantum chemical simulations presented in Fig. 3.2. The spectra are shown on an energy loss (ΔE) scale, defined as $\Delta E = \hbar\omega_I - \hbar\omega_S$ in the framework discussed in section 2.3. This aligns features with respect to the energy difference between the electronic ground state and the valence-excited state populated as final state of the

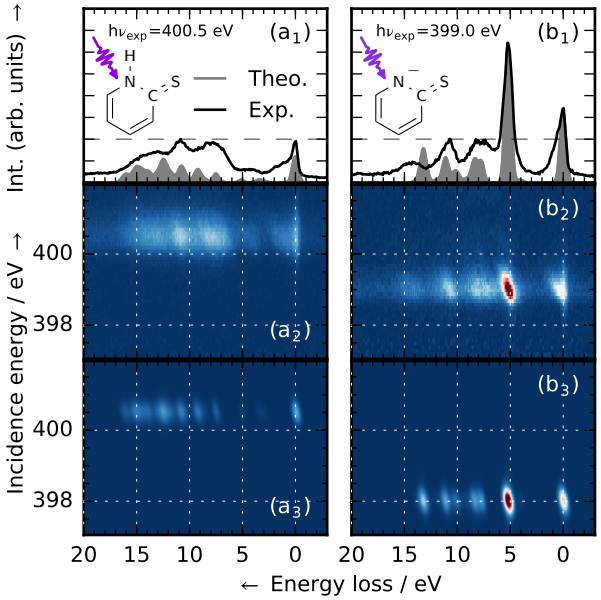

Figure 3.2: *N 1s RIXS signatures of (de-)protonation in 2-thiopyridone.* Integral and incidence energy resolved experimental and theoretical RIXS spectra of 2-TP (a_1-a_3) and 2-TP$^-$ (b_1-b_3). N deprotonation induces the presence of an intense electronically inelastic RIXS feature at ∼5 eV energy loss at the ∼1.5 eV redshifted absorption resonance. The theoretical simulations allow to assign this characteristic deprotonation signature to the presence of a N lone-pair orbital. The intensity of other spectral signatures remains almost unaffected by the deprotonation (see horizontal line in a_1 and b_1). Figure taken from **publication II**.

RIXS process. For excitations at the π^*-resonances of 2-TP and 2-TP$^-$ it allows to attribute the overlap of occupied valence orbitals to the detected RIXS spectral features. The increased overlap between the contracted occupied N lone pair orbital and the N 1s orbital drastically increases the transition dipole moment between them. Consequently an intense feature at ∼5 eV energy loss is present in the RIXS spectrum of 2-TP$^-$ for core-excitation at the shifted π^*-resonance shown in Fig. 3.2b. The cross section of other electronically inelastic RIXS transitions remains almost unaffected by the chemical deprotonation, as can be seen from a comparison of the RIXS spectra in Fig. 3.2a_1 and b_1. The attributed orbitals are delocalized across the molecular ring and are therefore not altered strongly by changes of N protonation. The inelastic RIXS feature resulting from emission from the contracted valence orbital is thus an ideal, unique deprotonation spectral fingerprint. An intensity increase in the same spectral range is identified on femtosecond timescales after 400 nm excitation of aqueous 2-TP in time-resolved N 1s RIXS measurements performed at the free-electron laser (FEL) LCLS. The data are presented in Fig. 3.3b and c. This intensity increase indicates that N deprotonation can occur on femtosecond timescales after photo excitation of 2-TP in a fraction of the excited molecules. The limited statistics of the recorded data set do not allow to quantify the yield of the detected ESPT process compared to other decay pathways across the excited state potential energy surfaces of the involved molecular species.

The three time-resolved studies by Du et al.[36], Van Kuiken et al.[37] and publication II differ in terms of the used solvent, the used excitation conditions or the investigated temporal range. To compare the different results and the proposed ESPT pathways, we consider the simulated energies of the molecular species 2-TP, 2-TP$^-$ and 2-MP on CASSCF level of theory including a polarizable continuum

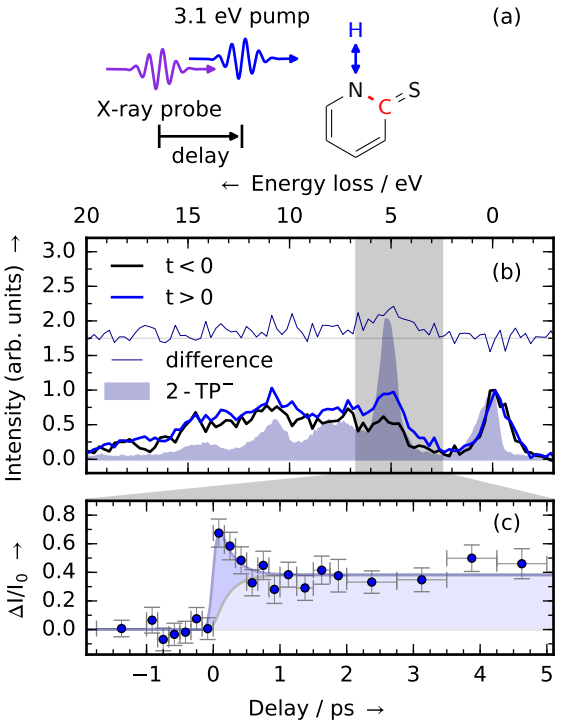

Figure 3.3: *Femtosecond N deprotonation of 2-TP:* (a) N–H dynamics in photo-excited 2-TP are investigated in an optical pump N 1s RIXS probe experimental scheme. (b) An intensity increase, in the range of the characteristic RIXS feature of 2-TP^- at ∼5 eV energy loss, is identified subsequent to the optical excitation ($t > 0$). (c) The delay-dependent intensity of the transient feature increases within the 167 fs bin width, indicating rapid photo-induced N–H dynamics. The constant offset at delays in the picosecond range indicates that the detected photochemical process occurs dominantly on ultrafast timescales. Figure taken from **publication II**.

model for water in Fig. 3.4. Du et al. proposed ESPT pathways of S_4-excited aqueous 2-TP based on their resonance Raman signatures of 2-MP on nanosecond timescales. One pathway considered relaxation among the excited states of 2-TP towards its T_1 state and finally ESPT to the S_0 state of 2-MP. The other pathways yielded direct ESPT via ISC or IC to the energetically accessible excited states of 2-MP and subsequent relaxation among them. Van Kuiken et al. identified signatures of 2-TP T_1 state population within the first nanosecond after 2-TP S_2 excitation in acetonitrile solution. They proposed the subsequent population of the 2-MP T_1 state based on their transient S K-edge spectral signatures on nanosecond timescales. The simulated energy levels presented in Fig. 3.4 indicate, that this state is inaccessible from the 2-TP T_1 state in an aqueous environment. Therefore, the proposed ESPT pathway does not yield the photo-induced 2-MP S_0 population detected by Du et al.. As can be seen in the UV-Vis spectrum of aqueous 2-TP in Fig. 3.5a (inset), the optical excitation at a wavelength of 400 nm was non-resonant for the data presented in publication II. Single photon absorption processes, in the tails of the S_2 optical absorption resonance, could have induced an inital S_2 population. In contrast, two photon absorption processes could have yielded a population of higher valence-excited states. The yield of fractional N deprotonation, which was detected on femtosecond timescales, can therefore not be directly ascribed to a specific excitation. The combination of these results thus do not allow for an unambiguous determination of dominant, possibly solvent and excited state dependent, decay pathways originating

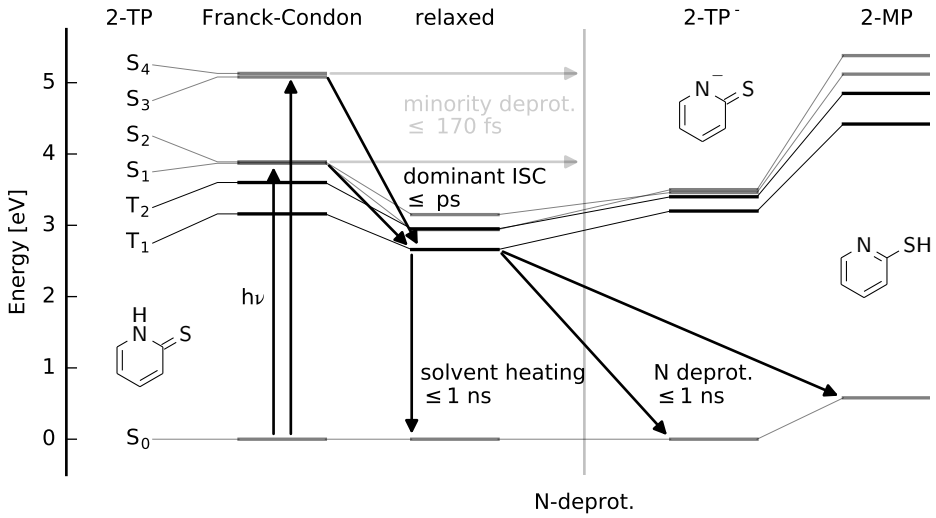

Figure 3.4: *Relaxation dynamics in 2-thiopyridone (aq, 2-TP) based on the results of transient N 1s spectroscopy.* The energy levels of ground and valence-excited states of the considered species simulated on CASSCF level of theory in a polarizable continuum model for water are illustrated. The T_3 and T_4 states of 2-TP were not simulated although they might be involved in the initial relaxation process upon S_4 excitation. Relaxation and ESPT pathways and the corresponding timescales which were identified using time-resolved N K-edge XAS and RIXS are indicated.

from the S_2 and S_4 states of 2-TP.

In **publication III**, we therefore investigated the pico- to nanosecond dynamics of aqueous 2-TP for resonant excitation of both optically accessible valence-excited states using transient N K-edge XAS. Transient spectra at different pump-probe delays are depicted in Fig. 3.5. We have found no differences of transient spectral signatures in the investigated temporal range for the S_2 and the S_4 optical excitations. Therefore, we conclude that the system reaches a common decay pathway on picosecond timescales. Electronic structure and spectrum simulations of ground and excited states of molecular species with different protonation states in comparison to the experimental data allow us to assign a dominant decay pathway valid for both valence-excitations. A detected transient N 1s resonance energetically below the ground state π^*-absorption, identified 0.1 ns after the optical excitation, matches exclusively with the simulated signatures of 2-TP in its S_2 or T_1 valence-excited states. These states are characterized by a $\pi \rightarrow \pi^*$ excitation with different spin configurations. They therefore open a new N 1s absorption resonance in comparison to 2-TP in its S_0 state. In contrast, the S_1 and the T_2 states of 2-TP are characterized by an excitation from a S centered non-bonding orbital $n \rightarrow \pi^*$ which does not overlap with the N 1s core hole and therefore does not open an additional resonance transiently. Due to the sub-nanosecond lifetime of the state and based on the ul-

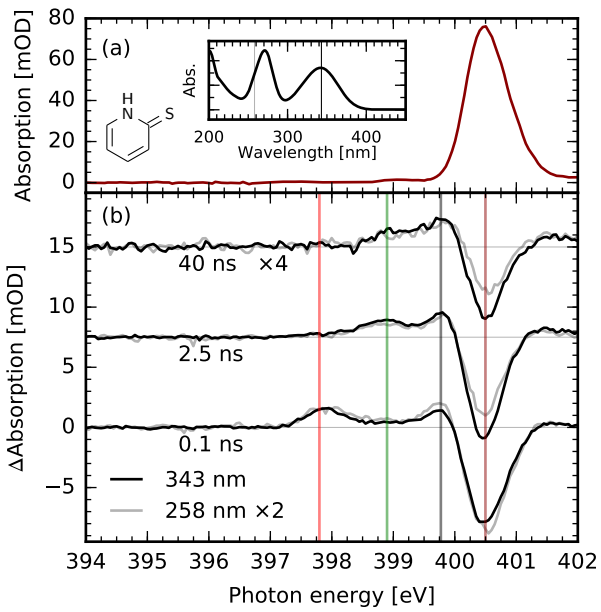

Figure 3.5: *ESPT of 2-TP on picosecond timescales mediated by its T_1 state.* Absorption around the N 1s π^*-resonance of 2-TP in its S_0 ground state (a) is altered transiently through optical S_2 and S_4 excitation [inset: UV-Vis spectrum of 2-TP (aq) with marked excitation wavelengths]. (b) The transient spectra at different pump probe delays for S_2 and S_4 excitation exhibit the same features, indicating a common decay pathway on picosecond timescales. The resonance at 397.8 eV at 0.1 ns delay is assigned to a 2-TP T_1 population. Upon its decay a resonance appears in the energy range of S_0 states of deprotonated species at $\sim$ 399 eV (spectrum at 2.5 ns delay). Figure taken from **publication III**.

trafast relaxation in similar S containing compounds, which could be disentangled using the previously discussed surface hopping method,[74] we assign the transient resonance to an efficient population of the lowest energy triplet state T_1 of 2-TP. In that context, the possibility for ISC is probably enhanced by the presence of the S atom, through an internal heavy atom effect. A subsequent decay yielding a population of an N site deprotonated species on sub-nanosecond timescales is identified from a transient resonance, exhibiting the previously discussed characteristic chemical shift with respect to the π^*-resonance of 2-TP in its ground state. Hence, we determined the 2-TP T_1 state with its sub-nanosecond lifetime as a mediator of ESPT in the system in an aqueous environment. An additional transient X-ray absorption increase exists in the transient spectra close to the 2-TP ground state π^*-resonance on nanosecond timescales. We interpret this signature as the competing dominant decay channel of the 2-TP T_1 state into the 2-TP S_0 state involving energy dissipation via thermalization with the surrounding solvent molecules. To compare our results to the results of Van Kuiken et al.[37], we extended our simulations towards S 1s XAS in the framework of a polarizable continuum model for acetonitrile. The simulations indicate, in contrast to the DFT based simulations by Van Kuiken et al., that the energy of the 2-MP T_1 state is higher than the energy of the 2-TP T_1 state. We therefore proposed a reassignment of the transient signature on nanosecond timescales in their data to a S K-edge resonance broadening or shift induced by the energy dissipation upon relaxation to the 2-TP S_0 state. With that we concluded that the dominant relaxation pathways and possible ESPT mechanisms proposed in publication III and summarized in Fig. 3.4 also qualitatively describe the dynamics

induced by S_2 excitation of 2-TP in acetonitrile.

In **publication II** we identified the character of the N 1s core-excited state in 2-TP from simulations of potential energy curves along N-H and N-C bonds. The N-H coordinate is bound in the core-excited state. In contrast, the N-C bond towards the S binding C site is dissociative and therefore photon energy dependent dynamics along selected coordinates can be induced in 2-TP. The results also underline the validity of N 1s RIXS as a sensitive probe for valence-excitation induced N-H dynamics in this particular system, as the dynamics on the core-excited state PES do not interfere with the optically driven coordinate.

The comparison of valence and core-excited state dynamics in 2-TP shows that adjustments of excitation photon energies yield bond deformations along different directions. In particular, the localized 1s core-excitation does not dissociate the molecule along all bonds of the core-excited site, but likely induces a dominant deformation of a single bond. The following study will show that the extend and directionality of such N 1s core-excited state dynamics can be largely affected by chemical environment dependent intra and intermolecular coordination.

3.2 Initial Response of Biomolecular Systems to Ionizing Radiation

For biomolecules core-excitation induced distortions of the molecular geometry can cause loss of their functionality and can have harmful carcinogenic consequences.[5,6] Whereas non-radiative decay processes subsequent to the absorption of a high energy photon can transfer the system into an dissociative ionic final state, chemical bonds within a molecule can already break upon propagation on the initially populated core-excited state potential. This ultrafast structural and electronic response can be monitored by transitions between the transforming molecular orbitals using RIXS. Using this technique, Blum et al. have demonstrated that N K-edge RIXS is sensitive to core-excited state proton dynamics in the amino-acid glycine which exhibits a single N site.[104] Meyer et al. further established N K-edge spectroscopic fingerprints of model compounds and amino acids.[105–107] Especially for the amino-acids histidine and proline a strong impact of core-excitation induced molecular fragmentation and membrane contamination in their liquid cell sample environment contaminated the spectra.[105] Using a liquid jet sample environment (see also section 4) avoids these contaminations. It therefore allows to shed light of the apparently strong N 1s core-excited state dynamics in these systems, as it was done for histidine in **publication IV**. Here, the propensity of histidine for core-excitation induced fragmentation was investigated dependent on its chemical environment.

The structure of aqueous histidine is depicted in Fig. 3.6. Two of the three N atoms of histidine are part of an imidazole ring and the third forms an amino group. They exhibit a pH-dependent protonation in aqueous environments.[49] We demonstrate that the local valence electronic structure at the imidazole N sites in the system can be accessed selectively in dependence on their protonation state through the

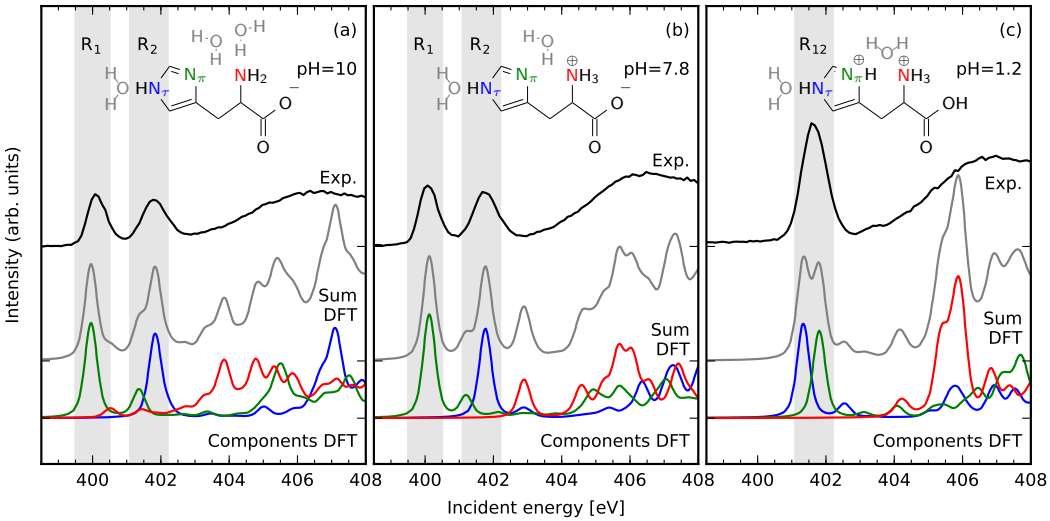

Figure 3.6: *Protonation-dependent access to N sites in the imidazole ring of histidine.* The N K-edge π^* absorption resonances of the N_τ and N_π sites are well separated due to their different protonation in basic (a) and neutral (b) environments, allowing to characterize the local electronic structure from emission spectra at the individual resonances. The chemical shift is reduced in an acidic environment (c) due to the protonation of both sides. Figure taken from **publication IV**.

chemical shift of their distinct N K-edge absorption resonances, as shown for basic and neutral conditions in Fig. 3.6a and b. Deprotonated imidazole N sites exhibit a red-shifted absorption resonance. The shift is of similar extend as the chemical shift between the resonances of 2-TP and 2-TP$^-$ presented in publication I. By tuning the energy to the isolated resonances of histidine in these environments, we could further establish an intense emission line originating from transitions between an occupied lone pair orbital and the N 1s core hole, equivalent to the deprotonation RIXS signature of 2-thiopyridone in publication II, as a unique RIXS fingerprint of deprotonated N sites in conjugated cycloorganic systems (see Fig. 3.7).

The extend of molecular deformation on the core-excited state PES within the duration of the scattering process is estimated from DFT based spectrum and dynamics simulations in the framework of the Z+1 equivalent core approximation (see Fig. 3.7 and 3.8). Solute solvent interaction is taken into account explicitly, through inclusion of surrounding water molecules in the simulation. We show that only minor structural deformations occur upon 1s core-excitation of the N sites in the imidazole ring of histidine (called N_π and N_τ) in a basic and neutral chemical environment. This yields the opportunity to characterize the detected transitions and their intensity with respect to the involved molecular orbitals. In contrast, the simulations presented in Fig. 3.8b, unravel a directional core-excitation induced N_τ-H dissociation for histidine in an acidic environment, which is present for excitations at both protonated imidazole N sites. This is reflected in drastic changes of the

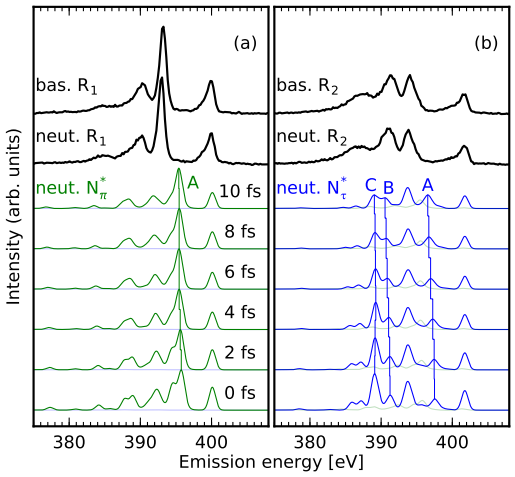

Figure 3.7: *N 1s emission signatures of protonation at the imidazole N sites of histidine.* Emission spectra from the deprotonated N site (a), here N_π, exhibit the characteristic fingerprint of an intense emission line originating from a N site centered lone pair orbital (see Fig. 3.8a). This feature is absent in the spectra for the protonated site (b), where a N–H binding sigma orbital is present instead. The simulated spectra for different propagation times within the Z+1 approximation remain nearly unaltered. Figure taken from **publication IV**.

electronic structure within the core hole lifetime (6.4 fs for N_2 [108]) and results in a loss of structure due to shifts and intensity changes of electronically inelastic transitions in the measured RIXS spectra. The site preference of core-excited state N-H dynamics is correlated with the local charge at the N_π and N_τ sites. Sites with higher local charge exhibit more drastic core-excited state dynamics. This correlation might allow

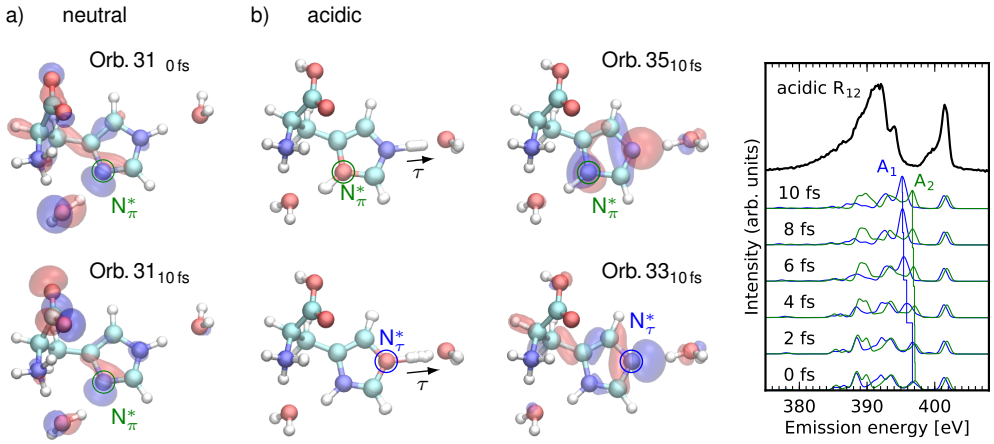

Figure 3.8: *N 1s core-excited state dynamics in histidine in the Z+1 approximation.* (a) Marginal dynamics in neutral and basic environments within 10 fs propagation allow to attribute intense emission lines to transitions from lone pair orbitals at deprotonated N sites in the imidazole ring. (b) In acidic solution, an excitation site independent N_τ deprotonation induces the formation of similar lone pair orbitals, altering the N_τ emission spectrum drastically within the scattering duration (feature A_1). Spectral features, as well as the local electronic structure at the N_π site remain mostly unaltered by the N_τ deprotonation (e.g. feature A_2). Figure taken and adapted from different figures in **publication IV**.

for estimations of N-H dissociation tendencies in N 1s core-excited states of other systems.

The highly directional dynamics of histidine in an acidic chemical environment in N 1s core-excited states exemplary illustrates that molecular geometries ranging from the ground state structure to configurations exhibiting fully dissociated bonds contribute to the RIXS intensity. The following section depicts how such directional structural deformations in core-excited states yield access to properties of molecular ground and valence-excited state potential energy surfaces.

3.3 Properties of Ground State Potentials from Core-Excited State Wave Packets

The energy of vibrationally excited states on a potential energy surface are defined by the chemical interactions within a molecule and with its chemical environment. Schreck et al. showed that populating the modes on the electronic ground state as RIXS final states allows to detect a fingerprint of the interaction between chloroform and acetone molecules in solution from high resolution RIXS spectra.[43] They proposed a method to extract potential energy surfaces from RIXS vibrational progressions. Eigenenergies of a Morse potential were fitted to peak positions in vibrationally resolved O K-edge RIXS spectra of pure acetone and acetone-chloroform mixtures. They seemed to yield direct access to the (hydrogen bond affected) molecular ground state potential along the O–C bond in acetone. The validity of this method was not confirmed from a theoretical perspective. For diatomic molecules in the gas phase the nuclear wave packet only propagates along the one existing inter-atomic bond in the core-excited state. Hence, the energy loss of the detected vibrational excitations can be directly related to the eigenenergies of the vibrational states on the one-dimensional potential energy curves.[40,45] For larger molecules the coupled motion along multiple nuclear coordinates has to be considered. Published vibrationally resolved RIXS data on triatomic or larger systems exist for liquid samples.[39,41,43,109] A direct comparison between the results of the potential extraction method and accurate quantum chemical potential simulations would be ideal to confirm the applicability of the potential reconstruction method. As intermolecular interactions are difficult to account for in simulations on a post HF level of theory, an isolated molecule in the gas phase consisting of at least three atoms would make an ideal test case.

The water molecule in its gas phase was investigated using O 1s RIXS by Weinhardt et al., who identified signatures of core-excited state dynamics in the detected electronically elastic RIXS transitions.[110] The experimental resolution in this study was insufficient to separate single vibrational peaks in the spectra. The gas phase water molecule thus exhibits all preconditions which are necessary to validate the potential reconstruction method. The system is small enough to simulate its potential energy surfaces along the O-H bonds and separately along the bending coordinate on post HF level of theory. The coupled stretch molecular dynamics can be simulated

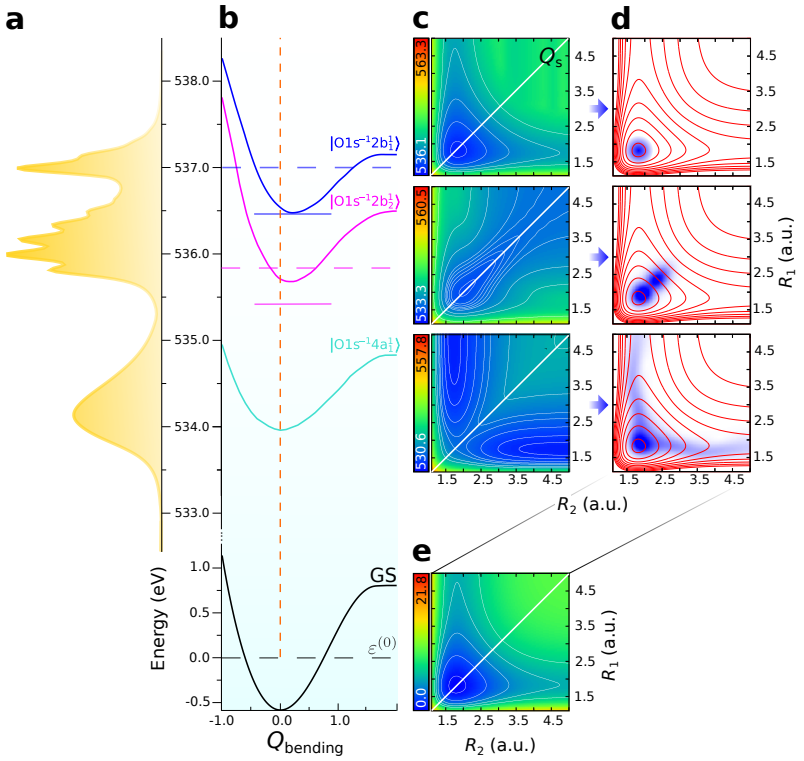

Figure 3.9: *Preparation of directional wave packets on the 1s core-excited state PESs of gas phase water.* The well separated X-ray absorption resonances (a) allow excitation of the nuclear wave packet from the ground state potential (b) bottom and (e) onto the potentials of the O 1s core-excited states (b) and (c). The potentials are shown along the bending coordinate (b) and the two O–H bond lengths R_1 and R_2 (c) and (e). The wave packets propagate dominantly along a single O–H bond, the symmetric stretch coordinate and the bending coordinate in the $|O1s^{-1}4a_1^1\rangle$, $|O1s^{-1}2b_2^1\rangle$ and $|O1s^{-1}2b_1^1\rangle$ states respectively. Figure taken from **publication V**.

using the wave packet formalism. The investigation of this computationally fully accessible system allows to identify the necessary properties of core-excited states and ground state vibrational modes yielding the possibility of a potential reconstruction, which is discussed in the publications V and VI. The studies are based on a comparison between vibrationally resolved O 1s RIXS spectra of gas phase water which we recorded with a resolution of 70 meV and the simulations. Under the mentioned experimental conditions, stretch and bending excitations as RIXS final states on the ground state PES are well separated.

In **publication V**, we discuss how directional and confined nuclear wave packets are generated in the different O 1s core-excited states. We show that their shape defines the transition rate into characteristically oriented vibrationally excited states on the ground state PES of the water molecule for electronically elastic RIXS transitions.

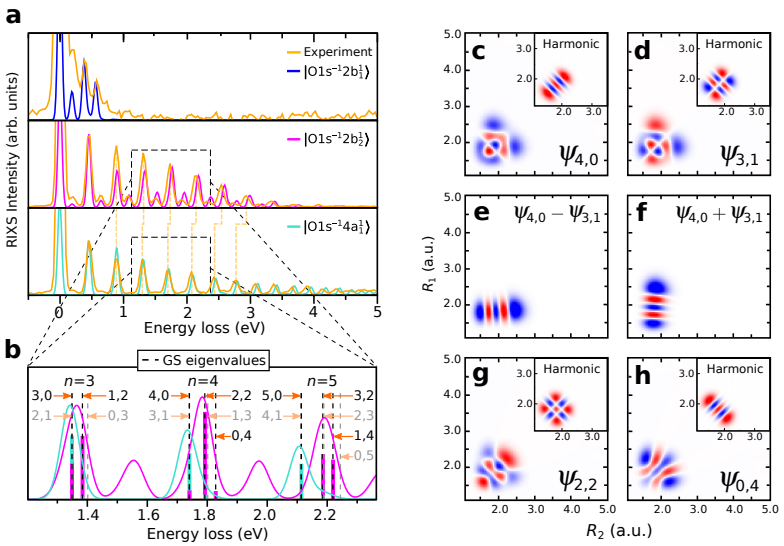

Figure 3.10: *Selective excitation of oriented ground state modes in the RIXS process.* A linear combination of nearly degenerate vibrational modes of the ground state potential allows to resemble the directionality defined by the O 1s core-excited state wave packets. The contribution of the modes (c-h) to the detected vibrational excitations in RIXS spectra at the different resonances (a) can be decomposed based on spectrum simulations (b). Figure taken from **publication V**.

The nuclear wave packets in three studied O 1s core-excited states are characterized dominantly by the determinants $|O1s^{-1}4a_1^1\rangle$, $|O1s^{-1}2b_2^1\rangle$ and $|O1s^{-1}2b_1^1\rangle$. The simulated propagated wave packets are depicted in Fig. 3.9. They are oriented almost exclusively along a single O–H bond R_1 or R_2, the symmetric stretch coordinate Q_s and the bending coordinate Q_b respectively. The projection of these confined, well oriented core-excited state wave packets onto the ground state vibrational modes in the emission step of the RIXS process yields a selective excitation of modes with the same orientation. In this context, we show that the coupled stretch modes can be sorted into groups with indices n according to their energy. The n-th group consists of $n+1$ nearly degenerate states of the coupled nuclear motion. A certain number of excited symmetric and anti-symmetric stretch quanta n_s and n_a, with $n = n_s + n_a$, can be assigned to each state within the n-th group. A linear-combination of states within these groups allows to generate the highly oriented states populated through the RIXS process, see Fig. 3.10.

On this foundation, we investigate how the wave packets and transition amplitudes into the individual vibrationally excited states are affected by deuteration and by alteration of the effective scattering time through detuning of the excitation photon energy from the individual resonances.[69] Furthermore, we identify and discuss spectral signatures of ultrafast dissociation processes in the spectra.[70]

In **publication VI**, we analytically derive how the confined wave packets yield

access to the eigenenergies of one-dimensional cuts through ground state PESs of a molecular system through the vibrational excitations detected in RIXS spectra. For that we link the RIXS transition amplitudes for a directionally confined core-excited state wave packet to the eigenenergies of a Hamiltonian defined by the one-dimensional cut through the ground state PES along the same direction in a system with coupled nuclear dynamics. Using this strict theoretical derivation, we validate the potential reconstruction method proposed by Schreck et al.[43] in the presence of highly directional core-excited state dynamics. Note that the nomenclature used here deviates slightly from the one used in publication V to be consistent with the wave packet formalism introduced in section 2.2.

We correlate the states of the n-th group on the potential energy surface j to RIXS features detected upon scattering through a single core-excited state C with the core-excited state Hamiltonian H_c. The fine structure of the transitions to the individual modes is expected to remain unresolved, e.g. due to a limited experimental resolution. Instead, a single vibrational emission line at the energy

$$\epsilon^{\mathrm{RIXS}} = \frac{\int_{\hbar\omega_{S,1}}^{\hbar\omega_{S,2}} \sigma(\hbar\omega_I, \hbar\omega_S)\hbar\omega_S \,\mathrm{d}\hbar\omega_S}{\int_{\hbar\omega_{S,1}}^{\hbar\omega_{S,2}} \sigma(\hbar\omega_I, \hbar\omega_S) \,\mathrm{d}\hbar\omega_S}$$

in the interval of scattering photon energies $[\hbar\omega_{S,1}, \hbar\omega_{S,2}]$ is detected. The scattering cross section σ results from the projection of the wave packet in equation 2.9 onto the vibrational states χ_{j,n_1n_2} of the surface j, integration for $T \to \infty$, summation over all modes, as well as taking the absolute square.

Here we neglect the dependence of the dipole moments between the electronic states on the nuclear coordinates and assume an infinite lifetime of the states on the surface j. We further assume that the RIXS process starts from the energetically lowest vibrational state of the electronic ground state with the energy $\epsilon_{1,00}$ and make use of the relation $\int_0^T e^{(-\alpha+i\beta)t}\,\mathrm{d}t = (-\alpha+i\beta)^{-1}[e^{(-\alpha+i\beta)T}-1]$. The expression for ϵ^{RIXS} thereby contracts to a sum over the states of the n-th group, if the considered energy interval is narrow enough and the states of different groups energetically well separable. The result reads

$$\epsilon_{j,n}^{\mathrm{RIXS}} = \frac{\sum_{n_1+n_2=n} |\langle\chi_{j,n_1n_2}|\tilde{\chi}^{\mathrm{C}}\rangle|^2 \epsilon_{j,n_1n_2}}{\sum_{n_1+n_2=n} |\langle\chi_{j,n_1n_2}|\tilde{\chi}^{C}\rangle|^2}, \tag{3.1}$$

$$|\tilde{\chi}^{\mathrm{C}}\rangle = \int_0^\infty e^{i(\hbar\omega_I+\epsilon_{1,00}+i\Gamma_{\mathrm{C}})t/\hbar} e^{-iH_ct}\chi_{1,00}. \tag{3.2}$$

$\tilde{\chi}^c$ defines the wave packet which was propagated on the core-excited state PES. * We will derive now how the projection of wave packets, which are strongly confined

*Note that the exponent in the integrand of the wave packet in formula 3.2 misses a term containing the energy difference between the electronic ground and the considered core-excited state, when compared to the derivation in publication VI. The difference originates from an increase of numerical precision for the wave packet propagation through redefinition of the energy of the PES with respect to the vertical transition energy and has no impact on the conclusions drawn here.

along a certain direction of Q_1 in the space or nuclear coordinates, is correlated with the eigenvalues of a one-dimensional Hamiltonian defined by the PES j along the coordinate Q_1 for the coupled stretch motion along two coordinates. Q_2 is defined to be orthogonal to Q_1. The confinement of $\tilde{\chi}^c$ along Q_1 at a certain $Q_2 = Q_{2e}$ is described as

$$\tilde{\chi}^{\mathrm{C}}(Q_1, Q_2) = \Phi(Q_1)\Delta(Q_2 - Q_{2e}),$$

where Δ is a sharp, normalized function. The Hamiltonian $\tilde{H}_j(Q_1)$ along Q_1 is generated from the Hamiltonian for nuclear motion in equation 2.4. For the coupled nuclear motion along the coordinates Q_1 and Q_2, with the reduced masses μ_1 and μ_2 it has the form

$$H_j(Q_1, Q_2) = -\frac{\partial^2_{Q_1}}{2\mu_1} - \frac{\partial^2_{Q_2}}{2\mu_2} - \zeta\partial_{Q_1}\partial_{Q_2} + E_j(Q_1, Q_2).$$

$\tilde{H}_j(Q_1)$ results as

$$\tilde{H}_j(Q_1) = \langle\Delta|H_j(Q_1, Q_2)|\Delta\rangle_{Q_2} \approx -\frac{\partial^2_{Q_1}}{2\mu_1} + E_j(Q_1, Q_{2e}) + c. \tag{3.3}$$

The term c contains a constant $\langle\Delta| - (2\mu_2)^{-1}\partial^2_{Q_2}|\Delta\rangle$ and higher order terms resulting from the expansion of $E_j(Q_1, Q_2)$ around $Q_2 = Q_{2e}$, which become negligible upon strong confinement of the wave packet. The mass polarization term in $H_j(Q_1, Q_2)$ yields

$$\begin{aligned}
-\zeta\langle\Delta|\partial_{Q_2}|\Delta\rangle\partial_{Q_1} &= -\zeta\int_{-\infty}^{\infty}\Delta(Q_2)\partial_{Q_2}\Delta(Q_2)\,\mathrm{d}Q_2\partial_{Q_1} \\
&= -\zeta\frac{1}{2}\int_{-\infty}^{\infty}\partial_{Q_2}\Delta(Q_2)^2\,\mathrm{d}Q_2\partial_{Q_1} \\
&= -\zeta\,\frac{1}{2}\Delta(Q_2)^2\Big|_{-\infty}^{\infty}\partial_{Q_1} = 0
\end{aligned}$$

and therefore does not contribute to $\tilde{H}_j(Q_1)$.

Now the core-excited state wave packet is expressed in the basis of eigenstates $\tilde{\psi}_n(Q_1)$ of the Hamiltonian $\tilde{H}_j(Q_1)$ with the eigenenergies $\tilde{\epsilon}_{j,n}$

$$\begin{aligned}
|\Phi\rangle &= |\tilde{\psi}_n\rangle\langle\psi_n|\Phi\rangle + \sum_{m\neq n}|\tilde{\psi}_m\rangle\langle\tilde{\psi}_m|\Phi\rangle, \\
\langle\chi_{j,n_1n_2}|\tilde{\chi}^{\mathrm{C}}\rangle &= \langle\chi_{j,n_1n_2}|\Delta\Phi\rangle \\
&= \langle\chi_{j,n_1n_2}|\Delta\tilde{\psi}_n\rangle\langle\tilde{\psi}_n|\Phi\rangle + \sum_{m\neq n}\langle\chi_{j,n_1n_2}|\Delta\tilde{\psi}_m\rangle\langle\tilde{\psi}_m|\Phi\rangle.
\end{aligned} \tag{3.4}$$

We also show that

$$\langle\chi_{j,n_1n_2}|\Delta\tilde{\psi}_m\rangle \approx 0, \quad n_1 + n_2 = n \neq m$$

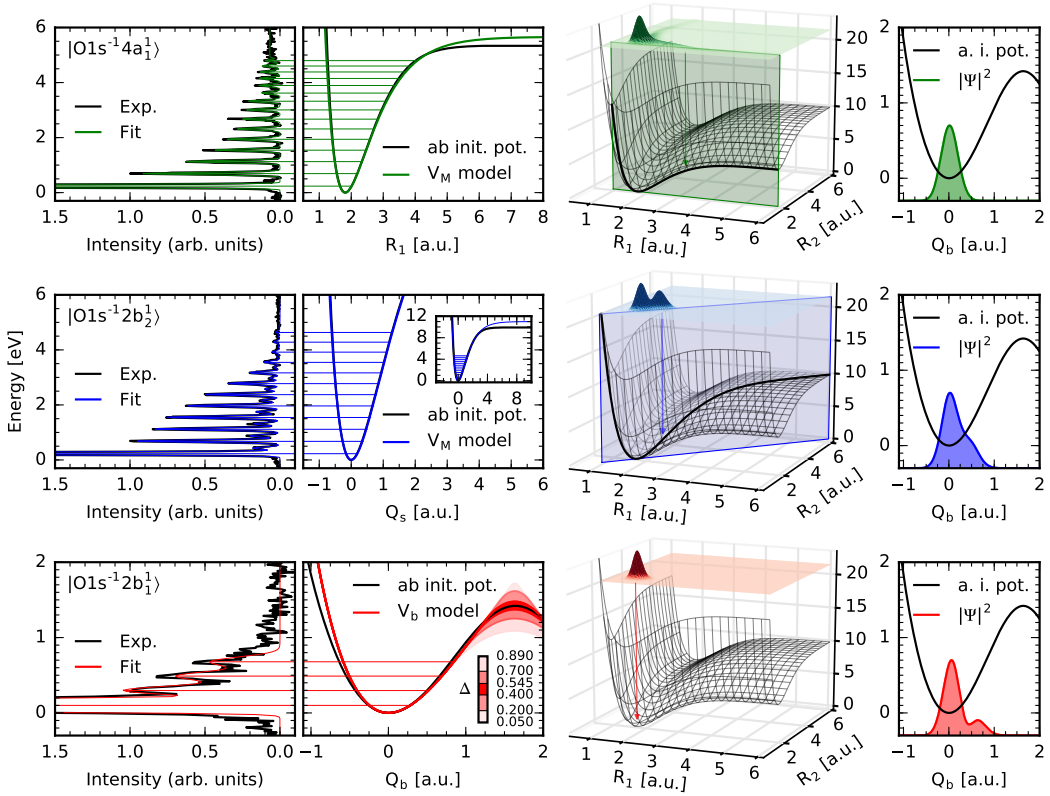

Figure 3.11: *One-dimensional ground state potential reconstruction from O 1s high resolution RIXS spectra of the water molecule.* RIXS spectra at the different O 1s resonances, reconstructed potentials in comparison to simulated one-dimensional cuts through the ground state potential and core-excited state wave packets along the different nuclear coordinates are shown from left to right. The strong confinement and orientation of the nuclear wave packets allows an accurate potential reconstruction along three distinct directions and in a wide range of molecular distortions. Figure partially taken and adapted from **publication VI**.

for the energetically well separated groups n and m. This can be used to further simplify expression 3.1 by implementing relation 3.4. We thus obtain

$$\begin{aligned}\epsilon_{j,n}^{\mathrm{RIXS}} &= \sum_{n_1+n_2=n} \langle \Delta\tilde{\psi}_n | \chi_{j,n_1n_2} \rangle \epsilon_{j,n_1n_2} \langle \chi_{j,n_1n_2} | \Delta\tilde{\psi}_n \rangle \\ &= \langle \Delta\tilde{\psi}_n | H_j | \Delta\tilde{\psi}_n \rangle = \langle \tilde{\psi}_n | \tilde{H}_j | \tilde{\psi}_n \rangle = \tilde{\epsilon}_{j,n}.\end{aligned}$$

The energy of the experimentally detected spectral lines therefore correspond to the eigenenergies $\tilde{\epsilon}_{j,n}$ of the reduced Hamiltonian $\tilde{H}_j$ along the coordinate Q_1 defined by the confinement of the core-excited state wave packet. This means, they can be used to reconstruct cuts through PESs along this confinement coordinate from vibrationally resolved RIXS spectra.

The concept is verified by direct comparison between the potentials extracted from experimental RIXS spectra of H_2O at the different O 1s resonances to the ones

along R_1, Q_s and Q_b resulting from ab-initio simulations of the system, presented in Fig. 3.11. Even though a simple Morse potential was used in the fitting routine, the approximated potentials along R_1 and Q_s show excellent agreement with the theoretical simulations the probed energy range up to 5 eV above the zero point vibrational mode. As only three bending excitations are visible in the $|O1s^{-1}2b_1^1\rangle$ spectrum, the reconstruction of the bending potential did not yield a precise estimate of the barrier height at a bond angle $\angle(HOH)$ of 180° but still confirmed the validity of the reconstruction principle.

Chapter 4

Soft X-ray Spectroscopy Instrumentation for Molecular Dynamics

The experimental infrastructure which enabled the soft X-ray spectroscopy studies of liquid and gaseous samples in the publications I-VI will be introduced here. It will be illustrated how accelerator based light sources provide soft X-ray radiation with sufficient intensity and the required temporal pulse structure for static and time-resolved X-ray absorption and RIXS investigations. The suitability of liquid jet and cell based sample environments for measurements under the necessary high and ultra-high vacuum conditions will be discussed. Their measurement scheme dependent implementation in different experimental setups will be outlined. In that context special properties of RIXS spectrometers used in the publications I, II, IV, V and VI are addressed. Technical developments for low-noise time-resolved XAS on picosecond timescales using liquid flat-jet technology are presented as publication VII. Efficient methods to temporally correlate optical and X-ray pulses are essential tools to compensate for pulse arrival time jitter at X-ray FELs and to temporally overlap and X-ray optical pulses in femtosecond time-resolved experiments. Concepts exploiting thin film interference effects have proven to yield an efficient detection of X-ray-induced optical reflectivity changes as a temporal cross-correlation method and a relative pulse arrival time monitor.[111–116] These concepts were extended towards the detection in optically induced X-ray reflectivity changes of multilayer structures in publication VIII. Thereby, an efficient X-ray optical cross-correlator for low-flux femtosecond X-ray sources has been developed.

4.1 Soft X-ray Light Sources

The spectroscopy techniques discussed above require high brilliance soft X-ray light sources as they rely on core-excitation of a sample using wavelength tunable radiation with narrow bandwidth in the photon energy range between 100 and 1000 eV. Despite pioneering efforts using high harmonic generation energy upconversion techniques driven by optical-laser systems,[26–31] third generation synchrotrons and

free electron lasers as accelerator based sources uniquely provide radiation fulfilling these requirements.

At these sources, synchrotron radiation is generated from electron bunches, traveling at relativistic energies, upon passage through magnetic fields. The high kinetic energy of the electrons, e.g. 1.7 GeV at the synchrotron BESSY II, causes the emitted radiation generated in an undulator, a section exhibiting alternating magnetic field B with the period λ_u, to be emitted dominantly in the propagation direction of the electron bunch and to exhibit a wavelength λ of

$$\lambda = \frac{\lambda_u}{2n\gamma^2}[1 + K^2/2 + (\theta\gamma)^2], \tag{4.1}$$

$$\text{with} \quad K = \frac{eB\lambda_u}{2\pi mc}.$$

Here, θ is the angle with respect to the undulator axis, n is the considered undulator harmonic, e and m are charge and mass of the electron and $\gamma = 1/\sqrt{1 - v^2/c^2}$ is the Lorentz factor with the velocity of the electrons v and the speed of light c. The magnetic structure usually consists of alternating pairs of permanent magnets and the emitted wavelength is adapted through magnetic field alterations. A two-fold relativistic correction through the factor γ^{-2} allows to generate radiation with nanometer wavelength using magnetic structures with periods in the ten millimeter range. The correction results from a length contraction of λ_u in the rest frame of the moving electrons in addition to a relativistic doppler effect between the radiation-emitting moving electrons and the laboratory frame. For $K \leq 1$ the magnetic structure is defined as an undulator. The magnetic field causes only a weak disturbance of the electron path inducing an approximately harmonic motion of the electrons in the periodic magnetic field and thus the first harmonic wavelength ($n = 1$ in equation 4.1) dominates the spectrum of emitted radiation. Higher K values yield stronger anharmonicities and thus a higher spectral contribution of higher harmonics ($n > 1$). Tuning K can conclusively be utilized to generate intense, narrow bandwidth radiation across a broad energy range. Special arrangement of the magnet pairs within undulator allows for the generation of linearly polarized light with a freely tunable polarization angle or even circular polarization.[117, p.141-188]

A pulsed source is required for optical pump X-ray probe experiments. At synchrotron light sources the electrons in the storage ring are kept at constant energy by a periodic potential. This induces the formation of electron bunches in potential buckets. These bunches generate light pulses with a duration in the picosecond range depending on the parameters of the storage ring. Laser systems can be frequency locked to the X-ray pulses originating from individual bunches. By that optical pump X-ray absorption probe studies can be performed routinely with picosecond resolution.[18–20,23,24] At dedicated beamlines femtosecond resolution is available at the cost of orders of magnitude reduced flux using the femtoslicing method.[118–121] At the synchrotron BESSY II the buckets are separated by 2 ns. In the regular operation mode, the bunches exhibit a length of approximately 50 ps, whereas few picoseconds long bunches are available in low-α operation.

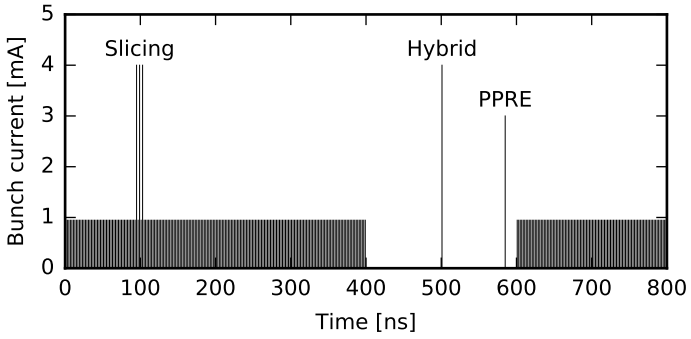

Figure 4.1: *BESSY II fill pattern with special bunches for time-resolved X-ray spectroscopy techniques.* Three bunches are used to generate femtosecond pulses at the slicing facility at kHz repetition rates. The isolated hybrid and PPRE bunches can be used for picosecond studies at MHz repetition rates.

The bunch filling pattern at BESSY II, depicted in Fig. 4.1 has a period of 800 ns, which corresponds to a single revolution of an electron bunch in the storage ring. It consists of a multi-bunch train of 600 ns length and a 200 ns gap with dominantly empty buckets. Five special bunches exhibiting a higher charge are available: the three slicing bunches located within the multi-bunch train, the hybrid bunch in the center of the gap and the PPRE (pulse picking by resonant excitation[122]) bunch at the end of the gap. The hybrid bunch is utilized in the context of this thesis in an optical pump transmission **X-ray absorption** probe experimental scheme, in combination with a MHz laser system, for investigations of photochemical processes in solution, which are discussed in more detail in section 4.5.

At high bunch currents and in long undulator sections the interaction between the electric field of radiation and the electrons can imprint a periodic substructure on the electron bunches, called microbunching. Through stimulated coherent emission of radiation by all electrons in the bunch a drastic gain in radiated intensity compared to classical undulator radiation can be achieved.[123] Based on this concept intense ultrashort X-ray pulses of coherent radiation are generated at FELs.[124]

RIXS studies of dilute molecular systems require the flux of all pulses with pulse arrival rates in the few hundred MHz range at modern synchrotron radiation light sources, due to the low yield of fluorescent decay pathways and a limited efficiency for the detection of inelastically scattered photons. A high average photon flux at synchrotrons on the order of 10^{12} ph/s in the required photon energy bandwidth on the sample (see also section 4.4) is necessary for reasonable acquisition times in a range minutes to hours. Therefore, X-ray FELs are used for time-resolved RIXS investigations. They generate narrow bandwidth soft X-ray radiation at comparable average flux, lower pulse arrival rates and femtosecond pulse lengths, making RIXS investigations of ultrafast molecular dynamics possible. The FEL LCLS was utilized in a time-resolved RIXS investigation discussed in publication II of this thesis. It provides pulses with a length on the order of 100 fs at a rate of 120 Hz.[124] They are frequency locked to optical laser pulses with equivalent length for optical pump X-ray probe experimental schemes.

4.2 Gas Phase and Liquid Sample Environments

The required sample geometry and dimension for a soft X-ray spectroscopy measurements depends on multiple parameters. Specific requirements of the used method, the available photon flux in relation to the detection efficiency, the temporal stability of the sample environment, the investigated absorption resonance, the elemental composition of solute and solvent in dilute samples, as well as the sample density have to be considered. Hard X-ray spectroscopy experiments can be performed partially under ambient pressure and with sub-millimeter sample thicknesses for transmission measurements.[125–131] The high absorption cross section of nitrogen and oxygen for soft X-ray radiation demands in-vacuum sample environments and photon detection schemes. Additionally, micrometer attenuation lengths in most materials in their condensed phases have to be taken into account.[132] A commonly applied method to prepare suitable liquid or gas volumes in the focus of an intense X-ray beam is utilizing membranes with thicknesses on the order of few ten to hundreds of nanometers to separate the sample liquid from the experimental vacuum chamber.[19,20,133–137] In this way gas phase and liquid sample environments can be established even in ultra high vacuum experimental chambers which were originally dedicated to solid sample environments. We implemented silicon-nitride and carbon membranes in a heatable cell for high resolution RIXS measurements in gaseous and liquid sample environments. I took part in the commissioning of the custom built cell, which was then used to acquire the high resolution oxygen 1s RIXS data set discussed in publications V and VI as well as the related studies[69,70].

Membranes can cause multiple experimental complications when in contact with the investigated sample. They can yield distortions of the measured signal or even make the experiment unfeasible. Examples are radiation damage of the membrane material through the exposure to intense synchrotron radiation and small focus sizes, adsorption of radiation damaged sample material on the membrane or in the solution in the interaction volume.[138,139] Thermal-load-induced strain and insufficient sample replenishment impair optical pump X-ray probe measurements. In-vacuum liquid jet technology allows to circumvent the mentioned deficits by spraying the sample liquid into the experimental vacuum chamber in form of a few micrometer to few ten micrometer thick liquid jet which is commonly frozen within a cryogenic trap after the interaction with the soft X-ray radiation, to avoid evaporation into the vacuum chamber.[140]

4.3 Liquid flexRIXS Experimental Setup

The liquid flexRIXS experimental setup, which was developed by the Helmholtz-Zentrum Berlin for static and time-resolved RIXS measurements of bulk and dilute liquid samples at synchrotrons and free electron lasers, employs a round in-vacuum liquid jet, with a diameter of 20 to 30 μm in combination with a compact RIXS spectrometer with high transmission.[140] It was used to acquire the data discussed in

publications I, II, IV and VI. I contributed to the optimization of the experimental endstation yielding improvements in efficiency and precision of the performed measurements at the synchrotron BESSY II.

The setup consists of a high vacuum chamber, housing the liquid jet, a differential pumping stage and a Scienta XES 350 RIXS spectrometer (see section 4.4) in slitless operation under 90° scattering geometry. The high vacuum chamber is operated at a pressure $< 10^{-2}$ mbar, which is achieved through turbo-molecular pumps and two liquid N_2 cooled cryogenic traps. In the first trap the sample liquid is frozen directly. The second trap reduces the load on the turbo pumps by freezing out evaporated sample. The experiment is coupled to the beamline via the differential pumping stage. The beamline consists of mirrors and gratings which guide, monochromatize and focus the X-ray beam from the undulator on its path to the experiment. To maximize the beamline transmission throughout the soft X-ray photon energy range and avoid contamination of optics, all beamline sections and optical elements are operated under ultra high vacuum conditions. Using the differential pumping stage, approximately five orders of magnitude pressure difference between the experiment and the beamline are bridged.

We upgraded the system by the implementation of a sample catcher system which avoids freezing the sample liquid within the experimental chamber and allows for lower sample consumption through optional recirculation. Operation of the setup with the catcher reduces the pressure in the chamber to approximately 5×10^{-4} mbar for aqueous sample solutions. This reduces the load on the cryogenic trap and allows for days of continuous measurement campaigns, instead of hours of operation with the first cryogenic trap. The liquid jet has to hit the center of the catcher opening with a diameter of 500 μm also upon changes of the alignment with respect to the synchrotron X-ray beam and the spectrometer. Hence, synchronized motorized motion of the jet and the catcher is a necessity to achieve efficient, stable and reproducible experimental conditions. In this context, the simultaneous motion of motors, control of beamline parameters and automatized measurement routines were implemented together with new hardware for motorization and data acquisition. In addition, online and post beamtime data analysis software was developed for the use within the FG-ISRR and for users of the endstation.

4.4 RIXS Spectrometers

The **Scienta XES 350** spectrometer is a medium resolution, high transmission instrument with a compact design. It consists of a set of three gold coated blazed spherical gratings, a slit with an adjustable width between 0 and 400 μm and an multi-channel plate (MCP) detector which are aligned in a Rowland circle geometry.[141] Its 1200 mm^{-1} grating exhibits a resolving power of $E/\Delta E \gtrsim 1000$ over the entire range of soft X-ray photon energies from 100 until 1000 eV. With a grazing incidence angle of 1.9° and a grating radius of 5 m, it has an entrance arm length of only 165.8 mm.[142,143] It is operated with the liquid jet as the source in an open slit configuration within

the liquid flexRIXS instrument resulting in slight deviations of the detector position from the Rowland circle geometry for an optimal resolution.[144] A CsI coated MCP detector, which is not sensitive to visible radiation, is used to detect the scattered X-ray photons, that originate from the liquid jet and are diffracted depending on their energy by the grating. The spectrometer can therefore be implemented in optical pump X-ray probe experimental schemes. The overall detection efficiency for isotropically emitted radiation from the sample is approximately 10^{-7}.[140] Considering a yield for fluorescent decay of the core-excited states on the order of 10^{-2}, photon count rates of 10^3 per second can be achieved for bulk sample materials illuminated with 10^{12} photons per second. For dilute samples, the count rate depends drastically on the investigated X-ray absorption edge and the elemental composition of the solvent. The measurements at the N K-edge edge of aqueous solutions were performed at sample concentrations in the 100 mM range. Here, count rates of $\sim 10^2$ per second could be achieved at the beamline U49-2_PGM-1 at the synchrotron BESSY II due to the high transmission of the solvent in the investigated range of photon energies.

The **SAXES** spectrometer is a dedicated high resolution instrument with a resolving power of $E/\Delta E \gtrsim 10000$ in an energy range from 400 to 1100 eV, which is attached to the RIXS endstation of the ADRESS beamline at the Swiss Light Source (SLS) in Villigen, Switzerland. It was used to record the vibrationally resolved RIXS spectra of the gas phase water molecule in publications V and VI. Its only optical element is, as for the Scienta XES 350, a spherical grating, which in contrast exhibits a variable line spacing. In addition to optical aberration minimization, this yields a less grazing incidence of the dispersed spectral lines on the detector, as they are focused at a position deviating from the Rowland circle geometry. CCD detectors can thus be used as analyzers. The high resolution is achieved through a high average grove density of the grating of 1500 or 3000 mm^{-1}[145], a substrate radius of 60 m and an 1050 mm entrance arm length. Hence, micrometer alignment precision and stability of the sample and the detector position is required for an ideal resolution. The instrument is also operated slitless. In an optimal alignment its resolution is limited by the energy bandwidth used to excite the sample, the focus size in the dispersive direction, which is below 5 μm, and the pixel size of the used detector.[95,146]

4.5 Time-resolved XAS in Transmission Mode

Transmission soft X-ray absorption measurements of liquid samples composed dominantly of light elements usually require sample thicknesses ranging from few micrometers down to few hundred nanometers. Thereby, a transmission and photon energy dependent transmission changes of the incident radiation on the order of percent is ensured.[132] This is required for a linear response of used detectors and electronics. Round jets are not well suited for transmission absorption measurements due to their uneven profile across the X-ray focal spot which usually has an expansion on the order of micrometers to few ten micrometers perpendicular to the direction of beam propagation. Free flowing flat liquid sheets with similar or greater

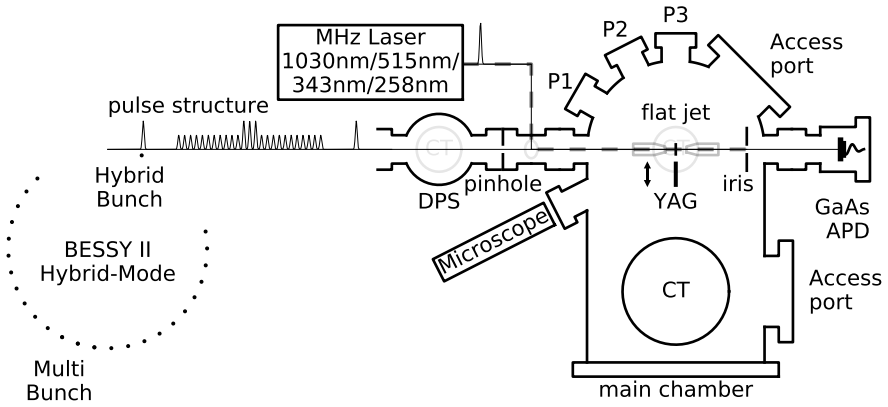

Figure 4.2: *Low noise transient transmission mode XAS on liquid samples.* Differential measurements of photo-induced transient X-ray absorption changes at MHz repetition rates are possible using laser pulses, which are frequency locked to the arrival rate of X-ray pulses originating from the hybrid bunch in the BESSY II pulse pattern. The intensity of individual X-ray pulses transmitting the sample is recorded as voltage pulses on an avalanche photo-diode. The liquid sample environment is established through collision of two round liquid jets forming a liquid sheet with micrometer to sub-micrometer thicknesses. Figure taken and adapted from **publication VII**.

thicknesses have been successfully implemented in pump probe experiments at hard X-ray synchrotrons.[125–131] Recent jet technology developments allow to generate in-vacuum free-standing liquid sheets with few-micrometer to sub-micrometer thicknesses suitable for soft X-ray absorption spectroscopy in a transmission experimental configuration.[62,147] One way to generate them is the collision of round jets with micrometer thicknesses. In **publication VI** we introduce an experimental setup which combines such a flat-jet with a MHz laser system and the dedicated X-ray pulse pattern of the synchrotron BESSY II for low–noise picosecond time-resolved optical pump soft X-ray probe measurements in a transmission experimental geometry.

A schematic overview of the experiment is presented in Fig. 4.2. We developed and commissioned the setup for the use at the open port beamline UE52_SGM. There, the pulses of a fiber laser system operated at a wavelength of 1030 nm are synchronized with the arrival of the X-ray pulses originating from the hybrid bunch in the gap of the BESSY II fill pattern. The fundamental wavelength and its harmonics are available for the excitation of the sample at fractions of the BESSY II pulse pattern repetition rate $1.25/n$ MHz, $n \in \mathbb{N}$. This enables the quasi simultaneous detection of the ground state and the photo excitation affected X-ray absorption signal in transmission mode. An avalanche photo-diode is used as a time sensitive X-ray intensity monitor. We demonstrate the feasibility to record static soft X-ray absorption spectra in a range of concentrations between tens of molar and tens of millimolar for bulk and dilute samples and for solutes below and above the main absorption edge of the solvent. Additionally, we benchmark the detection efficiency for transient photo-

excitation induced X-ray absorption changes at 208 kHz repetition rate and the available excitation wavelengths to be on a sub–mOD (optical density) level based on the transient absorption of photo-excited aqueous iron(II)-trisbipyridine.

4.6 Timing at Free Electron Lasers and Synchrotrons

The overlap between the optical and the X-ray pulse at the sample position are an essential precondition for successful time-resolved experiments. Spatially the two beam paths can be aligned on fluorescent screens positioned at the actual sample position which can be monitored visually using optical microscopy. The temporal overlap can be achieved to a precision of few ten picoseconds using silicon avalanche photo-diodes with a small active surface which yields a fast response to the impact of both optical and X-ray pulses. If the transient effect which is supposed to be induced by the impact of the optical pulses in the actual sample material can be detected efficiently with the X-ray probe technique, the temporal overlap of the pulses down to the pulse length limited precision can be established by changing the delay within a few ten picoseconds broad range. In experiments which require long acquisition times e.g. due to low flux provided by the X-ray source or if a photon hungry technique like RIXS is applied, the relative arrival time of the two pulses needs to be known more precisely, prior to the actual experiment. Voltage pulses resulting from the emission of photoelectrons from a conducting material can be monitored to achieve a temporal overlap with few picoseconds precision.[148] This timing method is only applicable, if sufficient intensity of both optical and X-ray pulses and short pulse lengths are available. The sampling rate of the electronics used to detect the impact of the light pulses limits the timing precision of this technique. The requirements for the mentioned method already indicates that different methods have to be applied dependent on the available X-ray pulse energy, if the temporal overlap needs to be established with sub-picosecond precision. To achieve a temporal overlap on a femtosecond timescale, we optimized the X-ray optical cross correlation contrast in specific reference pump-probe measurements which are tailored to application with intense ultrashort X-ray pulses and under low X-ray flux conditions.

To establish the temporal overlap for the time-resolved N K-edge RIXS measurements in publication II, concepts for X-ray optical temporal cross correlation methods at **free electron lasers** based on X-ray induced optical reflectivity changes (see Fig. 4.3 left) were optimized.[51] The results can be used to further improve existing schemes for the detection of the jitter affected relative pulse arrival time in the interaction region.[111–116] The method is based on changes of optical refractive indices induced by the absorption of intense X-ray pulses in semiconducting thin film samples. Non-radiative decay subsequent to soft X-ray absorption processes within semiconducting and insulating materials yields a high density of excitations across the band gap through cascading inelastic scattering events. This altered band population affects the refractive index of the excited material in dependence of the optical wavelength through bandgap shrinkage, bandfilling and free carrier absorption

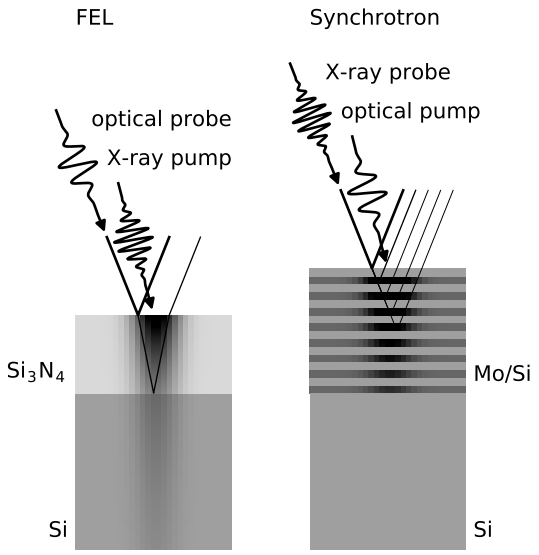

Figure 4.3: *Femtosecond temporal cross correlation at FELs and synchrotrons.* Both concepts are based on transient reflectivity changes of thin film samples for the used probe radiation, which can be maximized by choice of thin film structures and the experimental geometry. Interference between probe radiation reflected at the different interfaces of the thin film structures is altered by the impact of the pump pulse. Transient variation of optical refractive indices in silicon nitride and the silicon substrate yield the cross correlation contrast at the FEL, whereas the propagation of phonons in the molybdenum/silicon multilayer structure induces transient strain and layer expansion affecting the intensity and position of Bragg reflexes.

effects.[149] Additionally, the electronic system and the lattice thermalize on ultrafast timescales which also affects the width of the band gap and hence the refractive index after the excitation.[149] The resulting ultrafast changes of optical properties can be detected by transient optical reflectivity in an X-ray pump optical probe experimental scheme. Optimization of thin film thicknesses and the experimental geometry are key concepts to drastically alter the shape and amplitude of the relative reflectivity changes as the cross-correlation signal.[51] Interference between fractions of the optical probe radiation reflected at the different interfaces can be used to minimize the reflectivity of a sample in dependence on the used probe wavelength by adaption of the thin film thickness and the angle of incidence with respect to the sample surface. As this destructive interference is strongly dependent on the optical path-length within the thin film, transient changes of the real part of the refractive index, which are of particular interest for probe photon energies far below the band gap of the used thin film material, can be sensitively detected in this configuration. These concepts were used to successfully establish the temporal overlap for the time-resolved N K-edge RIXS measurements presented in publication II, using the transient reflectivity of a silicon nitride film on a silicon substrate.

In **publication VIII** an efficient method for X-ray optical cross-correlation at **synchrotron light sources** based on optically induced X-ray reflectivity changes of a thin film multilayer structure is discussed (see Fig. 4.3 right). As in the previously discussed method, interference conditions are transiently altered also in this scheme. We monitor the X-ray reflectivity of Bragg reflectors. At a fixed photon energy, the reflectivity strongly depends on the angle of the incoming X-ray beam with respect to the orientation of the layers, as well as on the thicknesses and refractive indices of the materials the multilayer structure is composed of.[150,151] Using a silicon-molybdenum

multilayer structure, we show that selective optical excitation of the molybdenum layers can be used as a versatile tool to establish the X-ray optical temporal overlap for pump probe experiments. The selective excitation of the superlattice structure, in the metallic and thus strongly absorbing molybdenum layers, alters its Bragg condition transiently. On sub-picosecond to few picosecond timescales after the optical excitation propagating phonons alter the intensity of the superlattice Bragg peaks periodically.[152,153] On few ten picosecond timescales thermalization induces an expansion of the lattice which shifts the entire Bragg peak in the reciprocal space. Both effects can be efficiently detected in an optical pump X-ray reflectivity probe experimental scheme and utilized to correlate the pulses on femtosecond and picosecond timescales.

Chapter 5

Publications

Publication I

Molecular structures and protonation state of 2-Mercaptopyridine in aqueous solution

S. Eckert, P.S. Miedema, W. Quevedo, B. O'Cinneide, M. Fondell, M. Beye, A. Pietzsch, M. Ross, M. Khalil, and A. Föhlisch

Chemical Physics Letters ***647****, 103-106 (2016)*

Publication II

Ultrafast Independent N-H and N-C Bond Deformation Investigated with Resonant Inelastic X-Ray Scattering

S. Eckert, J. Norell, P. S. Miedema, M. Beye, M. Fondell, W. Quevedo, B. Kennedy, M. Hantschmann, A. Pietzsch, B. van Kuiken, M. Ross, M. P. Minitti, S. P. Moeller, W. F. Schlotter, M. Khalil, M. Odelius, and A. Föhlisch

Angewandte Chemie International Edition ***56****, 6088-6092 (2017)*
Angewandte Chemie ***129****, 6184–6188 (2017)*[*]

[*]The german version of the article is not printed here. It can be accessed online through the DOI 10.1002/ange.201700239.

Publication III

T_1 Population as the Driver of Excited-State Proton Transfer in 2-Thiopyridone

S. Eckert, J. Norell, R. M. Jay, M. Fondell, R. Mitzner, M. Odelius, and A. Föhlisch

Submitted to the Chemistry – A European Journal (under review)

Publication IV

Valence orbitals and local bond dynamics around N atoms of histidine under X-ray irradiation

S. Eckert, J. Niskanen, R. M. Jay, P. S. Miedema, M. Fondell, B. Kennedy, W. Quevedo, M. Iannuzzi, and A. Föhlisch

Physical Chemistry Chemical Physics ***19****, 32091–32098 (2017)*

Publication V

Selective gating to vibrational modes through resonant X-ray scattering
R. C. Couto, V. Vaz da Cruz, E. Ertan, S. Eckert, M. Fondell, M. Dantz,B. Kennedy, T. Schmitt, A. Pietzsch, F. F. Guimarães, H. Ågren, F. Gel'mukhanov, M. Odelius, V. Kimberg, and A. Föhlisch
Nature Communications ***8****, 14165 (2017)*

Publication VI

One-dimensional cuts through multidimensional potential energy surfaces by tunable x rays

S. Eckert, V. Vaz da Cruz, F. Gel'mukhanov, E. Ertan, N. Ignatova, S. Polyutov, R. C. Couto, M. Fondell, M. Dantz, B. Kennedy, T. Schmitt, A. Pietzsch, M. Odelius, and A. Föhlisch

Physical Review A ***97****, 053410 (2018)*

Publication VII

Time-resolved soft X-ray absorption spectroscopy in transmission mode on liquids at MHz repetition rates

M. Fondell, S. Eckert, R. M. Jay, C. Weniger, W. Quevedo, J. Niskanen, B. Kennedy, F. Sorgenfrei, D. Schick, E. Giangrisostomi, R. Ovsyannikov, K. Adamczyk, N. Huse, Ph. Wernet, R. Mitzner, and A. Föhlisch

Structural Dynamics ***4****, 054902 (2017)*

Publication VIII

Versatile soft X-ray-optical cross-correlator for ultrafast applications
D. Schick, S. Eckert, N. Pontius, R. Mitzner, A. Föhlisch, K. Holldack, and F. Sorgenfrei
Structural Dynamics ***3****, 054304 (2016)*

Chapter 6

Conclusion and Future Prospects

In this thesis, photo-induced molecular proton dynamics were accessed at active atomic sites. The local detection of nitrogen and oxygen protonation enabled studies of proton dynamics in the electronic ground state and on both valence and core-excited state potential energy surfaces. The identification of transiently populated valence-excited states allowed to determine proton transfer mechanisms along relaxation pathways on femto- to nanosecond timescales. Access to proton dynamics in the electronic ground state and in core-excited states was gained through highly directional structural deformations within femtosecond core-hole lifetimes.

With the investigation of excited state proton transfer dynamics of 2-thiopyridone, we demonstrated the possibility to sensitively monitor nitrogen protonation along valence-excited state relaxation pathways and to identify mechanisms yielding N deprotonation in transiently populated configurations. The transient N K-edge X-ray spectroscopic signatures allowed us to propose a dominant relaxation pathway for the system. Thereby, we resolved contradictions in published results on the photo-induced dynamics of 2-thiopyridone on pico- and nanosecond timescales regarding a dependence on the used excitation wavelength and solvent. As a foundation, we established a 1.5 eV shift of a π^* absorption resonance (in publication I) and a strong intensity increase of an emission line in RIXS (in publication II) as fingerprints of N deprotonation from spectra of the system in neutral and basic aqueous environments. We identified an emission intensity increase in this fingerprint spectral range upon photo-excitation of the system in femtosecond time-resolved N 1s RIXS measurements. By that we demonstrated the feasibility of studies on ultrafast proton dynamics in liquids using N K-edge RIXS on femtosecond timescales at X-ray free electron lasers. Using transient N K-edge transmission XAS and ab-initio quantum-chemical simulations (in publication III), we detected a N deprotonation on picosecond timescales occurring from the T_1 state of 2-thiopyridone with a lifetime of 760 ps, which is efficiently populated upon valence-excitation. In summary we demonstrated that a fraction of photo-excited molecules undergo ultrafast deprotonation on femtosecond timescales prior to the intersystem crossing into the T_1 state of 2-thiopyridone. Excited state proton dynamics on picosecond timescales are mediated by this triplet

state. The origins of possible N deprotonation during the initial relaxation from the optically accessible S_2 and S_4 excited states remain to be determined.

We used the N K-edge spectroscopic signatures, which allowed us to monitor the N protonation in 2-thiopyridone, to characterize the core-excited state dynamics of aqueous histidine (in publication IV). We could selectively probe the impact of N 1s excitations at the two imidazole N sites of histidine on the electronic structure and the molecular geometry. They exhibit, equivalent to 2-thiopyridone, robust N K-edge spectroscopic signatures of N protonation. In particular, the N K-edge absorption resonances exhibit a N protonation-dependent characteristic shift. Moreover, an intense emission line is present or absent under deprotonated or protonated conditions respectively. In an acidic environment 1s core-excitation at each of the protonated imidazole N sites induces the dissociation of a specific N–H bond. We unraveled this directional core-excitation induced dissociation using simulations in the framework of the Z+1 equivalent core approximation. We demonstrated that the initial response of organic molecules to ionizing radiation, i.e. an ultrafast N deprotonation, can be monitored locally using N 1s RIXS also for molecules containing multiple N sites. Even in the presence of overlapping X-ray absorption resonances, a combination of RIXS measurements and quantum-chemical simulations yielded information on core-excited state dynamics at specific sites.

Access to proton dynamics in the molecular electronic ground state, in contrast to the previously investigated dynamics in valence and core-excited states, was gained through directional structural deformations induced by core-excitations. We validated a proposed method to reconstruct one-dimensional cuts through potential energy surfaces of polyatomic molecules based on vibrational excitations detected in high resolution RIXS spectra. Directional O 1s core-excited state wave packets were utilized by us to populate ground state vibrational modes of the water molecule with a specific orientation upon scattering events to the electronic ground state (in publication V). On a theoretical level we derived the relation between eigenenergies of a Hamiltonian defined by a one-dimensional cut through a potential energy surface and vibrational modes of coupled nuclear motion populated by the decay of a confined core-excited state nuclear wave packet (in publication VI). We confirmed the applicability of the proposed potential reconstruction method through the extraction of the ground state potential energy surface defining proton dynamics in the gas-phase water molecule. A comparison to ab-initio simulations yielded excellent agreement in the probed range of nuclear coordinates. This method is currently extended to extract signatures of intermolecular interactions from vibrationally resolved RIXS spectra of liquid samples.

To enable studies of valence-excited state molecular dynamics, like the investigation of the proton transfer capabilities of 2-thiopyridone on pico and nanosecond timescales, an experimental setup for liquid phase transient soft X-ray absorption measurements was developed (and was presented in publication VII). It uses the BESSY II fill pattern, which is optimized for pico- to nanosecond time-resolved studies, in combination with a transmission flat-jet sample environment and a fiber laser system, providing pulses

for the optical excitation of the sample at MHz repetition rates. This combination enabled a highly sensitive detection of transient absorption changes on a sub-mOD level. The used flat-jet sample environment makes the system particularly robust against radiation damage under high optical and X-ray flux densities. It provides a stable transmission sample environment in combination with sufficient sample replenishment. This allows for universal applicability in static and time-resolved soft X-ray spectroscopy studies at free-electron lasers, synchrotrons and laser driven sources.

Studies of femtosecond molecular dynamics using optical pump X-ray probe schemes rely on efficient methods to establish the X-ray optical temporal cross-correlation. The applicability of individual cross-correlation techniques depends on the available X-ray flux. A widely applied cross-correlation method based on X-ray induced transient optical reflectivity at free electron lasers can be optimized based on thin film interference effects. This method was crucial for the successful detection of femtosecond photo-induced proton dynamics of 2-thiopyridone at the free-electron laser LCLS. A similar concept was used to design a cross-correlator for application at low-flux X-ray sources providing femtosecond pulse durations (in publication VIII). It is based on the efficient detection of transient X-ray reflectivity changes. Intensity variations of super-lattice Bragg peaks, induced by the propagation of phonons in multilayer thin film structures, thereby yield a high cross-correlation contrast. As relative intensity variations on the order of few percent can be achieved using this method, it is implemented as a standard tool to establish the temporal X-ray optical cross-correlation at the femtoslicing facility of the synchrotron BESSY II. An optimization of the multilayer structure with respect to the excitation profile could yield even higher transient signal changes. Having both cross-correlation methods optimized and at hand is an essential precondition for femtosecond time-resolved soft X-ray studies of photo-induced molecular dynamics.

The presented results are based on the element-specific, site-selective and orbital-sensitive access of soft X-ray spectroscopy to local molecular electronic structure. It should be emphasized that the application of the discussed methods and infrastructure is not restricted to studies of classical photochemical processes of molecules in a solution environment and could be extended to some related research fields. Novel sample environments allowing for continuous sample replenishment, could enable investigations of solution-phase catalytic and electrochemical processes on an atomic level. The active sites in these processes could be accessed systematically using the selectivity of X-ray spectroscopy. Probing ground state potentials through vibrationally resolved RIXS could be of particularly high value to investigate the bond formation and dissociation at interfaces in functional devices. Time-resolved schemes would allow for studies of photo-electrochemical or photo-catalytic processes. Moreover, implementation of THz and infrared excitations in pump-probe experimental schemes might allow for investigations of thermally driven chemical processes. Thereby, access to properties of intermediate species present in chemical reactions could be gained through soft X-ray spectroscopy probes subsequent to controlled

vibrational excitation or temperature jumps of the solution. A scheme to study mixing and reaction kinetics in solution environments could be established using the flat-jet sample environment. The probed position on the liquid sheet, which can be generated from different chemicals in the two individual jets, can be utilized to spatially map kinetics within the flowing jet on microsecond timescales.

Based on the presented studies and the used infrastructure, prospective investigations of molecular dynamics at currently available and future light sources can be outlined. They largely depend on flux and pulse structure provided by the sources in combination with an optimization of the experiments with respect to the sample environment and the applied experimental scheme.

To study processes in the few picoseconds time domain at high signal to noise ratio, X-ray pulses in the BESSY II low-α operation mode can currently be used in the experimental configuration discussed in publication VII. In the future, the BESSY VSR scheme will provide compressed bunches in addition to the regular BESSY II fill pattern in the standard operation. Thereby, molecular dynamics in the few picosecond time domain would be routinely accessible.

Flat-jet instabilities and the resulting noise could be further reduced through advances in jet technology. This could enable longer counting times at stable conditions, which would benefit studies at sources with lower X-ray pulse repetition rates or with lower flux. It would enable transient X-ray absorption studies of liquid samples at synchrotron slicing and laser driven sources with femtosecond resolution, avoiding risks of radiation damage through continuous sample replenishment.

Femtosecond time-resolved RIXS studies focused on electronic transitions, using medium resolution instruments as in publication II, will largely benefit from higher repetition rates at the free-electron lasers European XFEL (Hamburg, Germany) and LCLS–II (Stanford, USA). They will enable studies at lower sample concentration and will reduce the contamination of spectra by molecules, which are sequentially excited within a single X-ray pulse. A higher repetition rate would also reduce noise in differential transmission measurements, induced by the mentioned flat-jet instabilities.

Research at existing RIXS instruments providing vibrational resolution is not focused on studies of molecular systems in gaseous and liquid environments. They allow only for the use of sample cells, causing the discussed experimental complications as a direct consequence. Currently, the experiments VERITAS at the synchrotron MAX IV, METRIXS at BESSY II and h-RIXS at the European XFEL are under development. They overcome these sample environment restrictions by the use of micro-jets. These instruments will allow for systematic vibrationally resolved RIXS studies on molecules in the future, even in a optical pump X-ray probe experimental configuration at the free-electron laser.

Bibliography

[1] P. E. M. Siegbahn. "A Structure-Consistent Mechanism for Dioxygen Formation in Photosystem II". *Chemistry - A European Journal* **14**, 8290 (2008).

[2] P. E. M. Siegbahn. "Structures and Energetics for O_2 Formation in Photosystem II". *Accounts of Chemical Research* **42**, 1871 (2009).

[3] H. B. Gray and A. W. Maverick. "Solar Chemistry of Metal Complexes". *Science* **214**, 1201 (1981).

[4] B. Mondal, F. Neese and S. Ye. "Toward Rational Design of 3d Transition Metal Catalysts for CO_2 Hydrogenation Based on Insights into Hydricity-Controlled Rate-Determining Steps". *Inorganic Chemistry* **55**, 5438 (2016).

[5] D. Goodhead. "Initial Events in the Cellular Effects of Ionizing Radiations: Clustered Damage in DNA". *International Journal of Radiation Biology* **65**, 7 (1994).

[6] National Research Council: Board on Radiation Effects Research Division on Earth and Life Studies. *Health Risks from Exposure to Low Levels of Ionizing Radiation* (National Academies Press, Washington, D.C., 2006).

[7] Y. Zhang, K. de La Harpe, A. A. Beckstead, R. Improta and B. Kohler. "UV-Induced Proton Transfer between DNA Strands". *Journal of the American Chemical Society* **137**, 7059 (2015).

[8] A. El Nahhas, T. Pascher, L. Leone, L. Panzella, A. Napolitano and V. Sundström. "Photochemistry of Pheomelanin Building Blocks and Model Chromophores: Excited-State Intra- and Intermolecular Proton Transfer". *The Journal of Physical Chemistry Letters* **5**, 2094 (2014).

[9] A. Corani, A. Huijser, T. Gustavsson, D. Markovitsi, P. Å. Malmqvist, A. Pezzella, M. D'Ischia and V. Sundström. "Superior photoprotective motifs and mechanisms in eumelanins uncovered". *Journal of the American Chemical Society* **136**, 11626 (2014).

[10] S. Olsen, J. Riesz, I. Mahadevan, A. Coutts, J. P. Bothma, B. J. Powell, R. H. McKenzie, S. C. Smith and P. Meredith. "Convergent Proton-Transfer

Photocycles Violate Mirror-Image Symmetry in a Key Melanin Monomer". *Journal of the American Chemical Society* **129**, 6672 (2007).

[11] M. L. Cowan, B. D. Bruner, N. Huse, J. R. Dwyer, B. Chugh, E. T. J. Nibbering, T. Elsaesser and R. J. D. Miller. "Ultrafast memory loss and energy redistribution in the hydrogen bond network of liquid H_2O". *Nature* **434**, 199 (2005).

[12] S. Baker, J. S. Robinson, C. A. Haworth, H. Teng, R. A. Smith, C. C. Chirila, M. Lein, J. W. G. Tisch and J. P. Marangos. "Probing Proton Dynamics in Molecules on an Attosecond Time Scale". *Science* **312**, 424 (2006).

[13] T. Elsaesser and H. J. Bakker (Eds.). *Ultrafast Hydrogen Bonding Dynamics and Proton Transfer Prosesses in the Condensed Phase* (Springer Netherlands, Dordrecht, 2002).

[14] A. Corani, A. Pezzella, T. Pascher, T. Gustavsson, D. Markovitsi, A. Huijser, M. D'Ischia and V. Sundström. "Excited-State Proton-Transfer Processes of DHICA Resolved: From Sub-Picoseconds to Nanoseconds". *The Journal of Physical Chemistry Letters* **4**, 1383 (2013).

[15] S. Banerjee, A. Pabbathi, M. C. Sekhar and A. Samanta. "Dual Fluorescence of Ellipticine: Excited State Proton Transfer from Solvent versus Solvent Mediated Intramolecular Proton Transfer". *The Journal of Physical Chemistry A* **115**, 9217 (2011).

[16] A. H. Zewail. "Femtochemistry". *Angew. Chem. Int. Ed.* **39**, 2586 (2001).

[17] J. Stöhr. *NEXAFS Spectroscopy*, vol. 25 of *Springer Series in Surface Sciences* (Springer Berlin Heidelberg, Berlin, Heidelberg, 1992).

[18] N. Huse, T. K. Kim, L. Jamula, J. K. McCusker, F. M. F. de Groot and R. W. Schoenlein. "Photo-Induced Spin-State Conversion in Solvated Transition Metal Complexes Probed via Time-Resolved Soft X-ray Spectroscopy". *Journal of the American Chemical Society* **132**, 6809 (2010).

[19] N. Huse, H. Wen, D. Nordlund, E. Szilagyi, D. Daranciang, T. A. Miller, A. Nilsson, R. W. Schoenlein and A. M. Lindenberg. "Probing the hydrogen-bond network of water via time-resolved soft X-ray spectroscopy". *Physical Chemistry Chemical Physics* **11**, 3951 (2009).

[20] P. Wernet, G. Gavrila, K. Godehusen, C. Weniger, E. T. J. Nibbering, T. Elsaesser and W. Eberhardt. "Ultrafast temperature jump in liquid water studied by a novel infrared pump-x-ray probe technique". *Applied Physics A* **92**, 511 (2008).

[21] M. Ochmann, I. von Ahnen, A. A. Cordones, A. Hussain, J. H. Lee, K. Hong, K. Adamczyk, O. Vendrell, T. K. Kim, R. W. Schoenlein and N. Huse. "Light-Induced Radical Formation and Isomerization of an Aromatic Thiol in Solution Followed by Time-Resolved X-ray Absorption Spectroscopy at the Sulfur K-Edge". *Journal of the American Chemical Society* **139**, 4797 (2017).

[22] M. Ochmann, A. Hussain, I. von Ahnen, A. A. Cordones, K. Hong, J. H. Lee, R. Ma, K. Adamczyk, T. K. Kim, R. W. Schoenlein, O. Vendrell and N. Huse. "UV-Photochemistry of the Disulfide Bond: Evolution of Early Photoproducts from Picosecond X-ray Absorption Spectroscopy at the Sulfur K-Edge". *Journal of the American Chemical Society* **140**, 6554 (2018).

[23] B. E. Van Kuiken, H. Cho, K. Hong, M. Khalil, R. W. Schoenlein, T. K. Kim and N. Huse. "Time-Resolved X-ray Spectroscopy in the Water Window: Elucidating Transient Valence Charge Distributions in an Aqueous Fe(II) Complex". *The Journal of Physical Chemistry Letters* **7**, 465 (2016).

[24] K. Hong, H. Cho, R. W. Schoenlein, T. K. Kim and N. Huse. "Element-Specific Characterization of Transient Electronic Structure of Solvated Fe(II) Complexes with Time-Resolved Soft X-ray Absorption Spectroscopy". *Accounts of Chemical Research* **48**, 2957 (2015).

[25] N. Huse, H. Cho, K. Hong, L. Jamula, F. M. F. de Groot, T. K. Kim, J. K. McCusker and R. W. Schoenlein. "Femtosecond Soft X-ray Spectroscopy of Solvated Transition-Metal Complexes: Deciphering the Interplay of Electronic and Structural Dynamics". *The Journal of Physical Chemistry Letters* **2**, 880 (2011).

[26] M. C. Chen, P. Arpin, T. Popmintchev, M. Gerrity, B. Zhang, M. Seaberg, D. Popmintchev, M. M. Murnane and H. C. Kapteyn. "Bright, coherent, ultrafast soft x-ray harmonics spanning the water window from a tabletop light source". *Physical Review Letters* **105**, 1 (2010).

[27] J. Seres, E. Seres, B. Landgraf, B. Ecker, B. Aurand, T. Kuehl and C. Spielmann. "High-harmonic generation and parametric amplification in the soft X-rays from extended electron trajectories". *Scientific Reports* **4**, 4234 (2015).

[28] Y. Pertot, C. Schmidt, M. Matthews, A. Chauvet, M. Huppert, V. Svoboda, A. von Conta, A. Tehlar, D. Baykusheva, J.-P. Wolf and H. J. Wörner. "Time-resolved x-ray absorption spectroscopy with a water window high-harmonic source". *Science* **355**, 264 (2017).

[29] D. Popmintchev, B. R. Galloway, M.-C. Chen, F. Dollar, C. A. Mancuso, A. Hankla, L. Miaja-Avila, G. O'Neil, J. M. Shaw, G. Fan, S. Ališauskas, G. Andriukaitis, T. Balčiunas, O. D. Mücke, A. Pugzlys, A. Baltuška, H. C. Kapteyn, T. Popmintchev and M. M. Murnane. "Near- and Extended-Edge

X-Ray-Absorption Fine-Structure Spectroscopy Using Ultrafast Coherent High-Order Harmonic Supercontinua". *Physical Review Letters* **120**, 093002 (2018).

[30] A. Bhattacherjee, C. D. Pemmaraju, K. Schnorr, A. R. Attar and S. R. Leone. "Ultrafast Intersystem Crossing in Acetylacetone via Femtosecond X-ray Transient Absorption at the Carbon K-Edge". *Journal of the American Chemical Society* **139**, 16576 (2017).

[31] A. R. Attar, A. Bhattacherjee, C. D. Pemmaraju, K. Schnorr, K. D. Closser, D. Prendergast and S. R. Leone. "Femtosecond x-ray spectroscopy of an electrocyclic ring-opening reaction". *Science* **356**, 54 (2017).

[32] P. Wernet, K. Kunnus, I. Josefsson, I. Rajkovic, W. Quevedo, M. Beye, S. Schreck, S. Grübel, M. Scholz, D. Nordlund, W. Zhang, R. W. Hartsock, W. F. Schlotter, J. J. Turner, B. Kennedy, F. Hennies, F. M. F. de Groot, K. J. Gaffney, S. Techert, M. Odelius and A. Föhlisch. "Orbital-specific mapping of the ligand exchange dynamics of $Fe(CO)_5$ in solution." *Nature* **520**, 78 (2015).

[33] M. Beye, H. Öberg, H. Xin, G. L. Dakovski, M. Dell'Angela, A. Föhlisch, J. Gladh, M. Hantschmann, F. Hieke, S. Kaya, D. Kühn, J. LaRue, G. Mercurio, M. P. Minitti, A. Mitra, S. P. Moeller, M. L. Ng, A. Nilsson, D. Nordlund, J. Nørskov, H. Öström, H. Ogasawara, M. Persson, W. F. Schlotter, J. A. Sellberg, M. Wolf, F. Abild-Pedersen, L. G. M. Pettersson and W. Wurth. "Chemical Bond Activation Observed with an X-ray Laser". *The Journal of Physical Chemistry Letters* **7**, 3647 (2016).

[34] J. LaRue, O. Krejčí, L. Yu, M. Beye, M. L. Ng, H. Öberg, H. Xin, G. Mercurio, S. Moeller, J. J. Turner, D. Nordlund, R. Coffee, M. P. Minitti, W. Wurth, L. G. M. Pettersson, H. Öström, A. Nilsson, F. Abild-Pedersen and H. Ogasawara. "Real-Time Elucidation of Catalytic Pathways in CO Hydrogenation on Ru". *The Journal of Physical Chemistry Letters* **8**, 3820 (2017).

[35] R. M. Jay, J. Norell, S. Eckert, M. Hantschmann, M. Beye, B. Kennedy, W. Quevedo, W. F. Schlotter, G. L. Dakovski, M. P. Minitti, M. C. Hoffmann, A. Mitra, S. P. Moeller, D. Nordlund, W. Zhang, H. W. Liang, K. Kunnus, K. Kubiček, S. A. Techert, M. Lundberg, P. Wernet, K. Gaffney, M. Odelius and A. Föhlisch. "Disentangling Transient Charge Density and Metal–Ligand Covalency in Photoexcited Ferricyanide with Femtosecond Resonant Inelastic Soft X-ray Scattering". *The Journal of Physical Chemistry Letters* **9**, 3538 (2018).

[36] R. Du, C. Liu, Y. Zhao, K.-M. Pei, H.-G. Wang, X. Zheng, M. Li, J.-D. Xue and D. L. Phillips. "Resonance Raman spectroscopic and theoretical investigation of the excited state proton transfer reaction dynamics of 2-thiopyridone." *The Journal of Physical Chemistry B* **115**, 8266 (2011).

[37] B. E. Van Kuiken, M. R. Ross, M. L. Strader, A. A. Cordones, H. Cho, J. H. Lee, R. W. Schoenlein and M. Khalil. "Picosecond sulfur K-edge X-ray absorption spectroscopy with applications to excited state proton transfer". *Structural Dynamics* **4**, 044021 (2017).

[38] F. Gel'mukhanov and H. Ågren. "Resonant X-ray Raman scattering". *Physics Reports* **312**, 87 (1999).

[39] Y.-P. Sun, F. Hennies, A. Pietzsch, B. Kennedy, T. Schmitt, V. N. Strocov, J. Andersson, M. Berglund, J.-E. Rubensson, K. Aidas, F. Gel'mukhanov, M. Odelius and A. Föhlisch. "Intramolecular soft modes and intermolecular interactions in liquid acetone". *Physical Review B* **84**, 132202 (2011).

[40] A. Pietzsch, Y.-P. Sun, F. Hennies, Z. Rinkevicius, H. O. Karlsson, T. Schmitt, V. N. Strocov, J. Andersson, B. Kennedy, J. Schlappa, A. Föhlisch, J.-E. Rubensson and F. Gel'mukhanov. "Spatial Quantum Beats in Vibrational Resonant Inelastic Soft X-Ray Scattering at Dissociating States in Oxygen". *Physical Review Letters* **106**, 153004 (2011).

[41] A. Pietzsch, F. Hennies, P. S. Miedema, B. Kennedy, J. Schlappa, T. Schmitt, V. N. Strocov and A. Föhlisch. "Snapshots of the Fluctuating Hydrogen Bond Network in Liquid Water on the Sub-Femtosecond Timescale with Vibrational Resonant Inelastic x-ray Scattering". *Physical Review Letters* **114**, 088302 (2015).

[42] R. C. Couto, M. Guarise, A. Nicolaou, N. Jaouen, G. S. Chiuzbăian, J. Lüning, V. Ekholm, J.-E. Rubensson, C. Såthe, F. Hennies, V. Kimberg, F. F. Guimarães, H. Agren, F. Gel'mukhanov, L. Journel and M. Simon. "Anomalously strong two-electron one-photon X-ray decay transitions in CO caused by avoided crossing". *Scientific Reports* **6**, 20947 (2016).

[43] S. Schreck, A. Pietzsch, B. Kennedy, C. Såthe, P. S. Miedema, S. Techert, V. N. Strocov, T. Schmitt, F. Hennies, J.-E. Rubensson and A. Föhlisch. "Ground state potential energy surfaces around selected atoms from resonant inelastic x-ray scattering". *Scientific Reports* **7**, 20054 (2016).

[44] S. Schreck, A. Pietzsch, K. Kunnus, B. Kennedy, W. Quevedo, P. S. Miedema, P. Wernet and A. Föhlisch. "Dynamics of the OH group and the electronic structure of liquid alcohols". *Structural Dynamics* **1**, 054901 (2014).

[45] F. Hennies, A. Pietzsch, M. Berglund, A. Föhlisch, T. Schmitt, V. Strocov, H. O. Karlsson, J. Andersson and J.-E. Rubensson. "Resonant Inelastic Scattering Spectra of Free Molecules with Vibrational Resolution". *Physical Review Letters* **104**, 193002 (2010).

[46] J.-E. Rubensson, F. Hennies and A. Pietzsch. "High-resolution resonant inelastic soft X-ray scattering applied to liquids". *Journal of Electron Spectroscopy and Related Phenomena* **188**, 79 (2013).

[47] F. Hennies, S. Polyutov, I. Minkov, A. Pietzsch, M. Nagasono, F. Gel'mukhanov, L. Triguero, M.-N. Piancastelli, W. Wurth, H. Ågren and A. Föhlisch. "Nonadiabatic Effects in Resonant Inelastic X-Ray Scattering". *Physical Review Letters* **95**, 163002 (2005).

[48] R. C. Couto, M. Guarise, A. Nicolaou, N. Jaouen, G. S. Chiuzbăian, J. Lüning, V. Ekholm, J.-E. Rubensson, C. Såthe, F. Hennies, F. F. Guimarães, H. Ågren, F. Gel'mukhanov, L. Journel, M. Simon and V. Kimberg. "Coupled electron-nuclear dynamics in resonant $1\sigma \rightarrow 2\pi$ x-ray Raman scattering of CO molecules". *Physical Review A* **93**, 032510 (2016).

[49] S. Li and M. Hong. "Protonation, Tautomerization, and Rotameric Structure of Histidine: A Comprehensive Study by Magic-Angle-Spinning Solid-State NMR". *Journal of the American Chemical Society* **133**, 1534 (2011).

[50] M. Ekimova, W. Quevedo, M. Faubel, P. Wernet and E. T. J. Nibbering. "A liquid flatjet system for solution phase soft-x-ray spectroscopy". *Structural Dynamics* **2**, 054301 (2015).

[51] S. Eckert, M. Beye, A. Pietzsch, W. Quevedo, M. Hantschmann, M. Ochmann, M. Ross, M. P. Minitti, J. J. Turner, S. P. Moeller, W. F. Schlotter, G. L. Dakovski, M. Khalil, N. Huse and A. Föhlisch. "Principles of femtosecond X-ray/optical cross-correlation with X-ray induced transient optical reflectivity in solids". *Applied Physics Letters* **106**, 061104 (2015).

[52] S.-Y. Lee and E. J. Heller. "Time-dependent theory of Raman scattering". *The Journal of Chemical Physics* **71**, 4777 (1979).

[53] M. Born and R. Oppenheimer. "Zur Quantentheorie der Molekeln". *Annalen der Physik* **389**, 457 (1927).

[54] J. I. Steinfeld. *Molecules and Radiation: An Introduction to Modern Molecular Spectroscopy* (MIT Press, Cambridge, MA, 1985), 2nd edition edn.

[55] P. Atkins and R. Friedman. *Molecular Quantum Mechanics* (Oxford Univ. Press, Oxford, 2005).

[56] I. Josefsson, K. Kunnus, S. Schreck, A. Föhlisch, F. de Groot, P. Wernet and M. Odelius. "Ab Initio Calculations of X-ray Spectra: Atomic Multiplet and Molecular Orbital Effects in a Multiconfigurational SCF Approach to the L-Edge Spectra of Transition Metal Complexes". *The Journal of Physical Chemistry Letters* **3**, 3565 (2012).

[57] L. Triguero, L. G. M. Pettersson and H. Ågren. "Calculations of near-edge x-ray-absorption spectra of gas-phase and chemisorbed molecules by means of density-functional and transition-potential theory". *Physical Review B* **58**, 8097 (1998).

[58] L. Triguero, L. G. M. Pettersson and H. Ågren. "Calculations of X-ray Emission Spectra of Molecules and Surface Adsorbates by Means of Density Functional Theory". *The Journal of Physical Chemistry A* **102**, 10599 (1998).

[59] M. Iannuzzi and J. Hutter. "Inner-shell spectroscopy by the Gaussian and augmented plane wave method". *Physical Chemistry Chemical Physics* **9**, 1599 (2007).

[60] J. Niskanen, N. Arul Murugan, Z. Rinkevicius, O. Vahtras, C. Li, S. Monti, V. Carravetta and H. Ågren. "Hybrid density functional–molecular mechanics calculations for core-electron binding energies of glycine in water solution". *Physical Chemistry Chemical Physics* **15**, 244 (2013).

[61] J. Niskanen, C. J. Sahle, I. Juurinen, J. Koskelo, S. Lehtola, R. Verbeni, H. Müller, M. Hakala and S. Huotari. "Protonation Dynamics and Hydrogen Bonding in Aqueous Sulfuric Acid". *The Journal of Physical Chemistry B* **119**, 11732 (2015).

[62] M. Ekimova, W. Quevedo, Ł. Szyc, M. Iannuzzi, P. Wernet, M. Odelius and E. T. J. Nibbering. "Aqueous Solvation of Ammonia and Ammonium: Probing Hydrogen Bond Motifs with FT-IR and Soft X-ray Spectroscopy". *Journal of the American Chemical Society* **139**, 12773 (2017).

[63] T. S. Rose, M. J. Rosker and A. H. Zewail. "Femtosecond real-tim probing of reactions. IV. The reactions of alkali halides". *Journal of Chemical Physics* **91**, 7415 (1989).

[64] N. F. Scherer, R. J. Carlson, A. Matro, M. Du, A. J. Ruggiero, V. Romero-Rochin, J. A. Cina, G. R. Fleming and S. A. Rice. "Fluorescence-detected wave packet interferometry: Time resolved molecular spectroscopy with sequences of femtosecond phase-locked pulses". *The Journal of Chemical Physics* **95**, 1487 (1991).

[65] W. T. Pollard, H. L. Fragnito, J. Y. Bigot, C. V. Shank and R. A. Mathies. "Quantum-mechanical theory for 6 fs dynamic absorption spectroscopy and its application to nile blue". *Chemical Physics Letters* **168**, 239 (1990).

[66] C. Meier and V. Engel. "Electron kinetic energy distributions from multiphoton ionization of Na_2 with femtosecond laser pulses". *Chemical Physics Letters* **212**, 691 (1993).

[67] M. Simon, L. Journel, R. Guillemin, W. C. Stolte, I. Minkov, F. Gel'mukhanov, P. Sałek, H. Ågren, S. Carniato, R. Taïeb, A. C. Hudson and D. W. Lindle. "Femtosecond nuclear motion of HCl probed by resonant x-ray Raman scattering in the Cl 1s region". *Physical Review A* **73**, 020706 (2006).

[68] F. Gelmukhanov and H. Ågren. "X-ray resonant scattering involving dissociative states". *Physical Review A* **54**, 379 (1996).

[69] V. Vaz da Cruz, E. Ertan, R. C. Couto, S. Eckert, M. Fondell, M. Dantz, B. Kennedy, T. Schmitt, A. Pietzsch, F. F. Guimarães, H. Ågren, F. Gel'mukhanov, M. Odelius, A. Föhlisch and V. Kimberg. "A study of the water molecule using frequency control over nuclear dynamics in resonant X-ray scattering". *Physical Chemistry Chemical Physics* **19**, 19573 (2017).

[70] E. Ertan, V. Savchenko, N. Ignatova, V. Vaz da Cruz, R. C. Couto, S. Eckert, M. Fondell, M. Dantz, B. Kennedy, T. Schmitt, A. Pietzsch, A. Föhlisch, F. Gel'mukhanov, M. Odelius and V. Kimberg. "Ultrafast dissociation features in RIXS spectra of the water molecule". *Physical Chemistry Chemical Physics* **20**, 14384 (2018).

[71] J. C. Tully. "Molecular dynamics with electronic transitions". *The Journal of Chemical Physics* **93**, 1061 (1990).

[72] M. Richter, P. Marquetand, J. González-Vázquez, I. Sola and L. González. "SHARC: ab Initio Molecular Dynamics with Surface Hopping in the Adiabatic Representation Including Arbitrary Couplings". *Journal of Chemical Theory and Computation* **7**, 1253 (2011).

[73] S. Mai, P. Marquetand and L. González. "A general method to describe intersystem crossing dynamics in trajectory surface hopping". *International Journal of Quantum Chemistry* **115**, 1215 (2015).

[74] S. Mai, M. Pollum, L. Martínez-Fernández, N. Dunn, P. Marquetand, I. Corral, C. E. Crespo-Hernández and L. González. "The origin of efficient triplet state population in sulfur-substituted nucleobases". *Nature Communications* **7**, 1 (2016).

[75] S. Mai, P. Marquetand and L. González. "Intersystem Crossing Pathways in the Noncanonical Nucleobase 2-Thiouracil: A Time-Dependent Picture". *The Journal of Physical Chemistry Letters* **7**, 1978 (2016).

[76] D. Sebilleau. *Magnetism: A Synchrotron Radiation Approach*, vol. 697 of *Lecture Notes in Physics* (Springer Berlin Heidelberg, 2006).

[77] A. Sanchez-Gonzalez, T. R. Barillot, R. J. Squibb, P. Kolorenč, M. Agaker, V. Averbukh, M. J. Bearpark, C. Bostedt, J. D. Bozek, S. Bruce, S. C. Montero, R. N. Coffee, B. Cooper, J. P. Cryan, M. Dong, J. H. D. Eland, L. Fang, H. Fukuzawa, M. Guehr, M. Ilchen, A. S. Johnsson, C. Liekhus-S, A. Marinelli, T. Maxwell, K. Motomura, M. Mucke, A. Natan, T. Osipov, C. Östlin, M. Pernpointner, V. S. Petrovic, M. A. Robb, C. Sathe, E. R. Simpson, J. G. Underwood, M. Vacher, D. J. Walke, T. J. A. Wolf, V. Zhaunerchyk, J.-E. Rubensson, N. Berrah, P. H. Bucksbaum, K. Ueda, R. Feifel, L. J. Frasinski, Marangos and J. P. "Auger electron and photoabsorption spectra of glycine in the vicinity of the oxygen K-edge measured with an X-FEL". *Journal of Physics B: Atomic, Molecular and Optical Physics* **48**, 234004 (2015).

[78] T. Wolf, F. Holzmeier, I. Wagner, N. Berrah, C. Bostedt, J. Bozek, P. Bucksbaum, R. Coffee, J. Cryan, J. Farrell, R. Feifel, T. Martinez, B. McFarland, M. Mucke, S. Nandi, F. Tarantelli, I. Fischer and M. Gühr. "Observing Femtosecond Fragmentation Using Ultrafast X-ray-Induced Auger Spectra". *Applied Sciences* **7**, 681 (2017).

[79] O. Gessner and M. Gühr. "Monitoring Ultrafast Chemical Dynamics by Time-Domain X-ray Photo- and Auger-Electron Spectroscopy". *Accounts of Chemical Research* **49**, 138 (2016).

[80] T. J. Wolf, R. H. Myhre, J. P. Cryan, S. Coriani, R. J. Squibb, A. Battistoni, N. Berrah, C. Bostedt, P. Bucksbaum, G. Coslovich, R. Feifel, K. J. Gaffney, J. Grilj, T. J. Martinez, S. Miyabe, S. P. Moeller, M. Mucke, A. Natan, R. Obaid, T. Osipov, O. Plekan, S. Wang, H. Koch and M. Gühr. "Probing ultrafast $\pi\pi^*/n\pi^*$ internal conversion in organic chromophores via K-edge resonant absorption". *Nature Communications* **8**, 1 (2017).

[81] R. Manne and H. Ågren. "Auger transition amplitudes from general many-electron wavefunctions". *Chemical Physics* **93**, 201 (1985).

[82] G. Wentzel. "Über strahlungslose Quantensprünge". *Zeitschrift für Physik* **43**, 524 (1927).

[83] H. I. B. Banks, D. A. Little, J. Tennyson and A. Emmanouilidou. "Interaction of molecular nitrogen with free-electron-laser radiation". *Physical Chemistry Chemical Physics* **19**, 19794 (2017).

[84] M. O. Krause. "Atomic radiative and radiationless yields for K and L shells". *Journal of Physical and Chemical Reference Data* **8**, 307 (1979).

[85] F. T. Smith. "Diabatic and Adiabatic Representations for Atomic Collision Problems". *Physical Review* **179**, 111 (1969).

[86] P. Avouris, W. M. Gelbart and M. A. El-Sayed. "Nonradiative electronic relaxation under collision-free conditions". *Chemical Reviews* **77**, 793 (1977).

[87] P. A. M. Dirac. "The Quantum Theory of the Emission and Absorption of Radiation". *Proceedings of the Royal Society A: Mathematical, Physical and Engineering Sciences* **114**, 243 (1927).

[88] H. A. Kramers and W. Heisenberg. "Über die Streuung von Strahlung durch Atome". *Zeitschrift für Physik* **31**, 681 (1925).

[89] S. Hüfner. *Photoelectron Spectroscopy*. Advanced Texts in Physics (Springer Berlin Heidelberg, Berlin, Heidelberg, 2003).

[90] R. Manne. "Molecular Orbital Interpretation of X-Ray Emission Spectra: Simple Hydrocarbons and Carbon Oxides". *The Journal of Chemical Physics* **52**, 5733 (1970).

[91] K. Kunnus. "Probing dynamic pathways and electronic structure of coordination complexes with soft x-ray spectroscopy". Ph.D. thesis, University of Potsdam (2014).

[92] D. Maganas, S. DeBeer and F. Neese. "A Restricted Open Configuration Interaction with Singles Method To Calculate Valence-to-Core Resonant X-ray Emission Spectra: A Case Study". *Inorganic Chemistry* **56**, 11819 (2017).

[93] A. Kotani, K. O. Kvashnina, S. M. Butorin and P. Glatzel. "Spectator and participator processes in the resonant photon-in and photon-out spectra at the Ce L_3 edge of CeO_2". *The European Physical Journal B* **85**, 257 (2012).

[94] M. Kavčič, M. Žitnik, K. Bučar, A. Mihelič, S. Carniato, L. Journel, R. Guillemin and M. Simon. "Electronic State Interferences in Resonant X-Ray Emission after K-Shell Excitation in HCl". *Physical Review Letters* **105**, 113004 (2010).

[95] G. Ghiringhelli, A. Piazzalunga, C. Dallera, G. Trezzi, L. Braicovich, T. Schmitt, V. N. Strocov, R. Betemps, L. Patthey, X. Wang and M. Grioni. "SAXES, a high resolution spectrometer for resonant x-ray emission in the 400–1600eV energy range". *Review of Scientific Instruments* **77**, 113108 (2006).

[96] B. Johansson and N. Mårtensson. "Core-level binding-energy shifts for the metallic elements". *Physical Review B* **21**, 4427 (1980).

[97] B. Brena, D. Nordlund, M. Odelius, H. Ogasawara, A. Nilsson and L. G. M. Pettersson. "Ultrafast Molecular Dissociation of Water in Ice". *Physical Review Letters* **93**, 148302 (2004).

[98] M. Odelius, H. Ogasawara, D. Nordlund, O. Fuchs, L. Weinhardt, F. Maier, E. Umbach, C. Heske, Y. Zubavichus, M. Grunze, J. D. Denlinger, L. G. M. Pettersson and A. Nilsson. "Ultrafast Core-Hole-Induced Dynamics in Water Probed by X-Ray Emission Spectroscopy". *Physical Review Letters* **94**, 227401 (2005).

[99] M. Odelius. "Information Content in O[1s] K-edge X-ray Emission Spectroscopy of Liquid Water". *The Journal of Physical Chemistry A* **113**, 8176 (2009).

[100] J. Niskanen, K. Kooser, J. Koskelo, T. Käämbre, K. Kunnus, A. Pietzsch, W. Quevedo, M. Hakala, A. Föhlisch, S. Huotari and E. Kukk. "Density functional simulation of resonant inelastic X-ray scattering experiments in liquids: acetonitrile". *Physical Chemistry Chemical Physics* **18**, 26026 (2016).

[101] P. Beak. "Energies and alkylations of tautomeric heterocyclic compounds: old problems-new answers". *Accounts of chemical research* **10**, 186 (1977).

[102] P. Beak and J. B. Covington. "Solvent Effects on Protomeric Equilibria: Quantitative Correlation with an Electrostatic Hyrdrogen-Bonding Model". *Journal of the American Chemical Society* **100**, 3961 (1978).

[103] P. Beak, J. B. Covington, S. G. Smith, J. M. White and J. M. Zeigler. "Displacement of protomeric equilibriums by self-association: hydroxypyridine-pyridone and mercaptopyridine-thiopyridone isomer pairs". *The Journal of Organic Chemistry* **45**, 1354 (1980).

[104] M. Blum, M. Odelius, L. Weinhardt, S. Pookpanratana, M. Bär, Y. Zhang, O. Fuchs, W. Yang, E. Umbach and C. Heske. "Ultrafast Proton Dynamics in Aqueous Amino Acid Solutions Studied by Resonant Inelastic Soft X-ray Scattering". *The Journal of Physical Chemistry B* **116**, 13757 (2012).

[105] F. Meyer. "Soft X-ray Spectroscopic Study of Amino Acid and Salt Solutions". Ph.D. thesis, Julius-Maximilians-Universität Würzburg (2015).

[106] F. Meyer, M. Blum, A. Benkert, D. Hauschild, Y. L. Jeyachandran, R. G. Wilks, W. Yang, M. Bär, C. Heske, F. Reinert, M. Zharnikov and L. Weinhardt. "X-ray Emission Spectroscopy of Proteinogenic Amino Acids at All Relevant Absorption Edges". *The Journal of Physical Chemistry B* **121**, 6549 (2017).

[107] F. Meyer, M. Blum, A. Benkert, D. Hauschild, Y. L. Jeyachandran, R. G. Wilks, W. Yang, M. Bär, F. Reinert, C. Heske, M. Zharnikov and L. Weinhardt. "Site-specific electronic structure of imidazole and imidazolium in aqueous solutions". *Physical Chemistry Chemical Physics* **20**, 8302 (2018).

[108] B. Kempgens, A. Kivimäki, M. Neeb, H. M. Köppe, A. M. Bradshaw and J. Feldhaus. "A high-resolution N 1s photoionization study of the molecule in the near-threshold region". *Journal of Physics B: Atomic, Molecular and Optical Physics* **29**, 5389 (1996).

[109] Y. Harada, T. Tokushima, Y. Horikawa, O. Takahashi, H. Niwa, M. Kobayashi, M. Oshima, Y. Senba, H. Ohashi, K. T. Wikfeldt, A. Nilsson, L. G. M. Pettersson and S. Shin. "Selective probing of the OH or OD stretch vibration in liquid water using resonant inelastic soft-X-ray scattering". *Physical Review Letters* **111**, 1 (2013).

[110] L. Weinhardt, A. Benkert, F. Meyer, M. Blum, R. G. Wilks, W. Yang, M. Bär, F. Reinert and C. Heske. "Nuclear dynamics and spectator effects in resonant inelastic soft x-ray scattering of gas-phase water molecules". *The Journal of Chemical Physics* **136**, 144311 (2012).

[111] M. Beye, O. Krupin, G. Hays, A. H. Reid, D. Rupp, S. D. Jong, S. Lee, W.-S. Lee, Y.-D. Chuang, R. Coffee, J. P. Cryan, J. M. Glownia, A. Föhlisch, M. R. Holmes, A. R. Fry, W. E. White, C. Bostedt, A. O. Scherz, H. A. Durr and W. F. Schlotter. "X-ray pulse preserving single-shot optical cross-correlation method

for improved experimental temporal resolution". *Applied Physics Letters* **100**, 121108 (2012).

[112] M. R. Bionta, N. Hartmann, M. Weaver, D. French, D. J. Nicholson, J. P. Cryan, J. M. Glownia, K. Baker, C. Bostedt, M. Chollet, Y. Ding, D. M. Fritz, A. R. Fry, D. J. Kane, J. Krzywinski, H. T. Lemke, M. Messerschmidt, S. Schorb, D. Zhu, W. E. White and R. N. Coffee. "Spectral encoding method for measuring the relative arrival time between x-ray/optical pulses". *Review of Scientific Instruments* **85**, 083116 (2014).

[113] T. Maltezopoulos, S. Cunovic, M. Wieland, M. Beye, A. Azima, H. Redlin, M. Krikunova, R. Kalms, U. Frühling, F. Budzyn, W. Wurth, A. Föhlisch and M. Drescher. "Single-shot timing measurement of extreme-ultraviolet free-electron laser pulses". *New Journal of Physics* **10**, 033026 (2008).

[114] C. Gahl, A. Azima, M. Beye, M. Deppe, K. Döbrich, U. Hasslinger, F. Hennies, A. Melnikov, M. Nagasono, A. Pietzsch, M. Wolf, W. Wurth and A. Föhlisch. "A femtosecond X-ray/optical cross-correlator". *Nature Photonics* **2**, 165 (2008).

[115] O. Krupin, M. Trigo, W. F. Schlotter, M. Beye, F. Sorgenfrei, J. J. Turner, D. A. Reis, N. Gerken, S. Lee, W. S. Lee, G. Hays, Y. Acremann, B. Abbey, R. Coffee, M. Messerschmidt, S. P. Hau-Riege, G. Lapertot, J. Lüning, P. Heimann, R. Soufli, M. Fernández-Perea, M. Rowen, M. Holmes, S. L. Molodtsov, A. Föhlisch and W. Wurth. "Temporal cross-correlation of x-ray free electron and optical lasers using soft x-ray pulse induced transient reflectivity". *Optics Express* **20**, 11396 (2012).

[116] M. B. Danailov, F. Bencivenga, F. Capotondi, F. Casolari, P. Cinquegrana, A. Demidovich, E. Giangrisostomi, M. P. Kiskinova, G. Kurdi, M. Manfredda, C. Masciovecchio, R. Mincigrucci, I. P. Nikolov, E. Pedersoli, E. Principi and P. Sigalotti. "Towards jitter-free pump-probe measurements at seeded free electron laser facilities". *Optics Express* **22**, 12869 (2014).

[117] D. Attwood. *Soft X-rays and Extreme Ultraviolet Radiation* (Cambridge University Press, Cambridge, 1999).

[118] A. A. Zholents and M. S. Zolotorev. "Femtosecond X-Ray Pulses of Synchrotron Radiation". *Physical Review Letters* **76**, 912 (1996).

[119] R. Schoenlein, S. Chattopadhyay, H. Chong, T. Glover, P. Heimann, W. Leemans, C. Shank, A. Zholents and M. Zolotorev. "Generation of femtosecond X-ray pulses via laser–electron beam interaction". *Applied Physics B* **71**, 1 (2000).

[120] S. Khan. "Femtoslicing in Storage Rings". In *Proceedings of the 2005 Particle Accelerator Conference*, vol. 2005, 590–594 (IEEE, 2005).

[121] K. Holldack, T. Kachel, S. Khan, R. Mitzner and T. Quast. "Characterization of laser-electron interaction at the BESSY II femtoslicing source". *Physical Review Special Topics - Accelerators and Beams* **8**, 040704 (2005).

[122] K. Holldack, R. Ovsyannikov, P. Kuske, R. Müller, A. Schälicke, M. Scheer, M. Gorgoi, D. Kühn, T. Leitner, S. Svensson, N. Martensson and A. Föhlisch. "Single bunch X-ray pulses on demand from a multi-bunch synchrotron radiation source". *Nature Communications* **5**, 1 (2014).

[123] J. M. J. Madey. "Stimulated Emission of Bremsstrahlung in a Periodic Magnetic Field". *Journal of Applied Physics* **42**, 1906 (1971).

[124] J. D. Bozek. "AMO instrumentation for the LCLS X-ray FEL". *The European Physical Journal Special Topics* **169**, 129 (2009).

[125] M. Saes, F. van Mourik, W. Gawelda, M. Kaiser, M. Chergui, C. Bressler, D. Grolimund, R. Abela, T. E. Glover, P. A. Heimann, R. W. Schoenlein, S. L. Johnson, A. M. Lindenberg and R. W. Falcone. "A setup for ultrafast time-resolved x-ray absorption spectroscopy". *Review of Scientific Instruments* **75**, 24 (2004).

[126] F. A. Lima, C. J. Milne, D. C. V. Amarasinghe, M. H. Rittmann-Frank, R. M. van der Veen, M. Reinhard, V.-T. Pham, S. Karlsson, S. L. Johnson, D. Grolimund, C. Borca, T. Huthwelker, M. Janousch, F. van Mourik, R. Abela and M. Chergui. "A high-repetition rate scheme for synchrotron-based picosecond laser pump/x-ray probe experiments on chemical and biological systems in solution". *Review of Scientific Instruments* **82**, 063111 (2011).

[127] A. M. March, A. Stickrath, G. Doumy, E. P. Kanter, B. Krässig, S. H. Southworth, K. Attenkofer, C. A. Kurtz, L. X. Chen and L. Young. "Development of high-repetition-rate laser pump/x-ray probe methodologies for synchrotron facilities". *Review of Scientific Instruments* **82**, 073110 (2011).

[128] D. Göries, B. Dicke, P. Roedig, N. Stübe, J. Meyer, A. Galler, W. Gawelda, A. Britz, P. Geßler, H. Sotoudi Namin, A. Beckmann, M. Schlie, M. Warmer, M. Naumova, C. Bressler, M. Rübhausen, E. Weckert and A. Meents. "Time-resolved pump and probe x-ray absorption fine structure spectroscopy at beamline P11 at PETRA III". *Review of Scientific Instruments* **87**, 053116 (2016).

[129] H. Cho, K. Hong, M. L. Strader, J. H. Lee, R. W. Schoenlein, N. Huse and T. K. Kim. "Electronic and Molecular Structure of the Transient Radical Photocatalyst $Mn(CO)_5$ and Its Parent Compound $Mn_2(CO)_{10}$". *Inorganic Chemistry* **55**, 5895 (2016).

[130] H. Wang, C. Yu, X. Wei, Z. Gao, G.-L. Xu, D.-R. Sun, Z. Li, Y. Zhou, Q.-J. Li, B.-B. Zhang, J.-Q. Xu, L. Wang, Y. Zhang, Y.-L. Tan and Y. Tao.

"Development of picosecond time-resolved X-ray absorption spectroscopy by high-repetition-rate laser pump/X-ray probe at Beijing Synchrotron Radiation Facility". *Journal of Synchrotron Radiation* **24**, 667 (2017).

[131] L. X. Chen and X. Zhang. "Photochemical Processes Revealed by X-ray Transient Absorption Spectroscopy". *The Journal of Physical Chemistry Letters* **4**, 4000 (2013).

[132] B. Henke, E. Gullikson and J. Davis. "X-Ray Interactions: Photoabsorption, Scattering, Transmission, and Reflection at E = 50-30,000 eV, Z = 1-92". *Atomic Data and Nuclear Data Tables* **54**, 181 (1993).

[133] M. Nagasaka, T. Hatsui, T. Horigome, Y. Hamamura and N. Kosugi. "Development of a liquid flow cell to measure soft X-ray absorption in transmission mode: A test for liquid water". *Journal of Electron Spectroscopy and Related Phenomena* **177**, 130 (2010).

[134] S. Schreck and P. Wernet. "Isotope effects in liquid water probed by transmission mode x-ray absorption spectroscopy at the oxygen K-edge". *The Journal of Chemical Physics* **145**, 104502 (2016).

[135] J. Meibohm, S. Schreck and P. Wernet. "Temperature dependent soft x-ray absorption spectroscopy of liquids". *Review of Scientific Instruments* **85**, 103102 (2014).

[136] S. Schreck, G. Gavrila, C. Weniger and P. Wernet. "A sample holder for soft x-ray absorption spectroscopy of liquids in transmission mode". *Review of Scientific Instruments* **82**, 103101 (2011).

[137] L.-Å. Näslund, J. Lüning, Y. Ufuktepe, H. Ogasawara, P. Wernet, U. Bergmann, L. G. M. Pettersson and A. Nilsson. "X-ray Absorption Spectroscopy Measurements of Liquid Water". *The Journal of Physical Chemistry B* **109**, 13835 (2005).

[138] L. Weinhardt, M. Blum, O. Fuchs, A. Benkert, F. Meyer, M. Bär, J. Denlinger, W. Yang, F. Reinert and C. Heske. "RIXS investigations of liquids, solutions, and liquid/solid interfaces". *Journal of Electron Spectroscopy and Related Phenomena* **188**, 111 (2013).

[139] M. Kubin, J. Kern, M. Guo, E. Källman, R. Mitzner, V. K. Yachandra, M. Lundberg, J. Yano and P. Wernet. "X-ray-induced sample damage at the Mn L-edge: a case study for soft X-ray spectroscopy of transition metal complexes in solution". *Physical Chemistry Chemical Physics* **20**, 16817 (2018).

[140] K. Kunnus, I. Rajkovic, S. Schreck, W. Quevedo, S. Eckert, M. Beye, E. Suljoti, C. Weniger, C. Kalus, S. Grübel, M. Scholz, D. Nordlund, W. Zhang, R. W. Hartsock, K. J. Gaffney, W. F. Schlotter, J. J. Turner, B. Kennedy, F. Hennies,

S. Techert, P. Wernet and A. Föhlisch. "A setup for resonant inelastic soft x-ray scattering on liquids at free electron laser light sources". *The Review of scientific instruments* **83**, 123109 (2012).

[141] H. A. Rowland. "XXIX. On concave gratings for optical purposes". *The London, Edinburgh, and Dublin Philosophical Magazine and Journal of Science* **16**, 197 (1883).

[142] J. Nordgren, G. Bray, S. Cramm, R. Nyholm, J.-E. Rubensson and N. Wassdahl. "Soft x-ray emission spectroscopy using monochromatized synchrotron radiation (invited)". *Review of Scientific Instruments* **60**, 1690 (1989).

[143] J. Nordgren and J. Guo. "Instrumentation for soft X-ray emission spectroscopy". *Journal of Electron Spectroscopy and Related Phenomena* **110-111**, 1 (2000).

[144] H. G. Beutler. "The Theory of the Concave Grating". *Journal of the Optical Society of America* **35**, 311 (1945).

[145] T. Schmitt. personal communication.

[146] T. Schmitt, V. N. Strocov, K.-J. Zhou, J. Schlappa, C. Monney, U. Flechsig and L. Patthey. "High-resolution resonant inelastic X-ray scattering with soft X-rays at the ADRESS beamline of the Swiss light source: Instrumental developments and scientific highlights". *Journal of Electron Spectroscopy and Related Phenomena* **188**, 38 (2013).

[147] M. Kubin, M. Guo, M. Ekimova, M. L. Baker, T. Kroll, E. Källman, J. Kern, V. K. Yachandra, J. Yano, E. T. J. Nibbering, M. Lundberg and P. Wernet. "Direct Determination of Absolute Absorption Cross Sections at the L-Edge of Dilute Mn Complexes in Solution Using a Transmission Flatjet". *Inorganic Chemistry* **57**, 5449 (2018).

[148] W. F. Schlotter, J. J. Turner, M. Rowen, P. Heimann, M. Holmes, O. Krupin, M. Messerschmidt, S. Moeller, J. Krzywinski, R. Soufli, M. Fernández-Perea, N. Kelez, S. Lee, R. Coffee, G. Hays, M. Beye, N. Gerken, F. Sorgenfrei, S. Hau-Riege, L. Juha, J. Chalupsky, V. Hajkova, A. P. Mancuso, A. Singer, O. Yefanov, I. A. Vartanyants, G. Cadenazzi, B. Abbey, K. A. Nugent, H. Sinn, J. Lüning, S. Schaffert, S. Eisebitt, W.-S. Lee, A. Scherz, A. R. Nilsson and W. Wurth. "The soft x-ray instrument for materials studies at the linac coherent light source x-ray free-electron laser". *Review of Scientific Instruments* **83**, 043107 (2012).

[149] B. Bennett, R. Soref and J. Del Alamo. "Carrier-induced change in refractive index of InP, GaAs and InGaAsP". *IEEE Journal of Quantum Electronics* **26**, 113 (1990).

[150] F. Schäfers. "Multilayers for the EUV/soft X-ray range". *Physica B: Condensed Matter* **283**, 119 (2000).

[151] S. Braun, R. Dietsch, M. Haidl, T. Holz, H. Mai, S. Müllender and R. Scholz. "Mo/Si-multilayers for EUV applications prepared by Pulsed Laser Deposition (PLD)". *Microelectronic Engineering* **57-58**, 9 (2001).

[152] A. Bojahr, D. Schick, L. Maerten, M. Herzog, I. Vrejoiu, C. von Korff Schmising, C. Milne, S. L. Johnson and M. Bargheer. "Comparing the oscillation phase in optical pump-probe spectra to ultrafast x-ray diffraction in the metal-dielectric $SrRuO_3$ /$SrTiO_3$ ". *Physical Review B* **85**, 224302 (2012).

[153] C. von Korff Schmising, M. Bargheer, M. Kiel, N. Zhavoronkov, M. Woerner, T. Elsaesser, I. Vrejoiu, D. Hesse and M. Alexe. "Accurate time delay determination for femtosecond X-ray diffraction experiments". *Applied Physics B* **88**, 1 (2007).

Appendix A

Presentation of the Results

In addition to the publications, I had the chance to present the results I summarized in this thesis at the following occasions.

Oral Presentations

Taipeh, Taiwan
Ultrafast bond deformations in molecular systems investigated with soft X-ray spectroscopy
Invited talk at the conference Synchrotron Radiation International 2018, 12.06.2018

Universität Potsdam, Potsdam, Germany
Probing photo-induced molecular dynamics with soft X-ray absorption spectroscopy and resonant inelastic X-ray scattering
Theorieseminar Theoretische Chemie und Computerchemie, 07.02.2018

HZB, Berlin, Germany
Ultrafast Independent N-H and N-C Bond Deformation Investigated with Resonant Inelastic X-Ray Scattering
Scientific Evaluation MATTER, 10.01.2018

Grainau, Germany
Photochemical processes in solution investigated with soft X-ray absorption spectroscopy
Helmholtz VI-419 Young Investigators Workshop, 24.04.2017

Reit im Winkl, Germany
2-Mercaptopyridine on Excited State Potential Energy Surfaces
Helmholtz VI-419 Young Investigators Workshop, 12.01.2016

HZB, Berlin, Germany
It's all about that base: Protonation of the nitrogen site in 2-Mercaptopyridine
Postgraduate seminar "Science with Synchrotron Methods" der Universität Potsdam / FG-ISRR Institute Seminar, 17.07.2015

Poster Presentation

DESY, Hamburg, Germany
2-Mercaptopyridine on Excited State Potential Energy Surfaces
From Matter to Materials and Life Workshop 2016 Research Topic 1, 15.12.2016

Appendix B

Supporting Information

Supporting Information for publications II, III, IV and V.

Supporting Information for

Selective gating to vibrational modes through resonant X-ray scattering

Acknowledgments

I would like to thank all scientific and technical staff I have had the pleasure to work with at the different research facilities in the last years for making nearly every project we worked on a success. In particular I would like to express my special thanks to ...

... Alexander Föhlisch for supervising my work, for being excited and encouraging in all projects we have been working on. Thank you for all the opportunities I have had from working under your guidance.

... Prof. Dr. Markus Gühr and Prof. Dr. Mathias Richter for reviewing this thesis.

... Raphael Jay, Mattis Fondell and Rolf Mitzner for the endless months of beamtime, work and effort we have spent together. We make a good team and I am very happy to be a part of it.

... Jesper Norell, Vinicius Vaz da Cruz, Michael Odelius and Faris Gel'mukhanov for your great theoretical simulations, derivations and explanations.

... Piter Midema and Johannes Niskannen for making sense of N K-edges with the help of your simulations.

... Annette Pietzsch, Brian Kennedy and Wilson Quevedo for our endless RIXS marathons.

... Christian Weniger and Thomas Blume for creating and improving our beautiful setups. Without your help many beamtimes would not have been successful.

... Philippe Wernet, Christian Schüßler-Langeheine, Niko Pontius, Karsten Holldack, Florian Sorgenfrei, Daniel Schick, Ruslan Ovsyannikov and Martin Beye for your always immediate help regarding scientific questions and technical hard and software issues.

... my family for always being by my side, supporting me and for bearing with me in stressful times. I am so lucky to have you!

Selbstständigkeitserklärung

Hiermit erkläre ich, dass die Arbeit an keiner anderen Hochschule eingereicht sowie selbständig von mir und nur mit den angegebenen Mitteln angefertigt wurde.

Potsdam, den

Sebastian Eckert